THE EFFECT OF FLOW GEOMETRY
ON CRITICAL HEAT FLUX

by

Khaled Joober

Submitted to the School of Graduate Studies of the University of Ottawa in partial fulfilment of the requirements for the degree of

MASTER OF APPLIED SCIENCE

in

Mechanical Engineering

ISBN 0-315-85863-X

ABSTRACT

An extensive and systematic literature review on the effect of flow geometry on the Critical Heat Flux (CHF) has been performed. This review covers most of the flow geometries that have been previously investigated such as tubes, concentric and eccentric annuli, rectangular channels, irregular-shaped channels and bundles.

Each of the above geometries is studied individually. The following geometric parameters have been found to strongly influence the CHF:

i) hydraulic-equivalent diameter,

ii) heated-equivalent diameter,

iii) gap size,

iv) unheated adjacent surface,

v) heated adjacent surface,

vi) curvature,

vii) eccentricity (including bowing), and

viii) channel shape.

It is found that some of the geometric effects on CHF depend on the flow conditions and the CHF type (six CHF types have been identified for convective boiling).

For each geometry the parametric trends have been described, whenever sufficient experimental results are available . A review and assessment of the available prediction methods is conducted. The observed trends are used to derive a correction factor to the reference CHF table values for an 8-mm tube.

In some cases, when the experimental data are limited, no correction factor is derived but only general recommendations are made for future work.

The following trends have been identified in this study: (i) in general the CHF in annuli (concentric and eccentric) is lower than that in tubes, especially for high quality and narrow gaps; (ii) for rectangular channels and irregular-shaped channels, corners can cause a large CHF reduction; (iii) the CHF for concave surface is significantly higher than the CHF for a convex surface; (iv) the effect of gap size in concentric annuli is different for a departure from nucleate boiling (DNB) type CHF and CHF type for the annular flow regime. For the first CHF type reduction in gap size results in a CHF decrease, while for the second CHF type it results in CHF enhancement; and (v) heating the adjacent surface results in a CHF increase.

Based on the observed trends, CHF correction factors have been derived for each geometry. Finally, an interim CHF prediction method for subchannels and flow conditions of interest to CANDU* reactors has been proposed.

---

* CANDU - CANada Deuterium Uranium, a registered trademark.

ACKNOWLEDGEMENTS

This study was performed at Atomic Energy of Canada Limited (AECL) at Chalk River Laboratories (CRL). I would like to express my gratitude to AECL for the permission to publish this material as a master's thesis.

I would like to express my appreciation to Dr. D.C. Groeneveld of AECL, who acted as my off-campus supervisor for providing help and assistance throughout the course of this work. I also appreciate the help, comments and suggestions of Dr. S.C. Cheng, my supervisor at the University of Ottawa. I also would like to thank Dr. S. Doerffer for his valuable comments, advice and his critical review of this thesis. I am also thankful to every person who helped directly or indirectly towards the completion of this work.

Finally, I am grateful to my family for everything they have done for me.

TABLE OF CONTENTS

LIST OF TABLES

LIST OF FIGURES

NOMENCLATURE

A_h	square area of the plate which heats the jet (mm^2 or m^2)
A_j	cross-sectional area of circular jet (mm^2 or m^2)
BO	boiling number = $\left[\frac{CHF}{G\,h_{fg}}\right]$
Cp_l	specific heat of liquid phase ($J.kg^{-1}.K^{-1}$)
CHF	critical heat flux ($kW.m^{-2}$)
D	tube diameter (mm or m)
d	rod diameter (mm or m)
D_b	bubble diameter (mm or m)
D_d	droplet diameter (mm or m)
D_{he}	heated equivalent diameter = $\left[\frac{4\ flow\ area}{heated\ perimeter}\right]$ (mm or m)
D_{hy}	hydraulic equivalent diameter = $\left[\frac{4\ flow\ area}{wetted\ perimeter}\right]$ (mm or m)
D_i	internal diameter of annulus (mm or m)
D_o	external diameter of annulus (mm or m)
f	Fanning friction factor
F	correction factor for subchannel geometry
g	acceleration due to gravity ($m.s^{-2}$)
G	mass flux ($Mg.m^{-2}.s^{-1}$)
G_D	local deposition rate ($Mg.m^{-2}.s^{-1}$)
h	enthalpy ($J.kg^{-1}$)
h_{fg}	latent heat ($J.kg^{-1}$)

Δh_c	subcooling at critical point, $h_f - h_c$ ($J.kg^{-1}$)
j_g	superficial velocity of gas phase ($m.s^{-1}$)
K	spacer plane loss coefficient
K_X	quality correction factor for annuli
K_δ	gap size correction factor for annuli
L	heated length (mm or m)
n	exponent used in Equations (3.1) and (4.1)
P	pressure (MPa)
P_{cr}	critical pressure (MPa)
rms	root mean square error = $\sqrt{\frac{\sum (relative\ error)^2}{number\ of\ data\ points}}$
r_i	internal radius of annulus (mm or m)
r_o	external radius of annulus (mm or m)
R	heat flux ratio for annuli = $\left[\frac{outer\ surface\ heat\ flux}{inner\ surface\ heat\ flux}\right]$
Re	Reynolds number = $\left[\frac{G\,D}{\mu}\right]$
Re_g	gas Reynolds number used in Equation (8.7)
s	height of rectangular cross section (mm or m)
T	temperature (K or ^oC)
u_g	maximum jet velocity for a stable column ($m.s^{-1}$)
X	thermodynamic equilibrium quality = $\left[\frac{h-h_f}{h_{fg}}\right]$
w	width of rectangular cross section (mm or m)
W_{LF}	film flow rate per unit width ($Mg.m^{-1}.s^{-1}$)

z axial coordinate (mm or m)

Greek Symbols

α void fraction = $\left[\frac{\textit{Cross Sectional Area Occupied by Gas}}{\textit{Total Cross Sectional Area of the Channel}}\right]$

β mixing coefficient = $\left[\frac{\textit{lateral mass flux in the element-element gap}}{\textit{axial mass flux}}\right]$

δ gap size (mm or m)

ε eccentricity = $\left[\frac{\delta_{conc} - \delta_{min}}{\delta_{conc}}\right]$

λ_T Taylor wavelength (m)

λ_{KH} Kelvin-Helmholtz wavelength (m)

μ viscosity ($kg.m^{-1}.s^{-1}$)

σ surface tension ($N.m^{-1}$)

ϕ surface heat flux ($kW.m^{-2}$)

ρ density ($kg.m^{-3}$)

Subscripts

ann annulus

b bulk liquid; bubble

c critical (CHF) conditions

d droplet

D=8mm reference tube of 8 mm in diameter

D=10mm reference tube of 10 mm in diameter

cf	cross flow effect
conc	concentric
D	deposition
eccn	eccentric
enh	enhancement effect in subchannels
f	saturated liquid
g	saturated vapour
hy	hydraulic
he	heated
i	inlet; internal
j	jet
l	liquid
LF	liquid film
mg	minimum gap effect
min	minimum
o	subcooled conditions; external
oaf	onset of annular flow
sat	saturated condition
sp	distance between spacers
sub	subcooled condition
X	quality effect

1. INTRODUCTION

During the past 40 years, the critical heat flux (CHF) has been studied extensively, as indicated by the proliferation of correlations (over 400 correlations can be found in the literature just for CHF in water-cooled tubes). Most of the prediction methods are designed exclusively for round tubes. These same predictions methods are usually applied to other geometries.

Developments in nuclear industry, steam generators and more recently in computers cooling systems have generated an increasing interest in the CHF in non-circular geometries. Therefore, there is a need for a prediction method to account for the effect of a change in flow geometry on CHF. The objective of this work is to develop such a prediction method.

The major importance of the effect of flow geometry on CHF comes from the nuclear industry. It is known that the CHF is one of the factors that limits the maximum power extractable from water-cooled nuclear reactors. Hence, the knowledge of the exact occurrence of CHF is essential in increasing the reactor power. However, round tube correlations are frequently applied to different geometries present in the reactor, such as subchannel-shaped geometries or bundles. Fuel bundle subchannels are usually defined as flow areas between fuel rods bounded by the rods themselves and imaginary lines linking adjacent rod centres, as illustrated in Figure 1.1 for the case of CANDU fuel bundle. This application of tube CHF correlations to these subchannel geometries is a source of possible large errors in CHF predictions, hence large safety margins are required to compensate for these potential errors. Another reason for the interest of analysts in the effect of geometry on CHF (particularly the effect of the presence of an unheated subchannel wall, the effect of element/element gap size, and the effect of element/pressure-tube gap size) is caused by the postulated geometry changes due to pressure-tube creep, fuel strain and element bowing, which can occur during normal operation or postulated loss of regulation (LOR) accident conditions. Figure 1.2 illustrates the different problems that might occur due to geometry changes in a nuclear fuel bundle.

The cost of experimentally investigating all these effects in full-scale simulated fuel-bundle geometries is prohibitive, as CHF experiments on each fuel-bundle geometry would typically cost from $2 to $5 Million. A number of geometries would be required to investigate each of the above effects.

Currently, the CHF for a CANDU fuel bundle or bundle subchannels is frequently predicted using the CHF look-up tables (Groeneveld *et al.* [1986a]). These tables provide the boiling-length-average CHF as a function of cross-sectional average flow conditions for a reference tube geometry. To account for the effect of a geometry change on CHF, any variation of each of the characteristic dimensions of a bundle or subchannel needs to be considered. These characteristic dimensions include:

- heated-equivalent diameter,
- hydraulic-equivalent diameter,
- inter-element gap size,
- element/pressure-tube gap size,

- curvature of the surfaces (heated and unheated), and
- subchannel shape.

In addition, the effect of the radial-flux distribution or variation of the heat flux around the subchannel perimeter needs to be considered.

The approach taken in this study is: (i) examine the effect of all flow-geometry parameters on CHF; (ii) determine the dominating parameters affecting the CHF; and (iii) use these parameters in deriving a correction factor to the CHF for the reference tube-CHF look-up table.

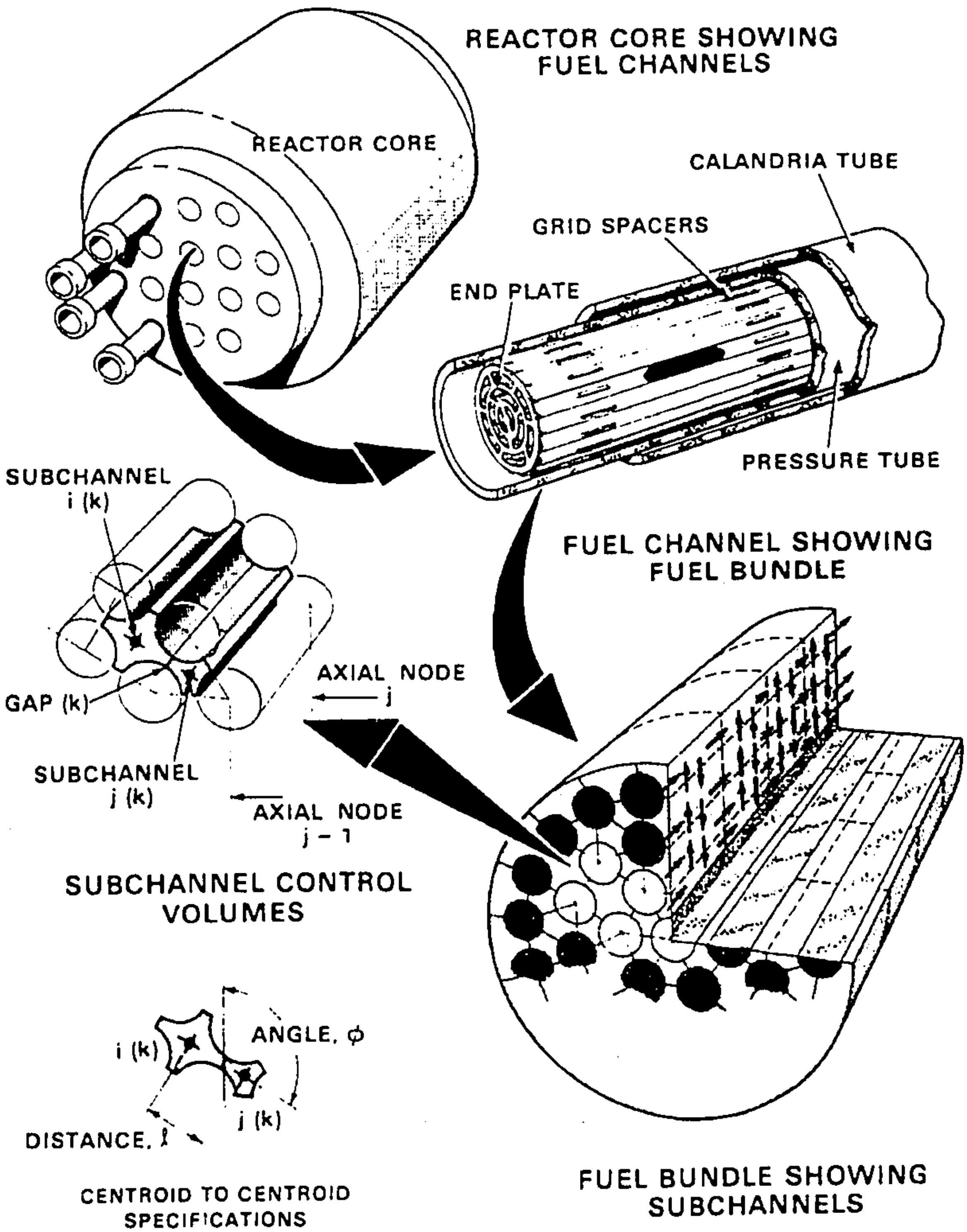

Figure 1.1: CANDU Subchannel Definition. From Judd *et al.* (1984).

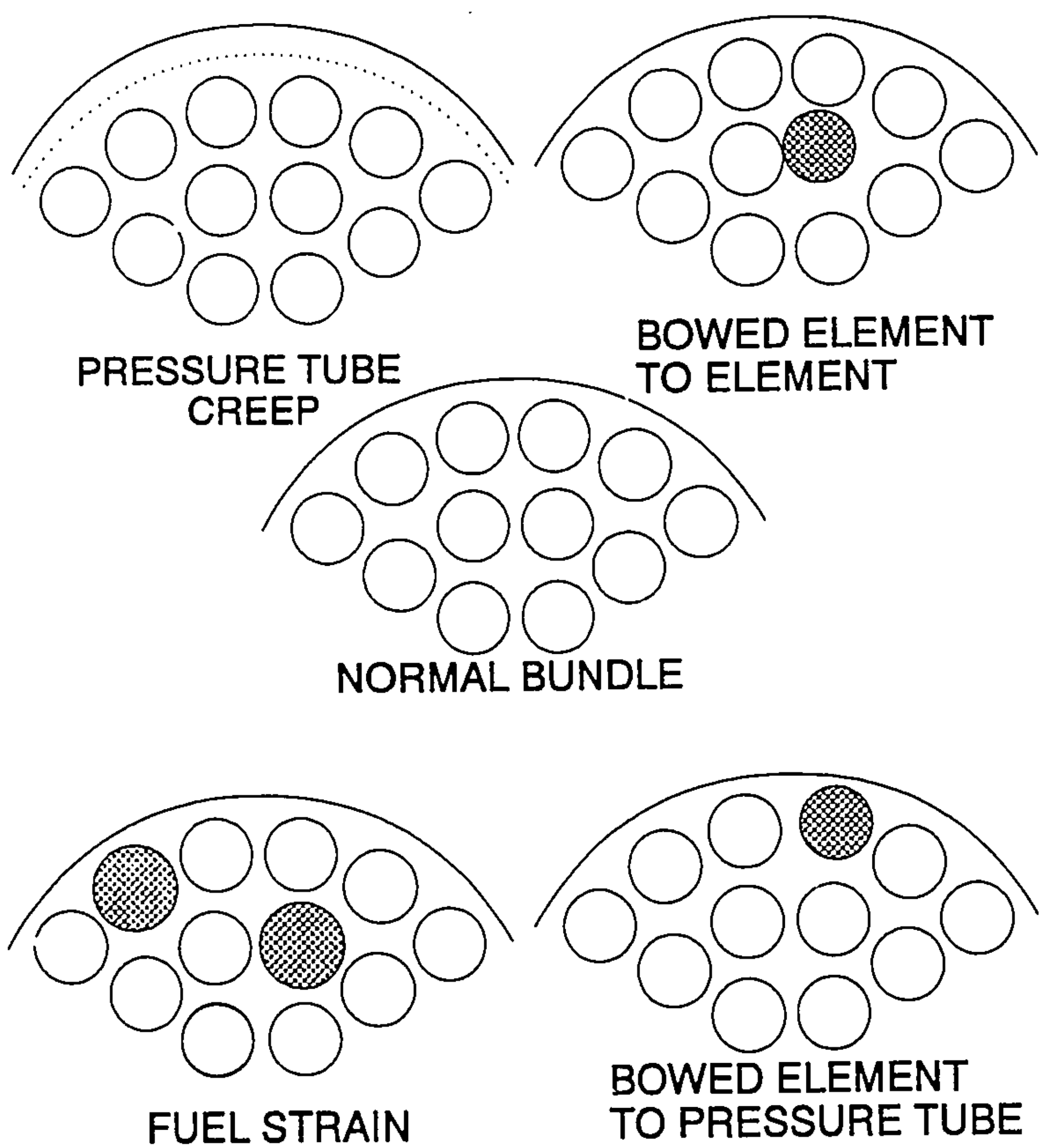

Figure 1.2: Problems That Might Happen During Normal Operations or Postulated Loss of Regulation Accident Conditions in CANDU Fuel Bundle.

2. REVIEW OF THE CHF LITERATURE

2.1 Introduction

When the heat flux applied to a surface in contact with boiling liquid is increased gradually, an insulating vapour layer builds up on the heated surface. This vapour layer causes a sudden decrease in heat transfer coefficient due to its low thermal conductivity. Simultaneously, if the heat flux is not reduced, the surface temperature rises dramatically. The magnitude of the temperature jump during this phenomenon depends upon the flow conditions and regimes. To describe this particular condition different terms have been used:

- burnout,
- dryout,
- critical heat flux (CHF) condition,
- departure from nucleate boiling (DNB) and
- boiling crisis.

None of these terms gives a general description of the physics. For instance, the term burnout implies a physical melting of the heated surface which does not necessarily occur (e.g., at high qualities the temperature excursion is not very important and does not lead to immediate damage of the surface). Under subcooled or saturated nucleate boiling conditions, this phenomenon is caused by a transition from nucleate boiling to film boiling, hence in this case the term "departure from nucleate boiling" is the most adequate. At high qualities, this phenomenon is associated with the dryout of the wall liquid-film, thus film dryout is the proper term for this case. In this thesis the above described phenomenon will be referred to as the critical heat flux condition, and the heat flux at which it occurs as the critical heat flux (CHF).

2.2 Boiling Curve

The boiling curve of a heated surface relates the surface heat flux to a temperature difference. In the case of pool boiling and for a temperature-controlled surface the boiling curve is shown in Figure 2.1a. The different regions of this curve are:

- the natural convection single-phase (liquid) region (A-B),
- the nucleate boiling region (B-C),
- the transition boiling region, where parts of the surface are in film boiling and others in nucleate boiling modes (C-D),
- the film boiling region (D-E).

The boiling curve of a heat-flux-controlled surface in pool boiling is shown in Figure 2.1b. Some parts of this curve are identical to Figure 2.1a. However, in this case when reaching point C (critical heat flux point), any slight increase in the surface heat flux results in a temperature jump from C to F. At point F, if the heat flux is increased the curve traces F-E, but if the heat flux is decreased the curve traces F-D and not F-C. Reaching point D (known as minimum film boiling point or Leidenfrost point), a further decrease in the heat flux results in the surface temperature following the path D-G. It is to be noted that the transition along C-F and D-G can only be achieved in one direction, as shown in Figure 2.1b.

The boiling curve in the case of flow boiling is similar in shape to the pool boiling curve but not exactly identical to it.

2.3 CHF Mechanisms

2.3.1 Pool Boiling

Depending on the fluid enthalpy, the following mechanisms govern the CHF occurrence in pool boiling:

(i) Saturated boiling: at these conditions vapour bubbles are generated at a very high rate, such that insufficient quantities of liquid can reach the surface. Bubbles form a barrier to the incoming liquid. The CHF prediction in this case is much simpler than in the flow boiling case. The theory predicts the CHF by determining the onset of the transition boiling region. According to this theory a heavy fluid on top of a light fluid layer is unstable (as the case for liquid and vapour). The layer collapses by a formation of waves, the wavelength is known as Taylor wavelength, λ_T, and is given by

$$\lambda_T = C \sqrt{\frac{\sigma}{(\rho_f - \rho_g)\, g}} \qquad (2.1)$$

where $C = 2\pi\sqrt{3}$ for one dimensional waves and $C = 2\pi\sqrt{6}$ for two dimensional waves. Vapour is removed from the surface vapour layer by rising vapour columns or jets forming at the peak amplitude position of the Taylor wave, as shown in Figure 2.2a for the case of a flat plate. Ultimately, when the vapour velocity in the columns reaches a critical value, the columns will collapse and become unstable. This is known as the Kelvin-Helmholtz instability. The maximum vapour velocity for a stable vapour column is given by

$$u_g = \sqrt{\frac{2\pi\sigma}{\rho_g\,\lambda_{KH}}} \tag{2.2}$$

where λ_{KH} is the disturbance wavelength as shown in Figure 2.2b. The CHF is obtained by a heat balance in the columns when the vapour velocity is equal to u_g

$$CHF = h_{fg}\,\rho_g\,u_g\left(\frac{A_j}{A_h}\right) \tag{2.3}$$

where A_j is the cross-sectional area of circular jet and A_h is the square area of the plate which heats the jet (see Figure 2.2a). For an infinite horizontal plate, substituting values for u_g and A_j/A_h into Equation (2.3) results in:

$$CHF_{sat} = K\,\rho_g^{1/2}\,h_{fg}\,\sqrt[4]{g\,(\rho_f-\rho_g)\,\sigma} \tag{2.4}$$

where K depends on the choice made for λ_{KH} and λ_T (Zuber [1959] suggested K=0.131 and Lienhard and Dhir [1973] suggested K=0.149). K=0.149 gives the closest results to the experimental data for a flat plate.

(ii) High subcooling: at very high subcooling it has been suggested that CHF can be caused by the complete evaporation the micro-layer (a very thin layer of liquid beneath an undetached bubble). At high heat flux levels dry-patch heats up very rapidly such that rewetting of this area is not possible. For subcooled conditions the correction suggested by Ivey and Morris [1962] is recommended for Equation (2.4) and given by

$$\frac{CHF_{sub}}{CHF_{sat}} = 1+0.1\left(\frac{Cp_l(T_{sat}-T_b)}{h_{fg}}\right)\left(\frac{\rho_f}{\rho_g}\right)^{3/4} \quad (2.5)$$

2.3.2 Forced Convective Boiling

Figure 2.3 illustrates the distribution of the flow regimes along a vertical uniformly-heated tube. The parameter characterizing the flow regimes in this figure is the thermodynamic quality, defined at any axial position, z, as

$$X(z) = \frac{h(z)-h_f}{h_{fg}} \quad (2.6)$$

The dryout point (CHF condition) is accompanied by a wall temperature rise. It is to be noted that this figure is for low heat flux (for high-quality CHF). Depending on the magnitude of heat flux, the CHF condition can be made to occur in any of the flow regimes as shown in Figure 2.4. Figure 2.4 illustrates the variation of the heat transfer coefficient with quality, X, with increasing heat flux as a parameter. Curve (i) of Figure 2.4 corresponds to the conditions shown in Figure 2.3. As the heat flux is increased for each case (curve ii to vii), subcooled boiling is initiated earlier and the CHF condition occurs at lower quality, hence in a different flow regime. CHF occurrence in different flow regimes (different local flow conditions) is one reason for the many CHF mechanistic descriptions present in the literature. A second reason for different CHF mechanisms is the geometry of the flow passage. Therefore, any mechanistic description of the geometry effect on CHF must be based on an understanding of the underlying CHF mechanisms. The following six CHF mechanisms have been identified for convective boiling:

(I) Liquid Starvation By Vapour Bridging. For certain combinations of flow geometry and flow conditions, the bubble can be of the same size as the transverse dimension of the flow geometry as shown in Figure 2.5. In this case, a bubble could locally bridge the complete cross section, resulting in a temporary interruption of the supply of liquid and a subsequent CHF occurrence due to blockage of the flow passage or a fraction of the flow passage. This mechanism is more likely to occur for:

(i) low pressures, where the liquid- to- vapour density-ratio is very high;

(ii) saturated boiling, where bubbles are large;

(iii) low flows, where the size of the discrete vapour cells (bubbles, slugs) is large; and

(iv) narrow flow passages.

For each of these conditions there is a thin liquid film which initially remains between the bubble and the heated wall. If the heat flux is high enough this film will evaporate and as a result a premature CHF occurs.

(II) Nucleation Induced. This type of CHF is also referred to by Collier [1981] as, "dryout under vapour clot". It is encountered at high subcoolings and very high heat fluxes. Here, a temporary dry patch is formed as a result of evaporation of the micro-layer under single bubble or coalescing bubbles as seen in Figure 2.5 (Collier [1981] and Groeneveld [1981]). At high heat-flux levels (close to the CHF), the high dry-patch surface temperature could prevent the rewetting of the surface, thus leading to the CHF condition. This type of CHF is characterized by a fast temperature rise (fast dryout).

(III) Bubble Clouding. This type of CHF is also known under "bubble crowding and vapour blanketing". At moderate subcooling (close to saturation), bubbles may form a bubble boundary layer in the vicinity of the heated surface [Tong, 1965]. This layer reduces the access of the liquid to the heated surface. This in turn causes an increase in near-wall liquid superheat, further increasing the near-wall bubble population, preventing fresh liquid from reaching the wall and eventually leading to vapour blanketing of the surface by increased nucleation/micro-layer evaporation and bubble coalescence (Figure 2.5). This phenomenon is also called the "boundary layer blow off". It is commonly accepted as the most general mechanism for low-quality region, with mechanism II occurring only at very high heat fluxes and mechanism I occurring only at low pressures and mass fluxes.

(IV) Entrainment-Controlled Film Dryout. Figure 2.6 [Hewitt and Hall-Taylor, 1970] shows the relation between the entrained-droplet flow rate and the local quality. Also shown in this figure is the hydrodynamic-equilibrium entrainment curve (dotted curve), where the entrainment is balanced by deposition for varying quality. The CHF condition is reached when the entrained-droplet flow equals the total-liquid flow. From this figure it is seen that the entrainment curve increases until crossing the hydrodynamic equilibrium curve and then decreases towards the CHF condition (burnout point). Hewitt and Hall-Taylor [1970] postulated that, "in the first part of the channel there is net liquid entrainment from the film and in the latter part of the channel there is net liquid deposition. The results are readily understood if it is realized that the flow will always be tending towards the hydrodynamic equilibrium". This type of CHF occurs in annular flow, but for a relatively shorter length and lower burnout qualities than the deposition-controlled film dryout described below. Figure 2.7 illustrates different zones of CHF occurrence, for various local qualities. The entrainment-controlled film dryout may occur either in Zone II or III and is accompanied by a moderate temperature rise. The liquid film depletion in this case may be enhanced by one of the following mechanisms:

- Thermocapillary effect: one of the most important source of entrainment in annular flow is the surface waves. These waves cause a non-uniform temperature distribution along the liquid-vapour interface; a maximum temperature in the valley and a minimum temperature at the wave tip. This in turn causes a surface tension gradient, which draws liquid to the higher surface tension area (wave tips) and eventually leads to a dryout in the wave valley.
- Nucleation induced film breakdown: when nucleation occurs in the annular flow regime, bubbles may cause a dry-patch in the liquid film if the bubble size is comparable to the film thickness. At high heat flux values, rewetting of this area could be prevented, thus leading to a CHF condition (N.B., this is unlikely to occur unless a local heat flux spike is present; high turbulence level in annular liquid film usually suppresses nucleation occurrence).

(V) Deposition-Controlled Film Dryout. The entrainment rate strongly depends on film thickness (Hewitt and Hall-Taylor, 1970), thicker films result in higher waves on the liquid film and the tips of the waves eventually become sheared off and entrained. At high qualities, the liquid film is thin and liquid entrainment is suppressed. In this region, the liquid-film flow rate is governed by evaporation and deposition. The following equation can be derived from the liquid-film mass balance

$$\frac{CHF}{h_{fg}} = G_D - \frac{dW_{LF}}{dz} \qquad (2.7)$$

where W_{LF} is the film flow rate per unit width and G_D is the local deposition rate.

If the last term in the above equation is zero, then the evaporation rate (from the liquid-film vapour interface) just balances the deposition rate and the CHF is said to be deposition controlled. Hewitt and Hall-Taylor [1970] concluded that the CHF for uniformly heated tubes becomes deposition controlled for long tube lengths (L/D >> 100). This type of CHF is illustrated in Figure 2.7 by Zone I.

(VI) Annular Film Dryout, No Entrained Droplets. This type of CHF mechanism occurs only at very low flows and high qualities, where all the liquid is in the liquid film on the walls of the flow geometry. Here, the CHF occurs when the quality approaches 100%.

2.4 CHF Prediction Methods

2.4.1 Correlations

Although correlations are quite valuable, the extrapolation to conditions outside their data range usually results in very large errors. Correlations are totally empirical; they do not use any assumptions about the actual CHF mechanistic process. CHF correlations can be divided into two main categories:

i- Local conditions correlations: these correlations are based on the local condition hypothesis suggested by Barnett [1963]. This hypothesis implies that the CHF depends only on the local conditions, i.e., CHF = f(P,G,X_c,cross-section geometry).

ii- Global conditions correlations: these correlations predict the CHF power as a function of the global conditions, i.e., CHF power = f(P,G,Δh_{in},L_{he}, cross-section geometry). This approach does not predict the axial location of CHF and it assumes steady state conditions and a uniform axial flux distribution. Bowring [1972] correlation is generally accepted as one of the most reliable correlation of this type for water.

It is to note that this functional relationship and the one proposed in the previous paragraph for the local condition hypothesis are connected by the heat balance equation.

2.4.2 Tabular Method

Doroshchuk *et al.* [1975] constructed a standard table of the CHF as a function of the local bulk conditions for an 8-mm tube. Note that this is basically a form of local condition hypothesis (i.e., CHF=f(P,G,X_c). The table approach has been continued at the University of Ottawa (UO) and Chalk River Laboratories (CRL) by Groeneveld *et al.* [1986a] using a much wider data base (15,000 tube CHF data). Similarly as the Doroshchuk table, the AECL-UO table (Groeneveld *et al.* [1986a]) presents the CHF as a function of P,G and X_c. The table covers a wide range of conditions:

- pressure (P) = 100-20000 kPa,

- mass flux (G) = 0-7500 $kg.m^{-2}.s^{-1}$,

- quality (X_c) = -50 to 100%.

The table is constructed for upward flow in a uniformly heated 8-mm tube. In order to obtain the CHF in any other configuration, correction factors are required:

$$CHF_{actual} = CHF_{8\text{-}mm}\, K_i\, K_j \cdots \tag{2.8}$$

where K_i, K_j... account for effects such as non-uniform flux distribution, spacer effects, transient effects, orientation effects, flow geometry effects, etc.. This study is concerned with the derivation of correction factors due to changes in cross-sectional flow geometry.

For fluids other than water, a dimensionless CHF table was constructed (Groeneveld *et al.*, [1986b]). The dimensional variables in the non-aqueous table are substituted by

- P by $\dfrac{\rho_f}{\rho_g}$

- CHF by $\dfrac{CHF}{G.h_{fg}}$

- G by $\psi_k = \dfrac{G.D^{0.5}}{\sigma^{0.5}\rho_f^{0.5}}$

2.4.3 Modelling Approach

Models are an analytical approach to characterize physically the CHF occurrence. Models may require a few optimized empirical constants obtained from experimental data. Theoretical models predict the CHF in a system within a set of conditions regardless of the fluid type. However, models are only valid for one flow regime and heat transfer configuration (e.g., annular flow and subcooled nucleate boiling).

A popular model for the annular flow regime was proposed by Hewitt and Hall-Taylor [1970] which assumes that the CHF occurs when the film flow rate goes to zero (film flow rate is affected by entrainment, deposition and evaporation).

A second model was developed by Weisman and Pei [1983] to predict CHF for low quality and high mass flux. This model uses the following assumptions for CHF prediction:

- Under subcooled conditions the CHF is a local phenomenon.
- Under subcooled conditions, the bubbly layer (the flow is divided into the bubbly layer and core region as shown in Figure 2.8) increases in thickness until the turbulent eddy size cannot move the bubbles radially.
- CHF occurs if the void fraction, α, in the bubbly layer exceeds 0.82.
- The void fraction in the bubbly layer is determined by a balance of the outward flow of vapour and the inward flow of liquid at the bubbly layer-core interface under the assumption of homogeneous two-phase flow in the bubbly layer.

A third CHF model proposed by Lee and Mudawwar [1988] for moderately subcooled flow conditions is based on the following assumptions:

- Vapour blankets are formed from small bubbles.
- The velocity of the vapour blanket is determined from the superposition

of the local liquid velocity and the relative vapour blanket velocity, determined by a balance between the buoyancy and drag forces exerted on the blanket.

- A dry-patch is formed after Helmholtz instability at the sublayer-blanket interface as shown in Figure 2.9. The length of the blanket is assumed equal to Helmholtz wavelength.
- CHF occurs when the rate of evaporation in the liquid sublayer exceeds that of the liquid entering the sublayer from the core region.

2.4.4 Subchannel Codes

Subchannel codes are computer programs that numerically solve for the thermal-hydraulic characteristics of a particular flow channel. The ASSERT (Advanced Solution of Subchannel Equations in Reactor Thermalhydraulics) code is an example of computer code developed at CRL for use in a nuclear rod bundle channel (the user manual is given by Judd *et al.* [1984]). ASSERT uses three CHF prediction methods and compares them against experimental data. One of the correlations used in ASSERT is the Westinghouse W-3 (i.e., Tong [1972]) correlation. The CHF look-up table of Groeneveld *et al.* [1986a] and the annular flow model developed by Whalley *et al.* [1974] are also tested in ASSERT.

2.4.5 CHF Fluid-to-Fluid Modelling

Performing CHF tests at typical nuclear reactor operating conditions is expensive and difficult. Hence, there is an increasing interest to use modelling fluids (Freons) to substitute for water. Since most of the prediction methods discussed before are for steam-water flow, a method is needed to relate water-steam systems to other fluids. Ahmad [1973] described one of the best known method, which uses dimensionless groups for scaling between the refrigerants and water systems. The modelling parameters in this scaling law are:

- $\left(\frac{L}{D}\right)$ for geometric similarity;

- $\left(\frac{\rho_\ell}{\rho_g}\right)$ for density ratio similarity;

- $\left(\frac{\Delta h_{in}}{h_{\ell g}}\right)$ for subcooling ratio similarity; and

- $\psi = \frac{G\,D_{hy}}{\mu_\ell}\left(\frac{\gamma^{1/2}\,\mu_\ell}{D_{hy}\rho_\ell}\right)^{2/3}\left(\frac{\mu_\ell}{\mu_g}\right)^{1/8}$ mass flux parameter similarity; where $\gamma = \frac{\partial\left(\frac{\rho_\ell}{\rho_g}\right)}{\partial P_{sat}}$.

If the above four dimensionless groups are the same in the two fluid systems, then the boiling number defined as, $BO = \frac{CHF}{G\,h_{\ell g}}$, is also the same for the two systems. Hence, the CHF can be obtained in any fluid system from another fluid system using these dimensionless groups.

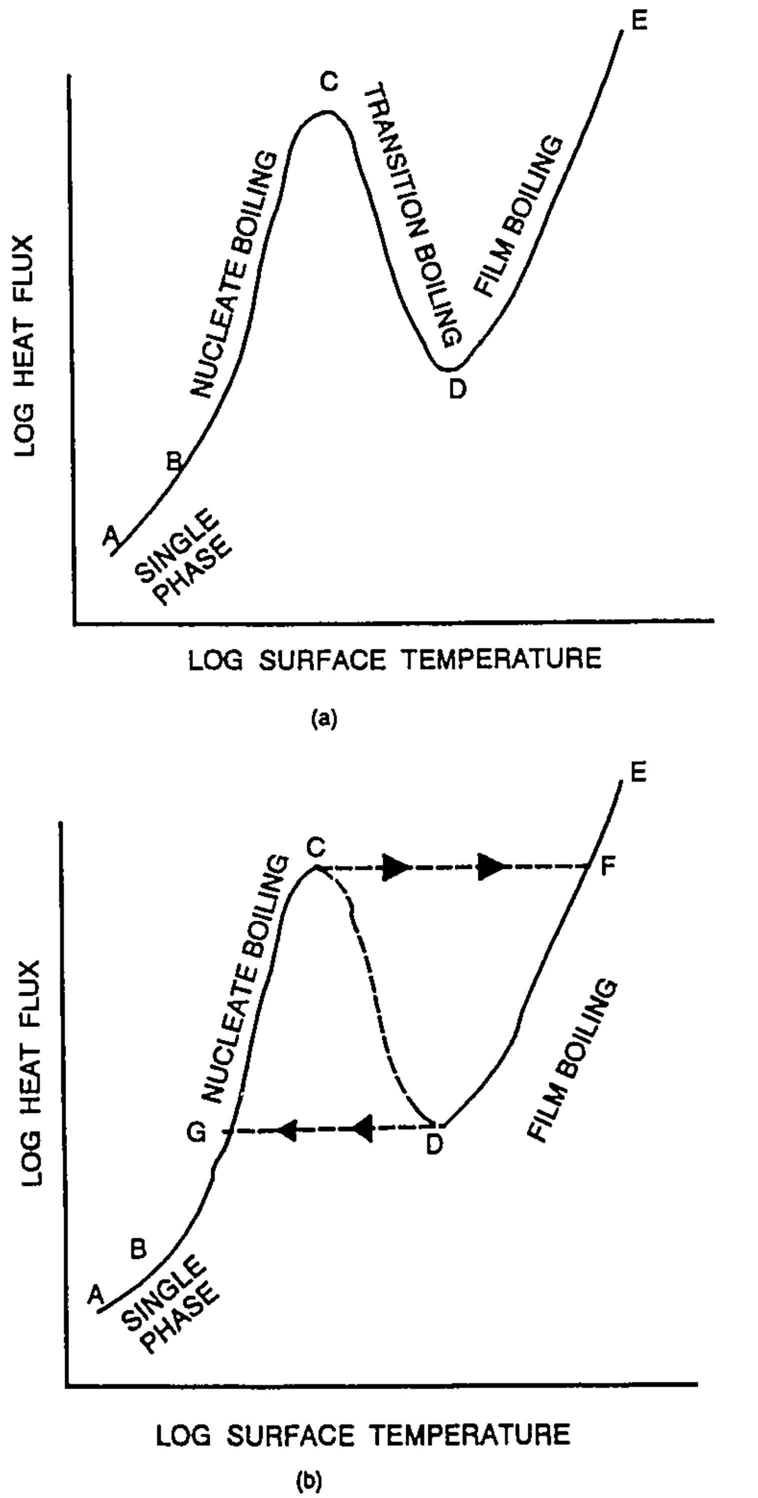

Figure 2.1: (a)- Pool Boiling Curve From a Temperature-Controlled Surface. (b)- Pool Boiling Curve From a Heat-Flux-Controlled Surface. From Macbeth [1968].

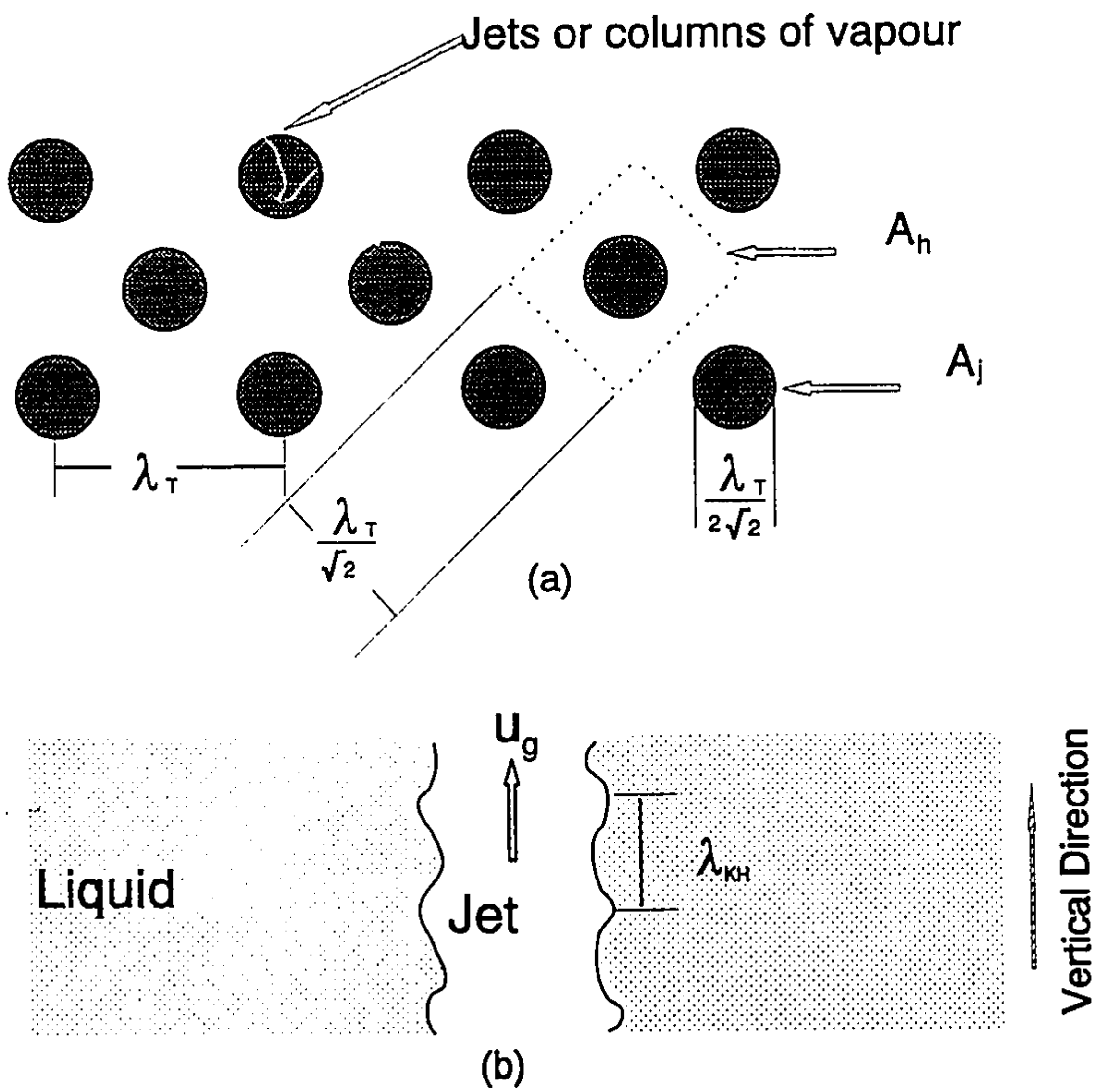

Figure 2.2: (a)- Vapour Jets Rising From a Flat Plate. (b)- Kelvin-Helmholtz Wavelength. From Whalley [1987].

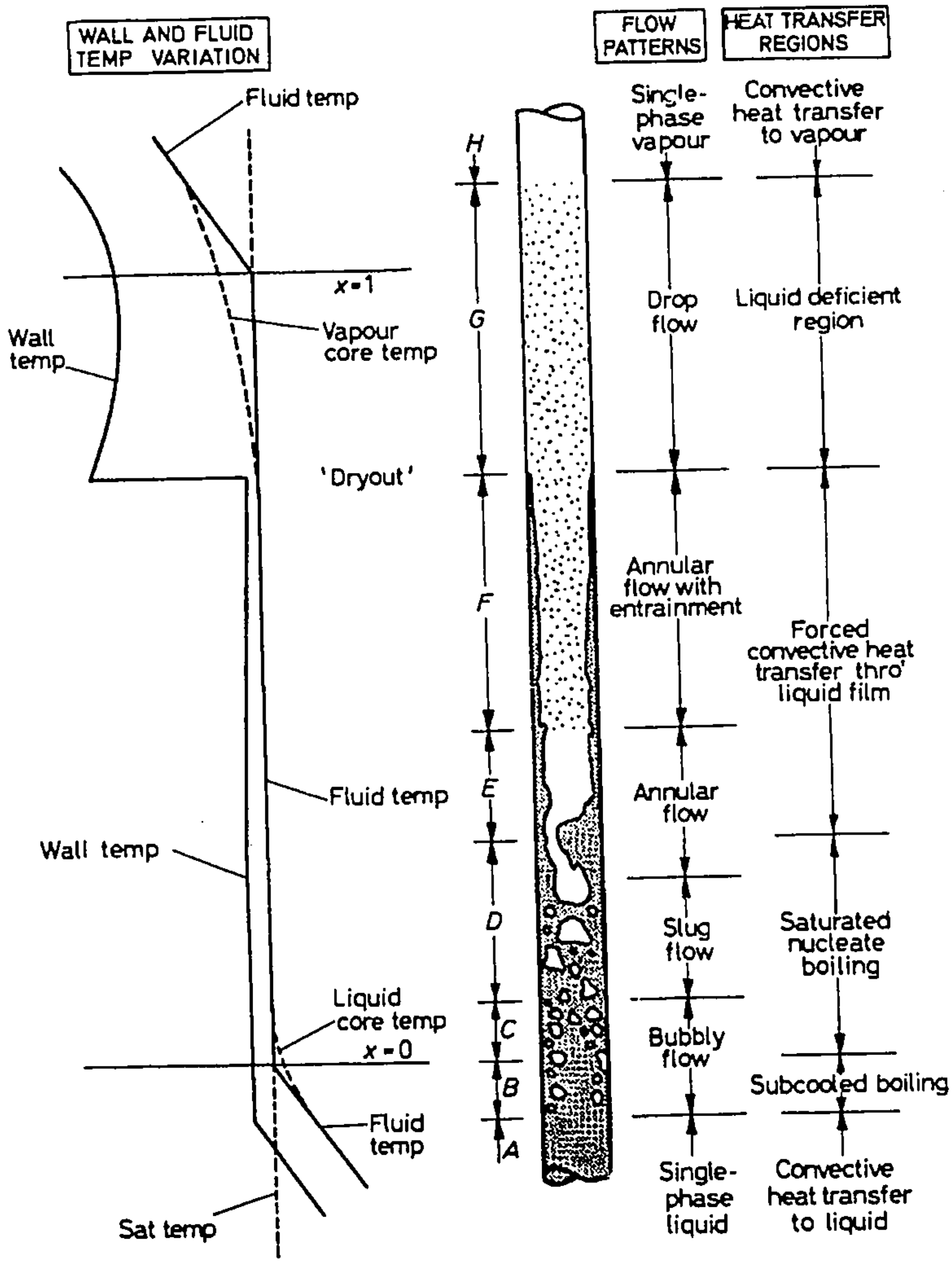

Figure 2.3: Heat Transfer Regions in Convective Boiling. From Collier [1981].

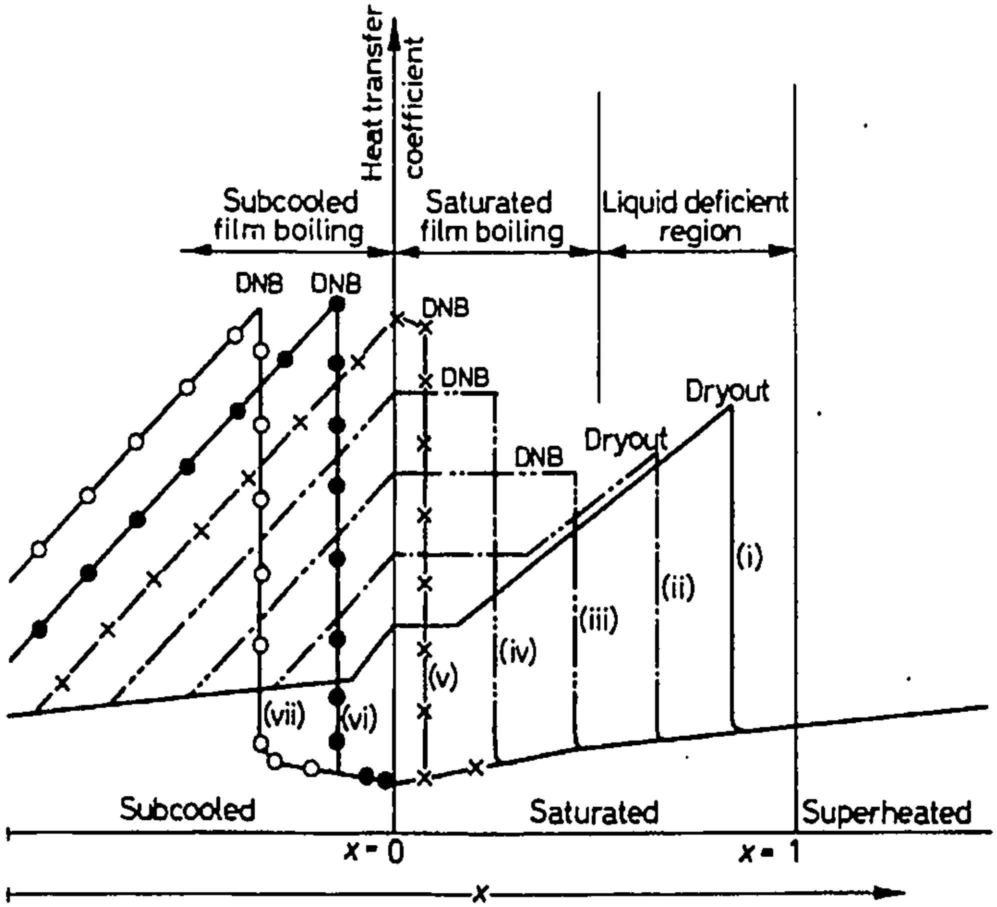

Figure 2.4: Variation of the Heat Transfer Coefficient With Quality With increasing Heat Flux as a Parameter. From Collier [1981].

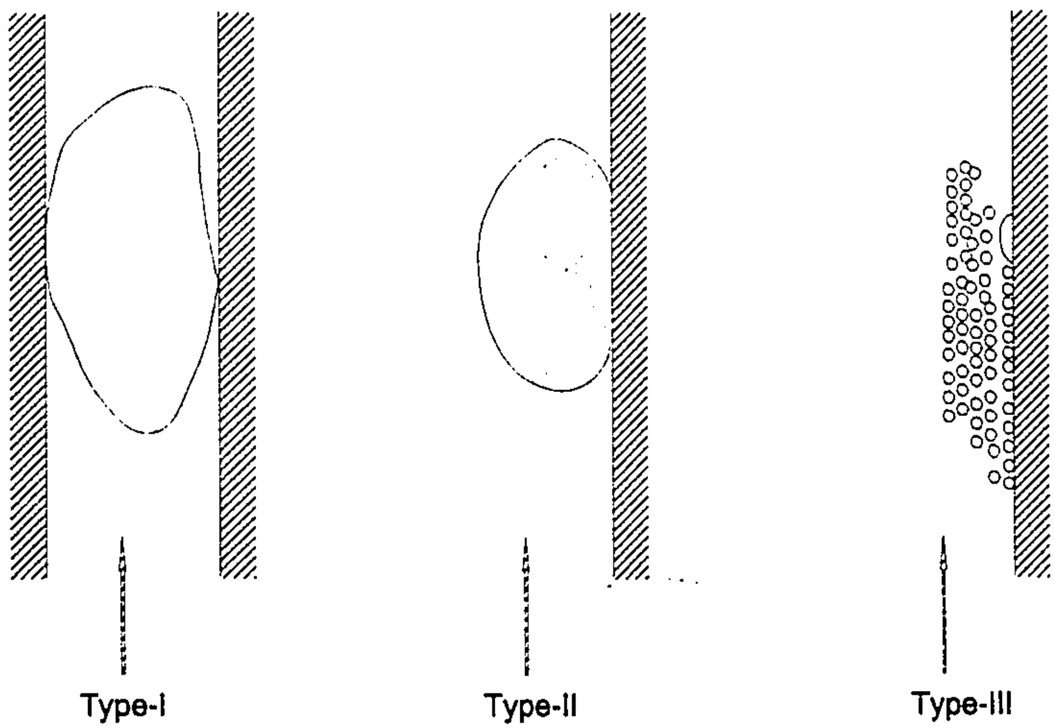

Figure 2.5: CHF Mechanisms in Forced Convective Boiling and Subcooled Conditions.

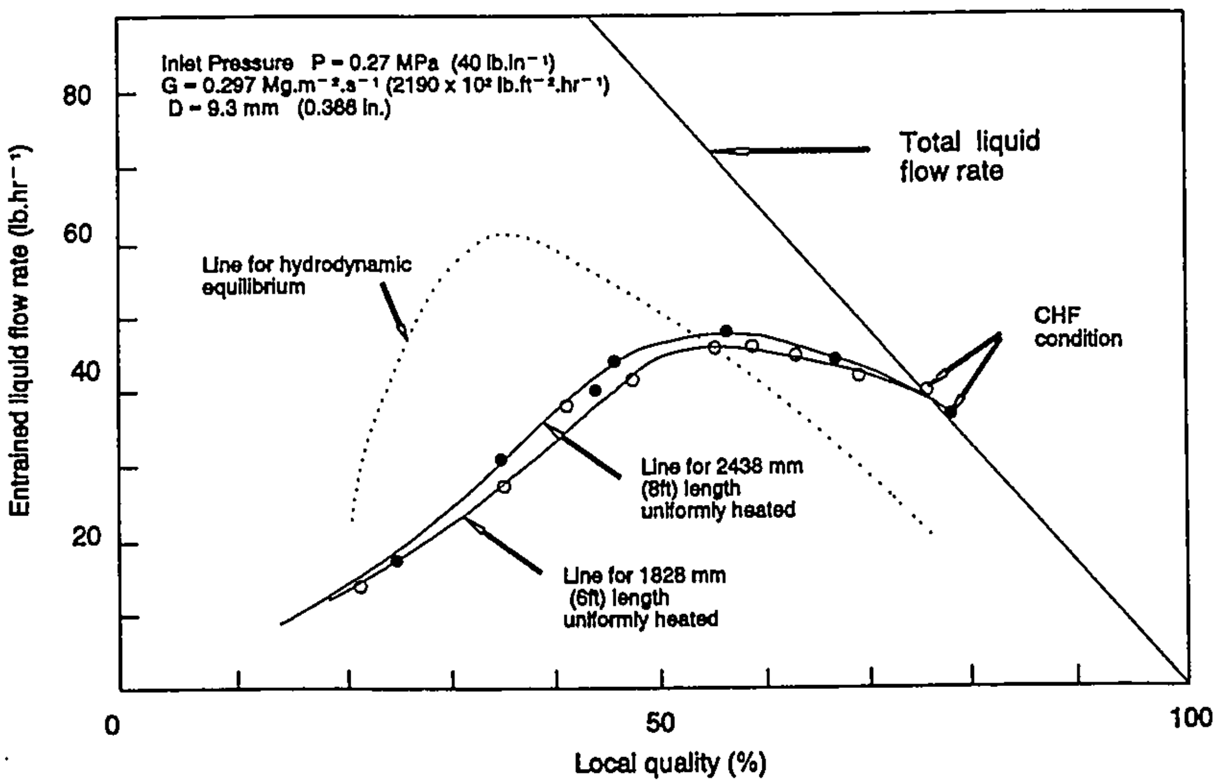

Figure 2.6: Entrainment Curves for Boiling in a Tube With Subcooled Water at the Inlet (the CHF Occurs at the Exit). From Hewitt and Hall-Taylor [1970].

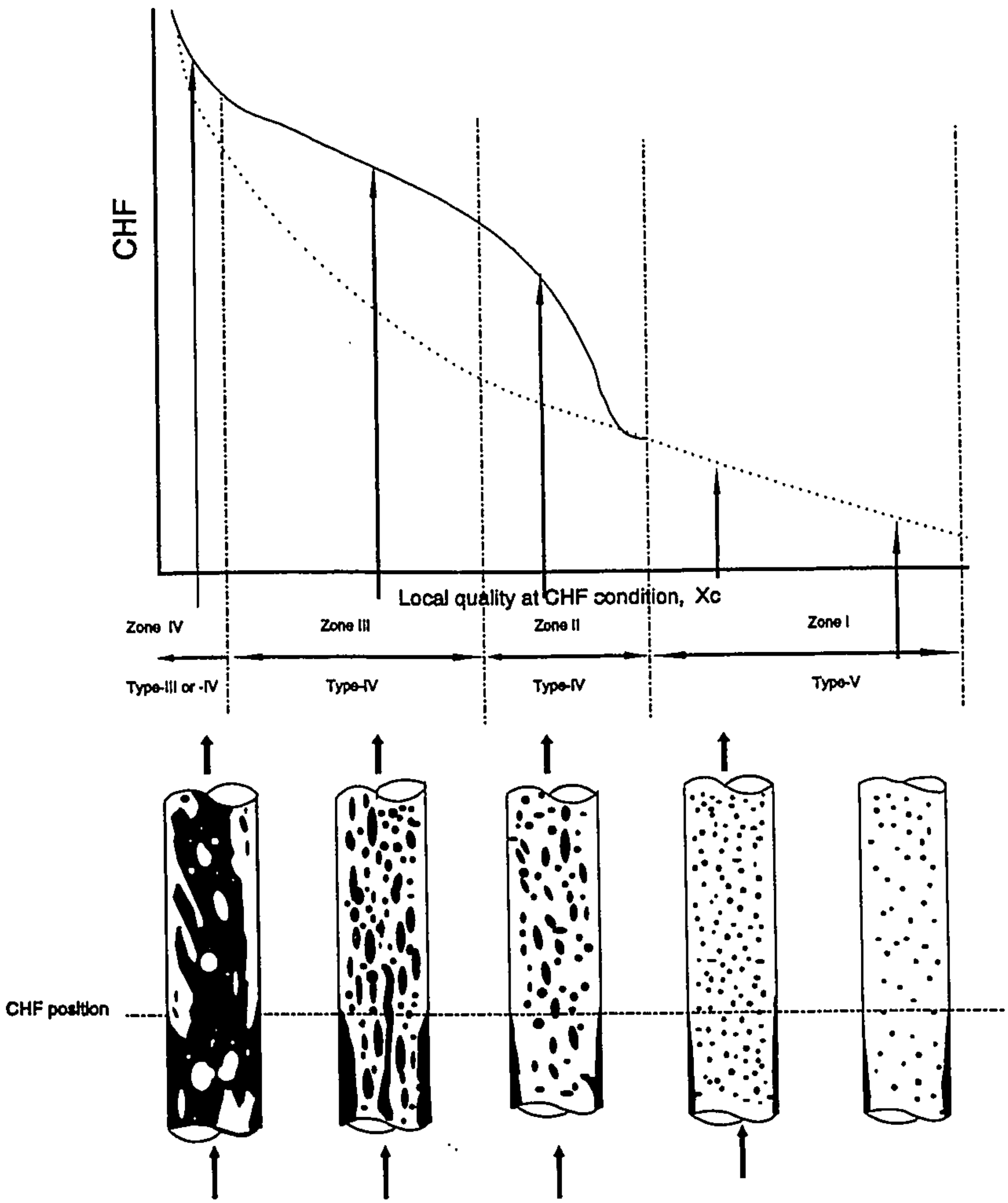

Figure 2.7: CHF Types in Forced Convective Boiling for Positive Qualities and for Uniformly Heated Tubes. From Hewitt and Hall-Taylor [1970].

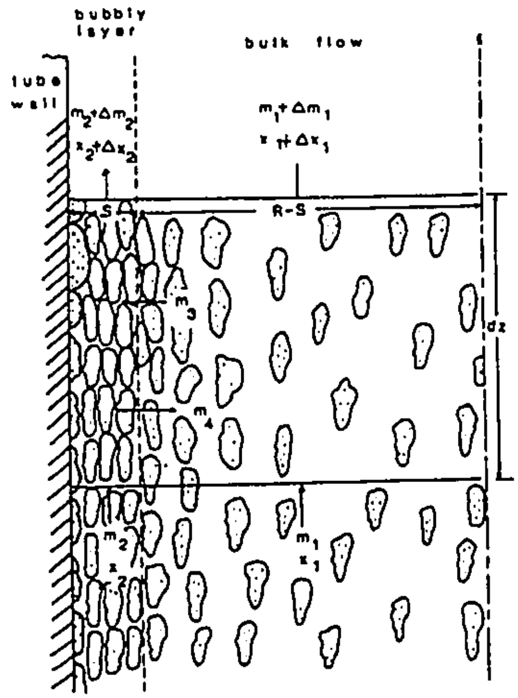

Figure 2.8: Schematic Diagram of Mass Transport Between Core and Bubbly Layer. From Weisman and Pei (1983).

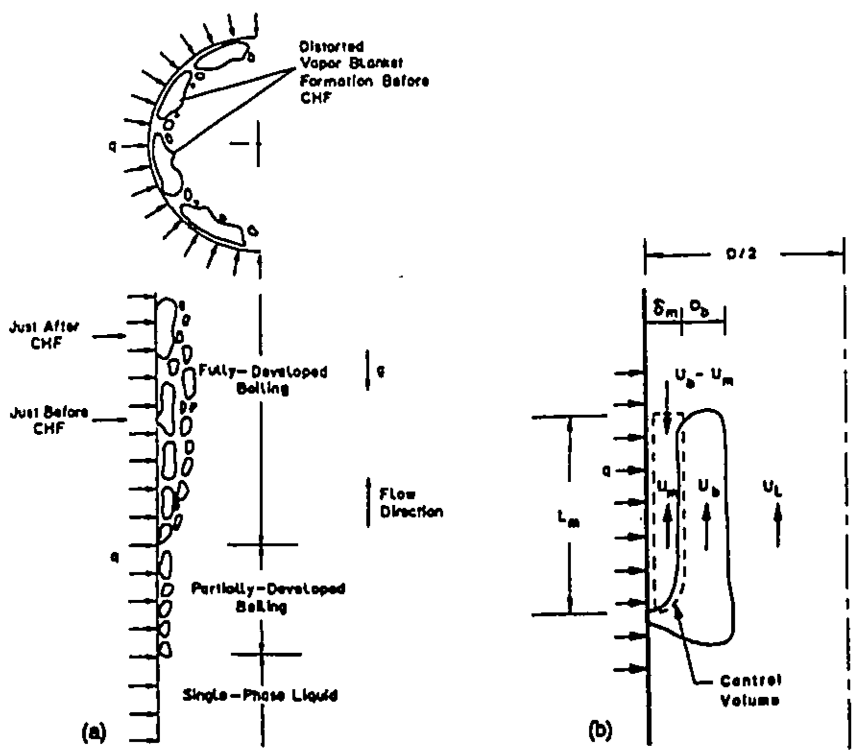

Figure 2.9: (a)- Subcooled Flow at High Pressure and Mass Velocity. (b)- Onset of Sublayer Dryout. From Lee and Mudawwar (1988).

3. TUBULAR GEOMETRIES

3.1 Observed Geometric Effects

Because of the importance of the tubular geometry in many industrial applications, a considerable amount of experimental CHF data is available for this geometry. For vertical, uniformly-heated tubes, the CHF occurs first at the outlet of the heated section in almost all cases. Thus, it can be postulated that the CHF for this simple test section is primarily a function of local exit conditions (local conditions hypothesis): pressure, mass flux, quality and diameter. It is agreed by most researchers that this assumption is true provided that the heated-length/diameter $\left(\frac{L}{D}\right)$ ratio is greater than 100. Figure 3.1 shows the breakdown of the local-conditions hypothesis for Freon 12 for low $\frac{L}{D}$ ratios. However, if $\frac{L}{D}$ > 100 the effect of heated length becomes negligible. The tube diameter, on the other hand, is shown to have a strong effect on the CHF (Figure 3.2): for dryout qualities greater than 0 (i.e., $X_c > 0$), the high CHF corresponds to a small tube diameter. Therefore, only the diameter is used to characterize the geometry effect for prediction methods based on local conditions.

Lee [1966] and Stevens *et al.* [1964] studies represent two of the few investigation that have focused entirely on the effect of tube diameter on the CHF. Their data indicate that the diameter effect on CHF becomes important only for small diameters. However, their data were not obtained for constant local CHF conditions which makes it difficult to interpret their results.

Bergles [1963] showed that, for constant outlet subcoolings and at low pressures, the CHF was lower for a large-diameter than a small-diameter tube. The diameter effect becomes more important as the tube diameter decreases. The diameter effect becomes less important at large diameter. Bergles *et al.* [1967] results strengthen the previous conclusions; they found that increasing the diameter by 4.15 mm (from 2 mm to 6.15 mm) results in 40% reduction in CHF at the same critical quality (25%). Similar Conclusions have been reached by Ornatskiy [1969a] who also indicated that the CHF approached approximately a constant value (depending on the mass flux) for large tube diameters.

Becker [1967] presented ratios of $CHF_D/CHF_{D=10\ mm}$ for various values of tube diameter at high-pressure. These ratios decrease with increasing diameter as shown in Table 3.1. Boltienko *et al.* [1988] obtained CHF data with 3 different tubes of 8-, 16- and 20-mm diameter using Freon as a coolant. Boltienko *et al.* [1988] concluded that the diameter effect on CHF depends on the dryout region or the CHF type: the CHF increased at the low-quality region (less than 0.2) as the tube diameter increases, however the CHF decreased at the high-quality region. Boltienko *et al.* [1989] used Equation (3.1) to correct for the diameter effect with a variable exponent, n. The exponent, n, varies for various pressure, mass flux and outlet quality as shown in Figure 3.3. This also means that this exponent, n, varies with CHF type as indicated in Table 3-1.

3.2 Prediction of Diameter Effect

CHF correlations have generally a limited range of application (only within the ranges of their data bases). Extrapolation to conditions far beyond these rHxges often leads to meaningless predictions (e.g., negative CHF predictions or high CHF values at qualities close to 100%), because of incorrect asymptotic trends. To overcome this problem, Doroshchuk *et al.* [1975] proposed the first CHF look-up table, which was a significant improvement over the CHF correlation approach, but did not cover all conditions of interest. Groeneveld *et al.* [1986a] ensured that the correct asymptotic and parametric trends were maintained at all conditions when they expanded the CHF look-up table approach of Doroshchuk *et al.* [1975] to a wider range of conditions. Their CHF table (see Table 3-2) provides a better accuracy in prediction and permits extrapolation outside the data base. Recently, Kirillov *et al.* [1989] improved Doroshchuk's CHF table with a larger data base, but the ranges of application remain narrower than those of Groeneveld's table.

Doroshchuk's, Kirillov's and Groeneveld's CHF tables are derived for an 8-mm tube with vertical flow. Correction factors have been suggested by these authors to account for the diameter effect. They are expressed in the form of

$$\frac{CHF_D}{CHF_{D=8}} = \left(\frac{8}{D} \right)^n \qquad (3.1)$$

where D is the tube diameter in mm. Table 3.1 presents the different recommended values of the exponent, n. These exponents are optimized, and are based on large CHF data banks. It may well be that the exponent, n, is also a function of pressure, mass flux, dryout quality and diameter. For example, the exponent for the diameter term in the Biasi correlation (Biasi *et al.*

[1967]) is 0.6 for a tube of diameter less than 10 mm, and 0.4 otherwise. Another example, is given by Boltienko *et al.* [1989] who presented the exponent, n, in a three dimensional plot as a function of quality and mass flux for P = 17.7 MPa (Figure 3.3). In view of the complexity involved to account for the diameter effect on CHF (could be the topic of a separate study), a simplified approach based on the form of correction factor as presented in Equation (3.1) is still recommended. A value of 1/3 is currently used in conjunction with the AECL-UO look-up table (Groeneveld *et al.* [1986a]).

Table 3.1: Prediction Methods of the Diameter Effect on CHF in Tubes

<table>
<tr><th>Prediction Methods</th><th>References</th><th>Comments</th></tr>
<tr><td>

$$\frac{CHF_D}{CHF_{D=8mm}} = \left(\frac{8}{D}\right)^{1/3} \quad for\ 4 < D < 16\ mm$$

</td><td>Groeneveld <u>et al.</u> [1986a]</td><td>For D > 16 mm this correction factor is eqaul to 0.79.</td></tr>
<tr><td>

$$\frac{CHF_D}{CHF_{D=8mm}} = \left(\frac{D}{8}\right)^{n} \quad n=f(P,G,X)$$

The values of n are given in the following table:

<table>
<tr><th>Pressure (MPa)</th><th>Type-II CHF</th><th>Type-III CHF</th><th>Type-IV or -V CHF</th></tr>
<tr><td>$1 < P \le 6$</td><td>0.188</td><td>-0.068</td><td>-0.266</td></tr>
<tr><td>$6 < P < 15$</td><td>0.263</td><td>-0.164</td><td>-0.197</td></tr>
<tr><td>$15 \le P \le 20$</td><td>0.418</td><td>-</td><td>-0.163</td></tr>
</table>

</td><td>Boltienko <u>et al.</u> [1989]</td><td>The exponent, n, varies with the CHF type. Fixing the pressure, the exponent, n, is determined from a three-dimensional diagram as shown in Figure 3.3.</td></tr>
<tr><td>

$$\frac{CHF_D}{CHF_{D=8mm}} = \left(\frac{8}{D}\right)^{1/2}$$

</td><td>Doroshchuk <u>et al.</u> [1975]</td><td>Valid for 4 < D <16 mm for ΔT_{sub}< 75°C and burnout of the first kind (not very high qualities).</td></tr>
<tr><td>

$$\frac{CHF_D}{CHF_{D=8mm}} = 1 + \frac{q_o}{CHF_{D=8}}\left(\sqrt[3]{\frac{8}{D}}-1\right)$$

</td><td>Doroshchuk <u>et al.</u> [1970]</td><td>Valid for positive qualities only; q_o=f(P).</td></tr>
<tr><td>

$$\frac{CHF_D}{CHF_{D=10mm}} = \left(\frac{10}{D}\right)^{n} \quad \begin{matrix} n=0.4\ if\ D > 10mm \\ n=0.6\ if\ D < 10mm \end{matrix}$$

</td><td>Biasi <u>et al.</u> [1967]</td><td>Ranges: D = 3-37.5 mm, P = 270-14000 kPa, G = 100-6000 $kg.m^{-2}.s^{-1}$ and $\frac{1}{1+\frac{\rho_l}{\rho_g}} < x < 1.0$</td></tr>
<tr><td>

$$\frac{CHF_D}{CHF_{D=10mm}} = f(D)$$

<table>
<tr><td>D</td><td>4</td><td>6</td><td>8</td><td>10</td><td>12</td><td>14</td><td>18</td><td>24</td><td>25</td></tr>
<tr><td>f</td><td>1.18</td><td>1.176</td><td>1.085</td><td>1.00</td><td>0.973</td><td>0.962</td><td>0.94</td><td>0.917</td><td>0.90</td></tr>
</table>

</td><td>Becker [1967]</td><td>Ranges: D = 4-25 mm, P = 270-10000 kPa, G = 120-5400 $Mg.m^{-2}.s^{-1}$, X = 0-0.5.</td></tr>
</table>

Table 3.2: Sample of the CHF Look-Up Table of Groeneveld *et al.* [1986a] for Light Water in 8-mm Tube (CHF in $kW.m^{-2}$ and G in $kg.m^{-2}.s^{-1}$).

P	G	Thermodynamic Quality, X																				
kPa		-.50	-.40	-.30	-.20	-.15	-.10	-.05	.00	.05	.10	.15	.20	.25	.30	.40	.50	.60	.70	.80	.90	1.00
3000	0				5971	4820	3700	2774	1450	277	262	248	233	219	204	175	146	117	87	58	29	0
3000	50				6044	4955	4000	3094	2313	1794	1641	1562	1483	1405	1326	1244	1044	650	600	574	571	0
3000	100				6099	5000	4100	3200	2600	2300	2100	2000	1900	1300	1200	1109	800	767	750	750	516	0
3000	200				6193	5200	4300	3400	2800	2500	2300	2150	1400	1297	1200	1180	1100	1000	1000	1000	514	0
3000	300				6278	5400	4450	3500	3000	2700	2400	2200	2150	2100	2000	1829	1497	904	417	400	350	0
3000	500				6433	5600	4650	3700	3150	2900	2500	2400	2300	2250	2226	1759	1388	659	250	200	200	0
3000	750				6610	5800	4850	3900	3300	3000	2650	2500	2314	2159	1818	1590	1463	1000	600	450	300	0
3000	1000				6775	6000	5000	4000	3400	3000	2600	2500	2134	1939	1800	1700	1600	1000	600	450	300	0
3000	1500				7083	6200	4600	3800	3300	3000	2600	2500	2350	2169	1800	1700	1500	1000	600	450	300	0
3000	2000				7370	6400	4500	4000	3500	3000	2600	2500	2150	2050	1800	1700	1400	1000	600	450	300	0
3000	3000				7905	7000	5742	4287	3900	3000	2600	2500	2150	2050	1800	1700	1400	1000	600	450	300	0
3000	4000				8600	8500	6411	4800	4500	3000	2600	2500	2150	2050	1800	1700	1400	1000	600	450	300	0
3000	5000				8880	6607	6120	5267	4845	3000	2600	2500	2150	2050	1800	1700	1400	1000	600	450	300	0
3000	7500				9990	6990	6465	5581	5077	3000	2600	2500	2150	2050	1800	1700	1400	1000	600	450	300	0
4500	0				5631	4650	3667	2683	1700	325	308	291	274	257	240	205	171	137	103	68	34	0
4500	50				5712	5063	4292	3296	2975	2481	2327	2248	2168	2014	1860	1551	1067	535	500	500	450	0
4500	100				5772	5200	4500	3500	3400	3200	3000	2900	2800	2600	2400	1160	900	870	850	800	504	0
4500	200				5877	5600	4700	3600	3500	3200	2900	2800	1600	1463	1400	1400	1376	1300	1200	1181	569	0
4500	300				5971	4592	3324	3300	3250	3200	2800	2700	2600	2500	2400	2176	1785	1043	438	400	362	0
4500	500				6142	4634	3367	3300	3250	3200	2700	2600	2600	2600	2500	1946	1341	811	200	200	200	0
4500	750				6338	6000	5000	3900	3800	3200	2800	2700	2586	2475	2402	1526	868	490	418	250	200	0
4500	1000				6521	6200	5200	4000	3900	3200	2600	2500	2395	2208	2100	1800	1500	1200	700	400	200	0
4500	1500				6862	6400	4154	4100	4000	3200	2600	2600	2538	2360	2100	1800	1500	1200	700	400	200	0
4500	2000				7180	6600	4300	4200	4100	3200	2600	2500	2294	2200	2100	1800	1500	1200	700	400	200	0
4500	3000				8000	7778	5690	4800	4706	3200	2600	2500	2294	2200	2100	1800	1500	1200	700	400	200	0
4500	4000				8600	8443	6302	4518	4400	3200	2600	2500	2294	2200	2100	1800	1500	1200	700	400	200	0
4500	5000				8852	5419	4851	3967	3525	3200	2600	2500	2294	2200	2100	1800	1500	1200	700	400	200	0
4500	7500				10082	5816	5198	4236	3630	3200	2600	2500	2300	2200	2100	1800	1500	1200	700	400	200	0
7000	0				5363	4540	4222	2000	1968	380	360	340	320	300	280	240	200	160	150	120	110	0
7000	50				5454	5035	4627	2330	2250	2195	2115	2035	1993	1950	1870	1860	1625	600	550	543	500	0
7000	100				5522	5200	4100	3400	2900	2800	2700	2600	2550	2200	2000	1500	1123	1112	984	908	595	0
7000	200				5639	5600	4150	3400	3000	2800	2600	2550	2500	2200	1700	1600	1500	1400	1306	890	595	0
7000	300				5745	4145	2896	2850	2825	2800	2600	2500	2450	2400	2400	2300	2161	1583	755	447	408	0
7000	500				5939	4187	2939	2900	2850	2800	2600	2400	2400	2400	2300	2245	1784	1123	451	250	236	0
7000	750				6159	6000	4300	3400	3100	2800	2600	2300	2150	2000	1900	1355	879	707	467	350	316	0
7000	1000				6365	6200	4400	3400	3200	2800	2600	2100	1966	1786	1200	700	606	593	500	300	200	0
7000	1500				6749	6400	4145	3060	3000	2800	2600	2100	2086	1500	1000	700	665	600	500	300	200	0
7000	2000				7108	6600	3521	3400	3300	2800	2600	2100	1800	1500	1200	1100	1000	700	500	300	200	0
7000	3000				7775	7500	5752	4146	3716	2800	2600	2200	1800	1500	1200	1100	1000	700	500	300	200	0
7000	4000				8399	8000	6210	4292	4076	2800	2600	2200	1800	1500	1200	1100	1000	700	500	300	200	0
7000	5000				8991	6619	6002	5440	3500	2800	2600	2200	1900	1500	1200	1100	1000	700	500	300	200	0
7000	7500				10376	6878	6271	5707	3600	2800	2600	2200	2000	1500	1200	1100	1000	700	500	300	200	0
10000	0			6548	5153	4482	4264	2059	1488	448	424	401	377	354	330	283	236	189	97	72	70	0
10000	50			6652	5260	5021	4669	2488	2300	2212	2056	1825	1594	1363	1133	971	809	500	450	404	400	0
10000	100			6730	5339	5200	4200	3500	3000	2800	2600	2300	2000	1700	1400	1200	1000	830	820	816	578	0
10000	200			6865	5477	5300	4250	3600	3200	3000	2900	2700	2600	2500	2200	2000	1800	1700	1403	913	649	0
10000	300			6986	5601	5400	4300	3700	3400	3000	2900	2700	2600	2550	2500	2500	2500	1892	1093	628	533	0
10000	500			7208	5827	5700	4400	3800	3500	3000	2900	2800	2700	2650	2600	2600	2568	1360	644	385	353	0
10000	750			7460	6085	6000	4600	3900	3600	3000	2700	2600	2500	2400	2300	2284	1398	680	450	426	420	0
10000	1000			7696	6326	6200	5060	4094	3600	3000	2800	2700	2700	2695	1600	1595	914	467	260	250	200	0
10000	1500			8136	6775	6400	4991	4025	3600	3000	2500	2400	2300	2284	1200	1166	745	259	199	175	150	0
10000	2000			8547	7195	6600	5200	4400	3600	3000	2500	2200	1800	1500	1300	1300	900	250	200	200	150	0
10000	3000			9312	7976	6800	5400	4600	3600	3000	2500	2200	1800	1500	1300	1200	900	250	200	200	150	0
10000	4000			10026	8705	7000	5600	4800	3600	3000	2500	2200	1800	1500	1300	1200	900	250	200	200	150	0
10000	5000			10705	9397	7200	5800	4900	3600	3000	2500	2200	1900	1500	1300	1200	900	250	200	200	150	0
10000	7500			12294	11018	7400	6000	5000	3600	3000	2500	2200	2000	1600	1300	1200	900	250	200	200	150	0

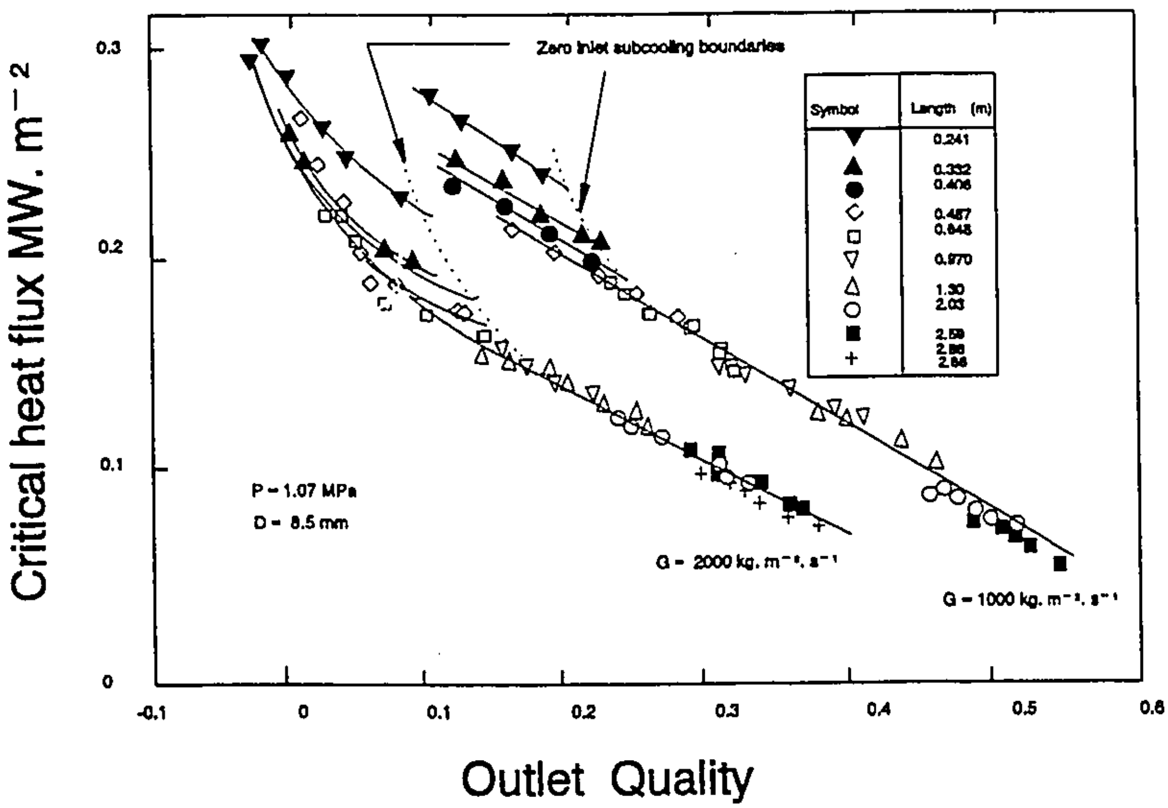

Figure 3.1: Breakdown of the Local Conditions Hypothesis for Freon-12 CHF Data. From Collier (1981).

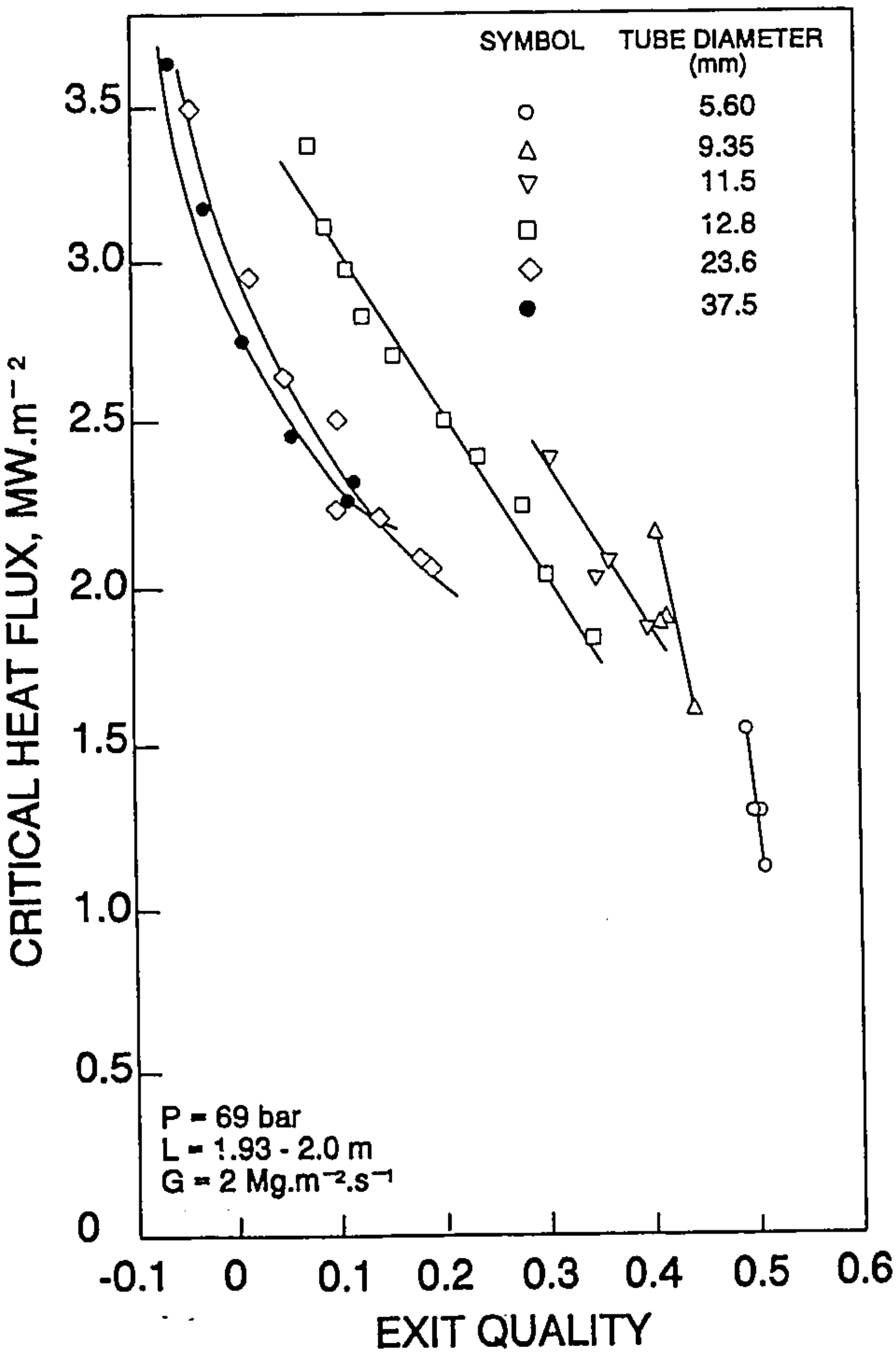

Figure 3.2: Effect of Diameter on CHF in Tube at Constant Dryout-Quality Conditions. From Collier [1981].

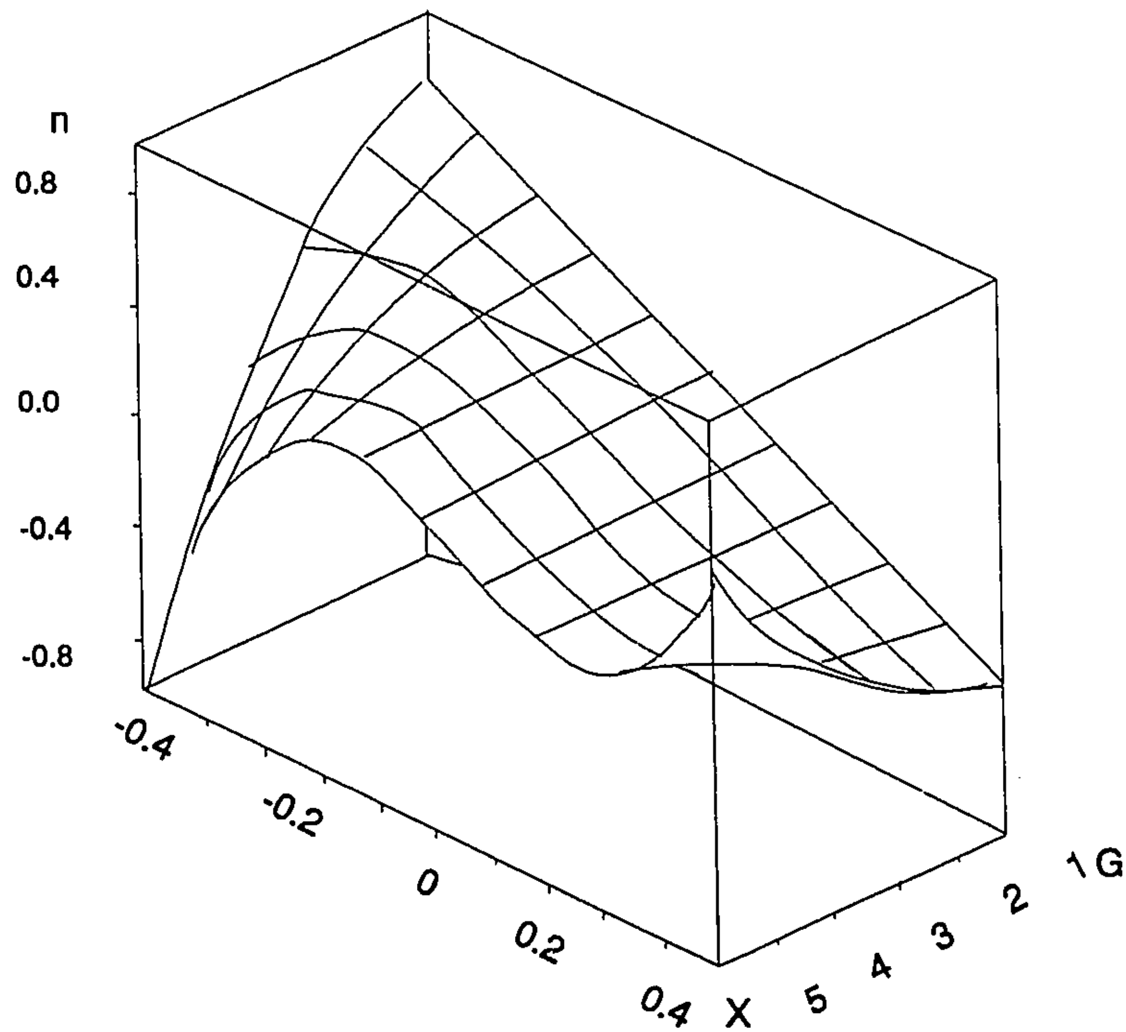

Figure 3.3: Dependence of the Exponent of Equation (3.1) on Mass Flux and Outlet Quality at P = 17.7 MPa (G in $Mg.m^{-2}.s^{-1}$). From Boltienko *et al.* [1989].

4. OBSERVED GEOMETRIC EFFECTS IN CONCENTRIC ANNULI

4.1 General

This chapter deals with various observations made from experiments performed in centrally heated annuli. It includes an examination of the effects of surface curvature and gap size. Table 4.1 gives a brief summary of the observed CHF trends in annuli. It also specifies the range of operating conditions and the details of the test-section geometries. Appendix A lists some of the CHF data for concentric annuli. In general, the CHF in an annulus is considerably lower than that in tubes, especially for annuli with narrow gaps for the same local conditions.

4.2 Effect of Gap Size on CHF

Janssen *et al.* [1963] compared CHF data sets obtained in annuli with different gap sizes. They noted that for 6.4 mm $\leq D_{hy} \leq$ 12.7 mm, the hydraulic diameter, D_{hy}, has little effect on the CHF. However, Figure 4.1 (Moeck *et al.* [1966]) shows that, at a constant mass flux and exit quality, the CHF increases as D_{hy} is increased from 2 mm to about 7.5 mm, and decreases as D_{hy} is increased further. This increasing trend agrees also with results obtained by Janssen *et al.* [1963] for D_{hy} less than 6.4 mm. Alvensleben *et al.* [1963] obtained CHF data for D_{hy} of 16 mm; his results are also shown in Figure 4.1.

In the case of externally heated annuli, Tolubinskiy *et al.* [1969] found that the effect of mass flux on CHF varies with gap size according to:

$$CHF \propto G^n \tag{4.1}$$

where the exponent n depends on the gap size, δ. For 0.1 mm $\leq \delta \leq$ 1.3 mm

$$n = 0.6\,[\tanh \delta]^{1/2} \tag{4.2}$$

The reduction in mass-flux effect is apparently due to a decrease of turbulence and the transverse fluctuations when the gap is reduced. Tolubinskiy stated that the CHF increases as the gap increases from 0.1 to 1.3 mm at constant critical quality. For δ greater than 1.3 mm, the gap-size effect almost vanishes. However, Tolubinskiy only performed tests at subcooled conditions with a test section having a short heated length (less than 150 mm), thus undeveloped flow conditions could have affected his results.

In a later study, Tolubinskiy *et al.* [1970a] found that, for internally heated annuli, increasing the gap size from 0.5 to 4.0 mm resulted in an increase in CHF. Although not clearly specified, it seems that this conclusion is for Type-II CHF (nucleation induced) or Type-III CHF (bubble clouding). Tolubinskiy expressed the gap-size effect on CHF by varying the exponent, n, in Equation (4.1) from 0.2 at δ = 0.5 mm to 0.6 at δ = 4.0 mm (a possible explanation is that the Reynolds number, Re (defined as $Re=(G\,\delta)/\mu$), increases with δ: higher values of Re corresponds to higher flow turbulence, better bubble removal and hence higher CHF). In both studies by Tolubinskiy, the length was very short, the mass flux was low, and the flow was subcooled.

Tolubinskiy *et al.* [1970b] concluded that with the increase of gap size from 0.5 mm to 1.5 mm, the CHF increases. Moreover, when the concentric gap size is more than 1.0 mm, the increase in the CHF is insignificant. A further increase in gap size beyond 1.5 mm results in no effect on CHF.

Ornatskiy [1969a] reached similar conclusions as Tolubinskiy *et al.* [1969, 1970a]. As the gap width of the annular channel is increased from 0.1 mm to 1-2 mm, the CHF increases. No effect on CHF was observed for larger gaps. Ornatskiy also observed that the gap-size limit (for which a further increase in the annular gap does not affect the CHF) increases with a decreasing pressure. However, his conclusions are based only on short L/D_{hy} (10 to 100) experiments in subcooled-water flow at high pressures (i.e., for Type-II (nucleation induced) or Type-III (bubble clouding) CHF). Ornatskiy *et al.* [1966] found no effect of gap size on CHF for the range of 1 to 2 mm gap size at 14.7 MPa and for G = 1.0 and 2.0 $Mg.m^{-2}.s^{-1}$ (Figure 4.2). Thus, for this pressure, increasing the gap size increases the CHF up to a gap size of 1 mm.

Hung and Yao [1983] observed the boiling behaviour of Freon-113 in an annulus with a quartz outer tube near the CHF condition. For a gap size of 2.58 mm, bubbles became large and slightly deformed when the heat flux was gradually increased to the CHF. When the gap size was reduced to 0.8 mm, bubbles started out spherical and, as they grew, they were squeezed due to the narrow gap between opposite walls. The flattened bubbles hence coalesced and formed vapour plugs. The thin liquid film between the vapour plug or bubble and the heated surface (microlayer) easily evaporated, causing the CHF to occur prematurely. A further reduction in gap size to 0.32 mm deformed the bubbles even more, leading to more coalescence and resulting in a further reduction in CHF. Hung and Yao [1983] concluded that the CHF decreased with a reduction in gap size for gaps less than 1.5 mm. The results of the tests performed by Hung and Yao [1983] are shown in Figure 4.3.

In conclusion, the CHF decreases as the gap is reduced below a particular gap size "δ_1" at constant local conditions. This particular gap size, δ_1, is dependent on the flow conditions and CHF type: different values of δ_1 have been quoted by various experimenters. Moreover, some authors (e.g., Janssen *et al.* [1963]) concluded that, when $\delta > \delta_1$, there is a range of gap sizes ($\delta_1 < \delta < \delta_2$) for which the CHF remains unaffected by gap size, while for $\delta > \delta_2$ the CHF will decrease with an increase in gap size. This increasing and decreasing trend is clearly illustrated in Figure 4.1. Note that the CHF trend for $\delta > \delta_2$ agrees with the observed trend in tubes, where an increase in D_{hy} also results in a decrease in CHF.

4.3 Discussion

A comparison of CHF data in annuli and tubes for the same local conditions shows that the CHF in a centrally heated annulus is generally lower. An explanation was presented by Tong [1972] who reported that, "a thick, cold liquid film is usually built up along an unheated wall, but it cannot be used to cool the heating surface. The liquid velocity in the cold film is therefore considered wasted or bypassed".

The differences in the D_{hy}-effect on CHF between tubes and annuli for small D_{hy} values were explained by Tolubinskiy [1969] as follows: "in boiling in cylindrical channels of small diameters, the accumulation of vapour bubbles and appearance of vapour plugs leads to an increase in the flow velocity in the blocked cross section; then, the stream pushes out the accumulated vapour and carries it away. The effect strengthens with a decrease in tube diameter. In annular channels, however, the accumulation of vapour bubbles and vapour plugs leads to blocking only some portion of the cross section between two walls and the liquid can move in the vapour-free cross section. Decrease of the gap width creates conditions which favour vapour locking of the cross section and, consequently, assist in the blocking of a part of the heating surface by a vapour film, thus decreasing the critical heat load". Tolubinskiy's explanation applies only to DNB-type CHF (Type-II or -III). No reference was made to the occurrence of this phenomenon at higher qualities, where the CHF mechanism is different.

Moeck *et al.* [1966] suggested two possible mechanisms to interpret the gap effect on CHF; one possibility is that, when reducing the gap size and keeping the same local conditions, the interfacial shear stress on the heated wall will increase. This increase in shear stress reduces the liquid-film flow rate by increasing the entrainment rate. A second possibility is that for narrow gaps, the 'roll' surface waves from the liquid film of the unheated wall will interact with the liquid film of the heated wall, thus increasing entrainment and reducing the CHF. This effect becomes negligible for large gap sizes. The above two mechanistic interpretations apply primarily for the entrainment-controlled film dryout (Type-IV CHF). However, the range of conditions covered by the experimental data also includes Type-III CHF (bubble clouding). For CHF of Type-II (nucleation induced) or Type-III (bubble clouding), decreasing the gap will reduce in the gap region the effect of flow turbulence and its transverse fluctuations, resulting in poor mixing and hence a lower CHF. These three interpretations support the behaviour shown in Figure 4.1 for gaps less than 0.8 mm. In this range a reduction in the hydraulic diameter, D_{hy}, results in CHF decrease. For D_{hy} greater than 0.8 mm the observed trend for annuli becomes similar to the tube that is the CHF decreases with increasing D_{hy}.

Hung and Yao's observations show that, for narrow gaps, the Type-I CHF can be encountered especially if bubble size is relatively large and is of the same order of magnitude as the gap size. Here again, the decrease occurs with a reduction in gap size. Thus, for all types of CHF, a reduction in CHF is expected for small gap sizes, especially within the range of 0 to 3 mm.

4.4 Recommended Prediction Method

Table 4-2 presents some of the CHF correlations for annuli available in the literature. Correlations by Tong [1972] and Tolubinskiy *et al.* [1969] have a relatively narrow application range and cannot be applied to CANDU conditions of interest. However for their correlations Barnett [1966] and Katto [1979] claimed a wide range of applicability.

Figure 4.4 shows examples of the comparison between Barnett's, Katto's correlations, AECL-UO look-up table predictions and experimental CHF data in annuli. All the experimental results used in this comparison came from Barnett [1966, 1968] data. Hence, Barnett's correlation fits best the experimental data, however it shows erroneous asymptotic trend (predicts negative CHF at high qualities). Katto's correlation does neither show good agreement with the experimental data nor the correct asymptotic trends. Figure 4.5 indicates a strong L/D_{he} effect for the above correlation, however experimental results (well represented by Barnett's correlation) did not reveal such strong effect. From Figure 4.4 it is also clear that CHF predictions from AECL-UO look-up table for tubes for the heated or hydraulic equivalent diameter and for an 8-mm tube will not satisfactorily predict the annuli CHF data.

To ensure a correct asymptotic trend, it was decided to predict the CHF using the 8-mm tube look-up table as a reference and apply a gap size and quality correction factors as follows:

(i) Quality correction factor, K_X: Figure 4.6 shows that as the quality increases the discrepancy between the CHF in annuli and the corresponding value from the AECL-UO CHF look-up table for an 8-mm tube increases as the quality increases. The following expression represents the quality correction factor:

$$K_X = \begin{cases} 1.0 & \text{for } X < -0.15 \\ 0.7942 - 1.375\,X & \text{for } -0.15 < X < 0.36 \\ 0.3 & \text{for } X > 0.36 \end{cases} \qquad (4.3)$$

This equation fits the 113 data points having a mass flux ≥ 2 $Mg.m^{-2}.s^{-1}$, with an rms error of 16.3%. The general decrease in CHF with quality may be explained in terms of the phase distribution. In general, the ratio $CHF_{ann}/CHF_{D=8mm}$ is close to one for the subcooled region (where the bulk temperature is the most important parameter and is relatively unaffected by the presence of an unheated wall). This ratio decreases gradually in the positive-quality region (entrainment-controlled CHF, because of the strong effect of the thicker liquid film on the unheated wall) and the ratio is least for the high-quality region where the deposition-controlled CHF becomes dominant (here, the presence of the liquid located on the unheated surface is felt most severely and has the greatest detrimental effect on CHF).

(ii) Gap-size correction factor, K_δ: Figure 4.7 shows the following trend: as the gap size increases from about 1.5 mm to 4.25 mm the ratio, $CHF_{ann}/CHF_{D=8mm}$, increases, then within the range of concentric gap size from 4.25 mm to 6.25 mm the gap size appears to have little or no effect on the CHF ratio and finally as the gap size increases beyond 6.25 mm the ratio start decreasing as is generally observed in tubes (see Chapter 3). The CHF in annuli is then predicted using the correction factor for the gap size with the correction factor for the quality (Equation 4.3) as follows:

$$CHF_{ann} = CHF_{D=8mm} \quad K_X \quad K_\delta \tag{4.4}$$

where the gap correction factor is given by the following expression:

$$K_\delta \begin{cases} = 0.3451 + 0.186\,\delta & \text{for } 0 < \delta \leq 4.3 \text{ mm} \\ = 1.1451 & \text{for } 4.3 < \delta < 6.25 \text{ mm} \\ = 2.271 - 0.1802\,\delta & \text{for } 6.25 \leq \delta < 9 \text{ mm.} \end{cases} \tag{4.5}$$

When using only the correction factor for quality as shown in Figure 4.9 the prediction improves. For the 113 CHF points used (for $G \geq 2$ $Mg.m^{-2}.s^{-1}$), the rms error was 13.3 % comparing to 91.4 % when no quality correction is applied (i.e., the comparison is between the CHF_{ann} and the predicted CHF values which are given by "$CHF_{D=8mm}\ K_X$" for the 13.3 % rms error and by "$CHF_{D=8mm}$" for the 91.4% rms error). Figure 4.8 also shows that when applying only the gap correction factor the prediction is improved (with respect to the 8-mm tube results; the ratio becomes closer to one). Employing both correction factors was found to also improve the prediction accuracy. Further work using a larger data base is required to determine whether individually extracted correction factors (e.g., K_δ and K_X) can be multiplied together as indicated by Equation (4.4) without altering the validity of the results.

Note also that a separate comparison using the ratio $CHF_{ann}/CHF_{D=Dhe}$ or $CHF_{ann}/CHF_{D=Dhy}$ yields much larger scatter among the data than that presented by using the 8-mm tube values as a reference.

Table 4.1: Concentric Annuli: Compilation of Gap Effect on CHF

References	Geometry*		Conditions Range			Comments*
	D_i/D_o (mm)	L(mm)	G(Mg/m²s)	P(MPa)	X_e	
Janssen and Kervinen [1963]	13.7/22.2, 9.5/22.2, 9.5/31.7, 9.5/18.0, 9.5/14.1, 12.7/25.4, 12.7/19.1	2591, 2743, 1829, 1778, 914 & 736	0.2 to 8.4	4.1 to 10	0 to 61.5%	Gap size, δ, was varied from 2.4 mm to 11.1 mm. The CHF decreased for gap sizes < 3.2 mm & > 6.35 mm. The optimum gap size (i.e., δ for a maximum CHF) for these flow conditions is between 3.2 mm and 6.35 mm.
Janssen and Kervinen [1964]	13.7/18.0 & 12.7/22.2	2730 & 6655	0.38 to 5.42	4.1 to 9.6	10 to 64%	Results were compared with their previous results [1963]. In general, there is good agreement between them. There was no significant effect of heated length.
Bennett, A.W. *et al.* [1964]	9.5/15.9, 9.5/14.2 & 11.1/15.9	736.6, 355.6, 177.8 & 88.9	0.678 to 4.068	0.52 to 8.62	0 to 74%	Two-phase inlet. The gap sizes used were 3.2, 2.3 and 2.4 mm. Within this range, no effect of gap size on CHF was observed.
Hoeck, E.O. *et al.* [1966]	76.3/79.6, 96.5/99.7 & 96.5/101.8	1882.6	0.678 to 6.78	6.89	−20 to 71%	Gap size varied from 2.6 to 1.6 mm. Results confirmed part of the observations by Janssen and Kervinen [1963]: the CHF decreases if the gap is reduced below 3.2 mm.
Ornatskiy, A.P. [1969a]	δ varies from 0.1 to 15 mm	Rel. Length 10 to 100	0.05 to 3.0	0.98 to 21.6	sub.	The study reviewed CHF data for subcooled water in annular channels. Ornatskiy concluded that as the gap size is increased from 0.1 to 1−2 mm the CHF increases. Further increase of the gap size did not affect the CHF.
Ornatskiy, A.P. *et al.* [1966]	10./11, 10/11.5& 10/12	49.5	1.0 & 2.0	14.7	−50 to 0%	CHF is of Type-II or III. External heating only. The gap width, δ, varied from 1 to 2 mm. Within this range, no effect of δ on CHF was noticed.
Tolubinskiy, V.I. *et al.* [1969]	D_w=2, 4, 8, 12, 16 & 26	20 to 150	0.05 to 0.8	5 to 21.6	Sub. to 30%	External heating. The CHF increased for gap size from 0.1 to 1.3 mm. For gaps greater than 1.3 mm, the effect of gap size on CHF was insignificant. Moreover, the CHF increased with an increase in mass flux G. The effect of G on CHF varied with gap size: $\phi \propto G^n$ where, n increases with gap width. The interpretation given was that reducing the gap decreased the flow turbulence and the transverse fluctuations.

continued...

Table 4.1 (concluded)

References	Geometry*		Conditions Range			Comments•
	D_i/D_o (mm)	L(mm)	G(Mg/m²s)	P(MPa)	X_e	
Tolubinskiy, V.I. *et al.* [1970a]	5/6 & 5/13	140 to 440	0.1 to 2.0	11.8 to 19.6	−70 to 40%	Internal heating. Increasing the annulus gap from 0.5 to 4 mm at the same local conditions increased the effect of G. The interpretation given was also (as given for external heating by Tolubinskiy [1969]) an increase in the flow turbulence and the transverse fluctuations; thus, the CHF also increased.
Tolubinskiy, V.I *et al.* [1977]	D_w = 1.0 to 5.0 mm	100 to 2000	0.25 to 2.0	5 to 20		Diameter of the rod was varied from 8 to 30 mm; the CHF increased at small rod radii. Increasing the curvature (reducing the diameter) results in a higher velocity gradient, which causes the increase in CHF. This interpretation seems only to be valid for Type-III CHF.
Hung and Yao [1983]	25.4/26.0, 25.4/27.0 & 25.4/30.6	76.2	0.124 to 1.145	0.132	Inlet sub. 12.8°C	Freon-113 was the working fluid. Gaps tested were 0.32, 0.80 and 2.58 mm. For a gap of 2.58 mm, little change in the bubble shape was observed when the CHF was reached. Reducing the gap size to 0.8 mm deformed bubbles and lowered the CHF. For a 0.32 mm gap size, bubbles were squeezed and coalesced together, a thin film developed beneath the coalesced bubbles, which was more likely to evaporate and lower the CHF even further. Comparison was affected by unequal local subcooling.

* D_i, D_o, and L are the internal diameter, external diameter and the heated length of the annulus, respectively.

• All these references are for vertical upflow of water and uniform Axial Flux Distribution (AFD) with unheated outside wall, unless otherwise specified.

Table 4.2: CHF Correlations for Annuli

Prediction Methods	References
Katto proposed separate equations for three regimes: - H-regime $\frac{CHF_O}{Gh_{fg}} = 0.12 \left(\frac{\rho_g}{\rho_f}\right)^{0.133} \left(\frac{\sigma \rho_f}{G^2 L}\right)^{1/3} \frac{1}{1 + 0.0081\ L/D_{ho}}$ - L-regime $\frac{CHF_O}{Gh_{fg}} = 0.25 \left(\frac{\sigma \rho_f}{G^2 L}\right)^{0.043} \frac{1}{L/D_{ho}}$ - N-regime $\frac{CHF_O}{Gh_{fg}} = 0.22 \left(\frac{\rho_g}{\rho_f}\right)^{0.133} \left(\frac{\sigma \rho_f}{G^2 L}\right)^{0.433} \frac{(L/D_{ho})^{0.171}}{1 + 0.0081\ L/D_{ho}}$ The regimes were distinguished by the following criteria: - between L- and H-regimes $\frac{L}{D_{ho}} = \frac{1}{0.48 \left(\frac{\rho_g}{\rho_f}\right)^{0.133} \left(\frac{\sigma \rho_f}{G^2 L}\right)^{0.29} - 0.0081}$ - between H- and N-regimes $\frac{L}{D_{he}} = \frac{0.0206}{\left(\frac{\sigma \rho_f}{G^2 L}\right)^{0.584}}$ The above equations refer to zero inlet subcooling (i.e. subscript O). When liquid is subcooled then the CHF can be calculated as: $CHF = CHF_O \left(1 + K \frac{\Delta h_i}{h_{fg}}\right)$ where K is a dimensionless parameter depending on the regime type.	Katto [1979]

continued...

Table 4.2 (continued)

Prediction Methods	References
Tong related the CHF for an annulus with that of a tube as predicted using the W-3 correlation: $$\frac{CHF_{unheated\ wall}}{CHF_{W-3,D_{he}}}=1.0-(1-\frac{D_{hy}}{D_{he}})\ [13.76-1.372\ e^{1.78x}$$ $$-4.732(\frac{G}{10^6})^{-0.0535}-0.0619(\frac{P}{10^3})^{0.14}-8.509D_{he}^{0.107}]$$ where $CHF_{W-3,Dhe}$ is calculated with the W-3 correlation based on D_{he} rather than D_{hy}. The correlation uses British units. The range of data used to develop this correlation is given by: $x_c \leq 0.1$ $1.356 \leq G \leq 6.78$ $Mg.m^{-2}.s^{-1}$ ($1.0 \leq G \leq 5.0$ $lb.h^{-1}.ft^{-2}$) $6.895 \leq P \leq 15.858$ Mpa ($1000 \leq P \leq 2300$ psia) $L \geq 254$ mm and $\delta \geq 2.54$ mm ($L \geq 10$ in and $\delta \geq 0.1$ in) Because of the relatively narrow range of qualities this correlation cannot be used generally, and thus has a limited range of applicability.	Tong [1972]
Tolubinskiy proposed the following correlation for CHF $$CHF_{sat.}=0.75\ 10^{-3}\ \frac{G^{0.6\sqrt{\delta}}}{\delta^{0.3}\ L}\ h_{fg}\sqrt{\rho_v}\ (1+\frac{\rho_v}{\rho_l})^{0.33}$$ This equation can be used for saturated water (x=C) at these ranges: $0.1 \leq \delta \leq 5$ mm. $20 \leq L \leq 200$ mm. $L/D_{hy} \leq 100$ $50 \leq G \leq 3000$ $kg.m^{-2}.s^{-1}$. $5 \leq P \leq 22$ MPa. For other values of local subcooling, Tolubinskiy modified the previous equation as follows $$CHF = CHF_{sat.}[1+1.2\ \ 10^{-2}\ \Delta h_{local\ sub.}(\frac{\delta}{L})^2]$$ Note that the short heated length may affect the trends of the correlations and could result in erroneous conclusions with the respect to the gap effect.	Tolubinskiy [1969]

continued...

Table 4.2 (concluded)

Prediction Methods	References
$$CHF \times 10^{-6} = \frac{A + B\,\Delta h_i}{C + L}$$ where $A = 67.45\, D_{hy}^{0.68} (G \times 10^{-6})^{0.192} [1 - 0.744 \exp(-6.512 D_{he} (G \times 10^{-6})]$ $B = 0.2587\, D_{hy}^{1.261} (G \times 10^{-6})^{0.817}$ $C = 185.0 D_{he}^{1.415} (G \times 10^{-6})^{0.212}$ This empirical correlation is developed at pressure of 1000 psia (6.9 MPa), which predicted 724 annuli data with an rms error of only 5.9%. This correlation uses British units and its data base covers the following range: $-\Delta h_i$: 0 to 412 Btu.lb^{-1} (0 to 0.958 MJ.kg^{-1}) -G: 0.14 to 6.20 (10^{-6}) lb.hr^{-1}.ft^{-2} (190 to 8430 kg.m^{-2}.s^{-1}) -L: 24.0 to 108.0 in. (0.61 to 2.74 m) $-D_i$: 0.375 to 3.798 in. (9.52 to 96.5 mm) $-D_o$: 0.551 to 4.006 in. (14 to 101.6 mm) For pressures other than 6.9 MPa, but within the range of 600 to 1400 psia (4.15 to 9.65 MPa), the previous equation is modified to: $$CHF \times 10^{-6} = \frac{A\left(\frac{h_{fg}}{649}\right) + B\,\Delta h_i}{C + L}$$ where h_{fg} is in Btu.lb^{-1}.	Barnett [1966]

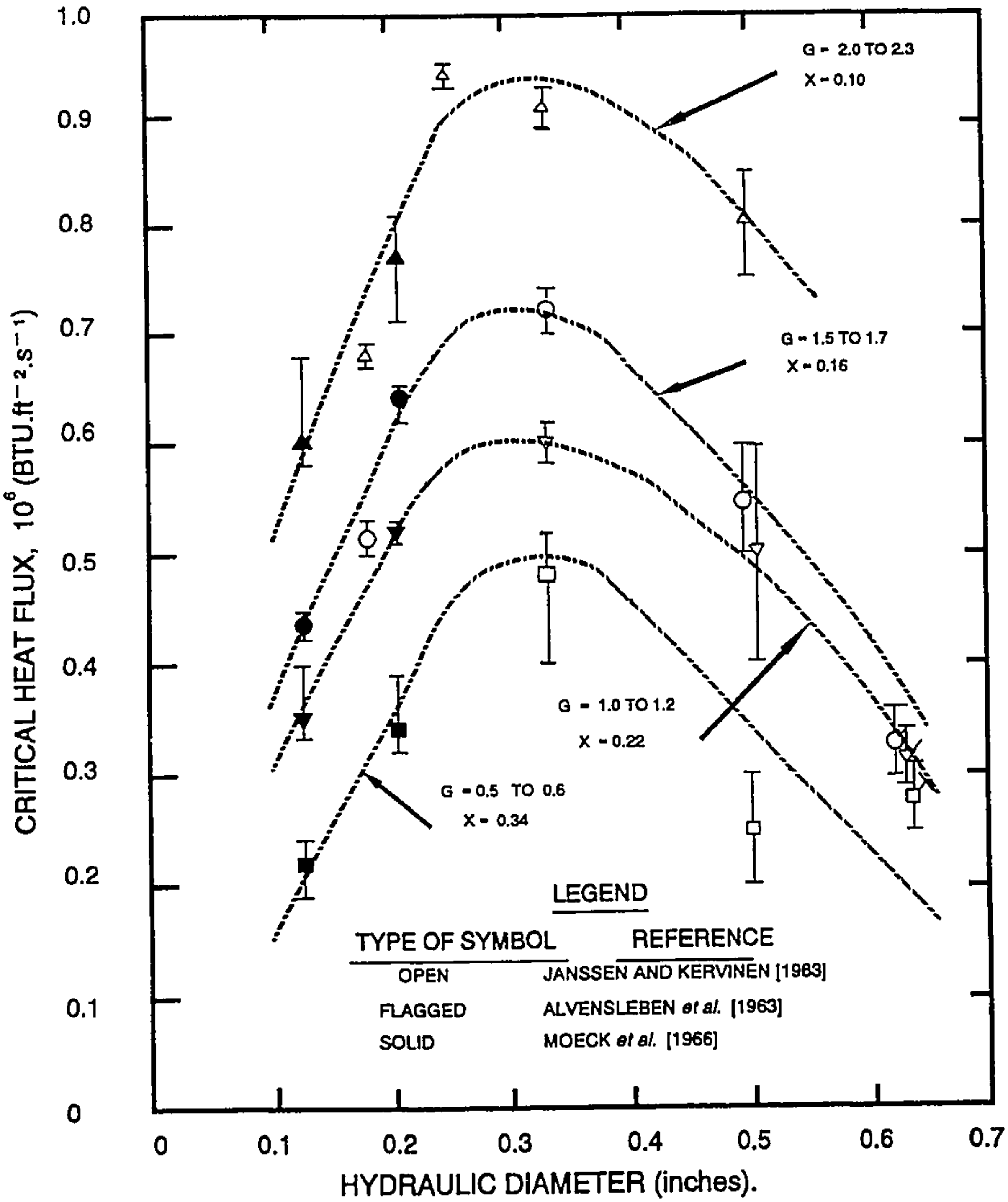

Figure 4.1: Effect of Hydraulic Diameter on CHF in Internally Heated Annuli (G in lb. hr^{-1}. ft^{-2}). From Moeck et al. [1966].

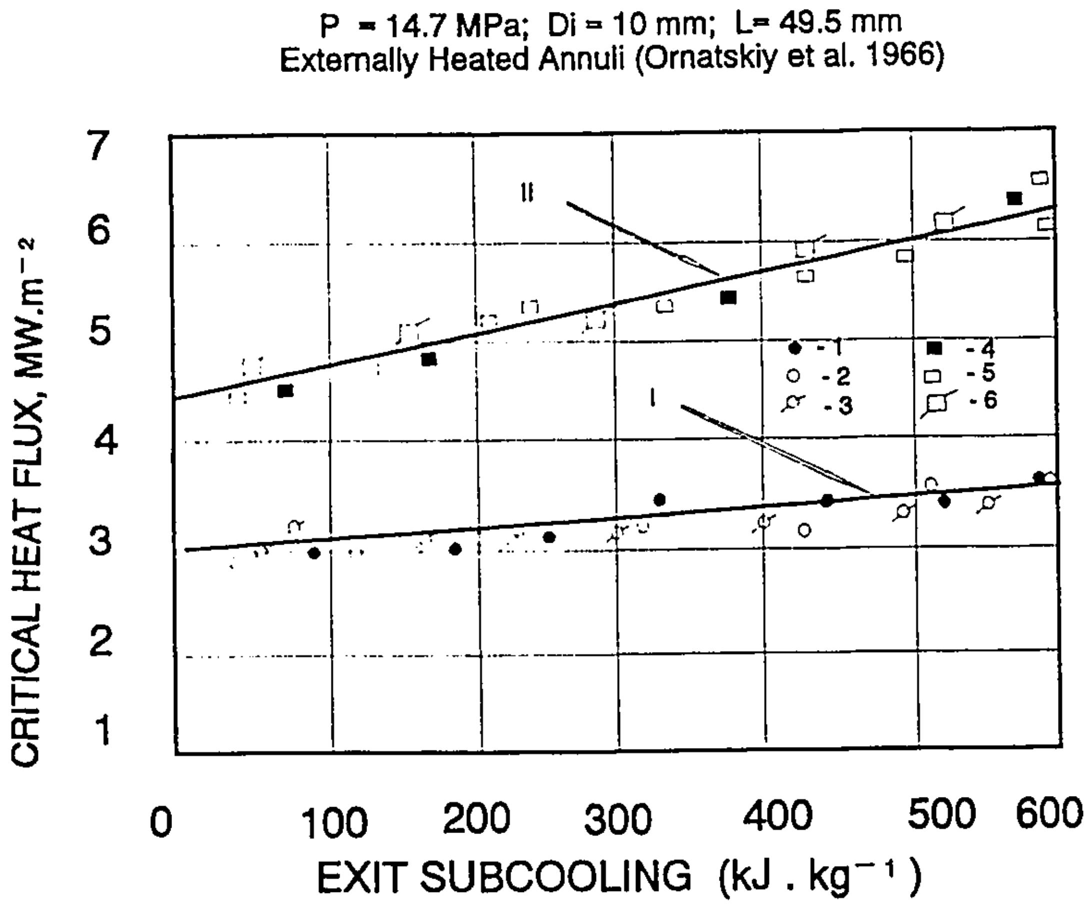

Figure 4.2: Effect of Gap Size on CHF. I– G=1.0 $Mg.m^{-2}.s^{-1}$; 1– δ=1.0 mm; 2– δ=1.5 mm; 3– δ=2.0 mm. II– G=2.0 $Mg.m^{-2}.s^{-1}$; 4– δ=1.0 mm; 5– δ=1.5 mm; 6– δ=2.0 mm.

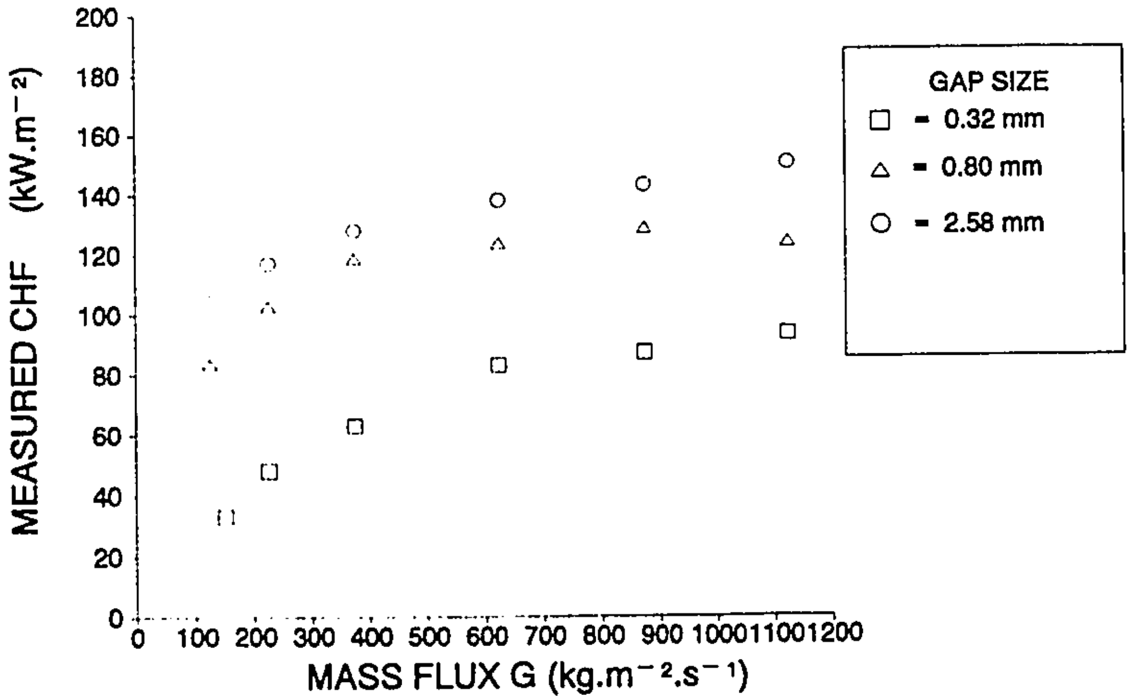

Figure 4.3: Effect of concentric Gap Size on CHF. From Hung and Yao [1983].

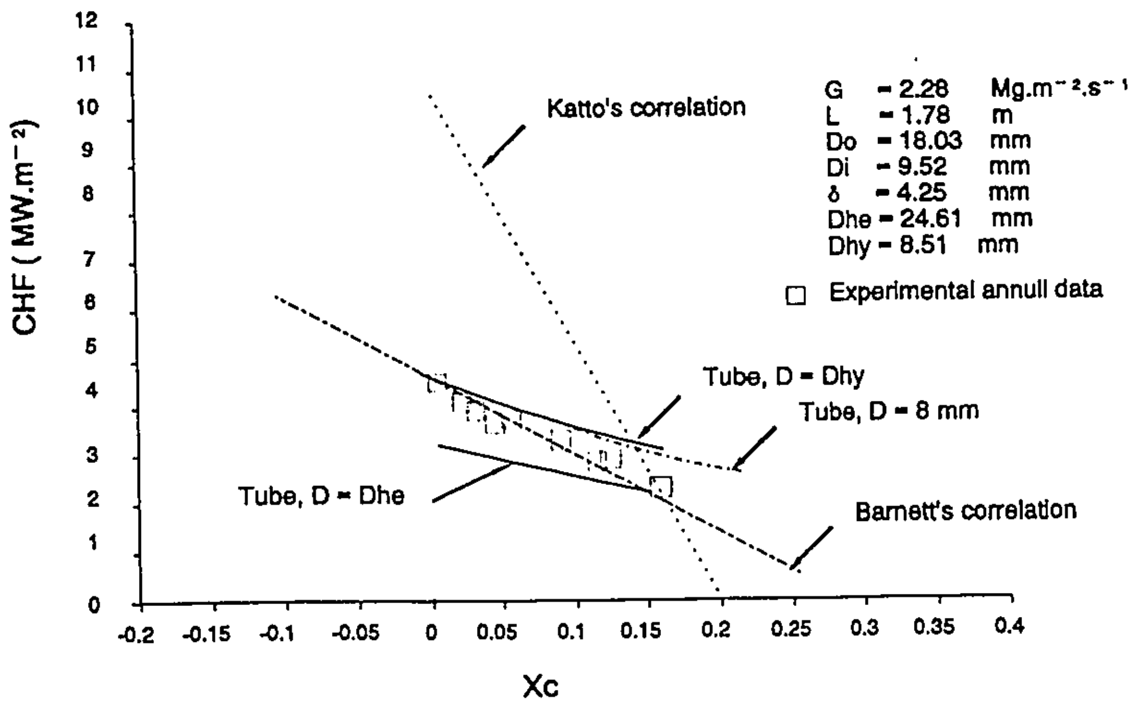

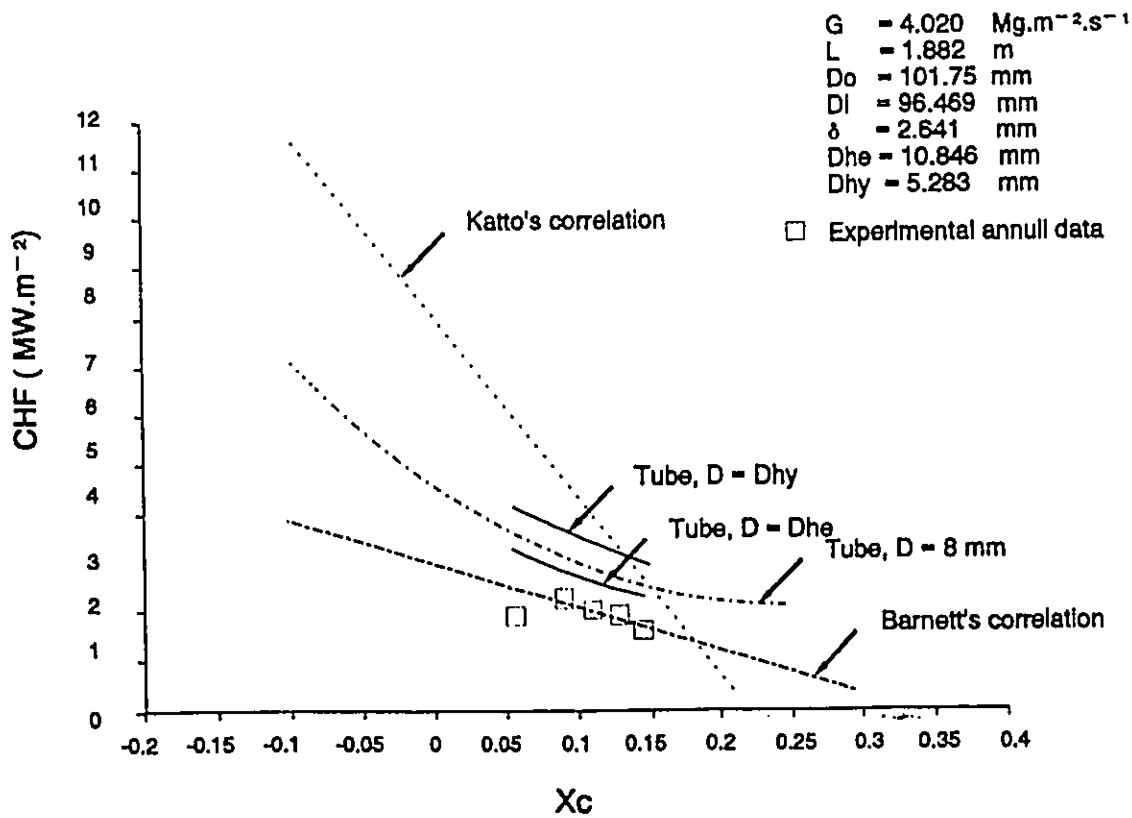

Figure 4.4: Comparison of Correlations and look-Up Table Predictions With Experimental Data in Annuli.

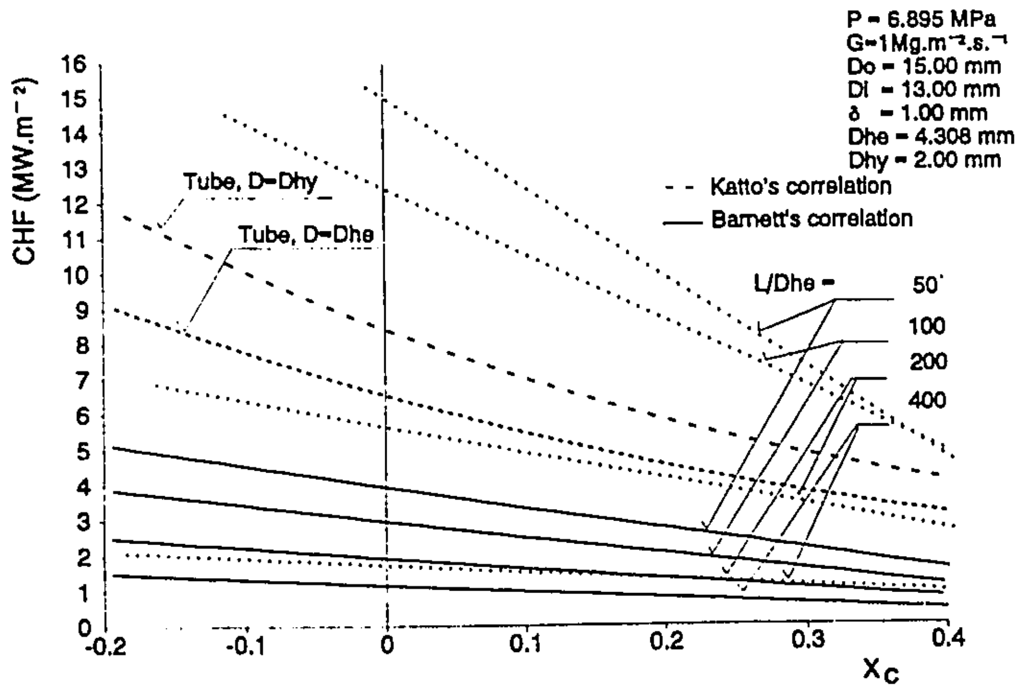

Figure 4.5: Prediction of L/D Ratio Effect on CHF in Annuli by Barnett's [1966] and Katto's [1979] Correlations.

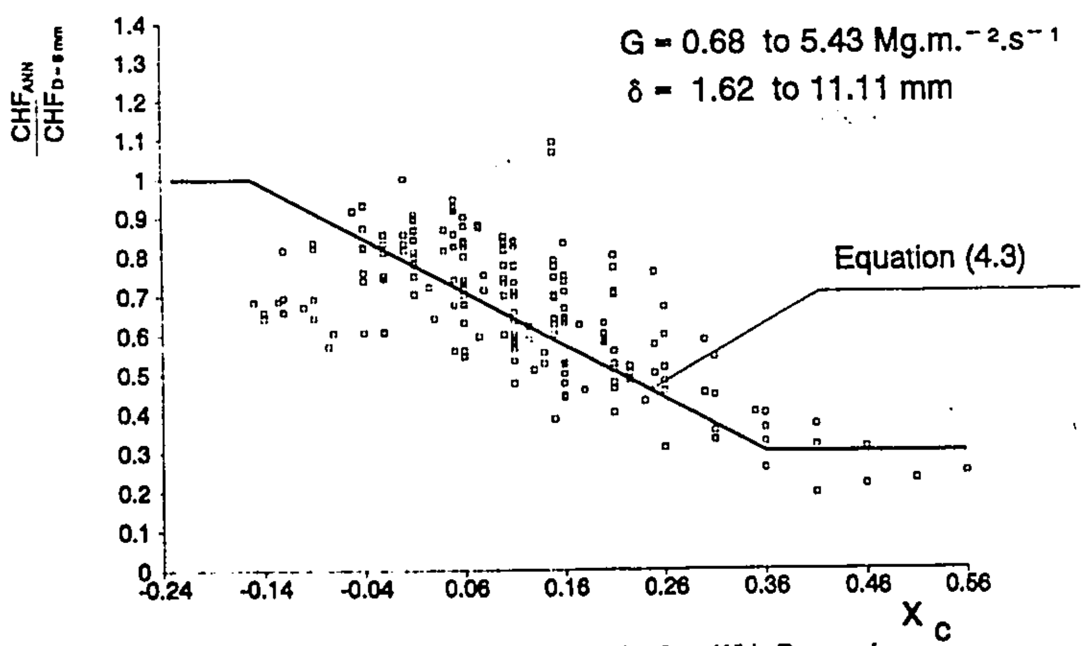

Figure 4.6: Ratio of CHF in Annuli and 8-mm Tube Over Wide Range of Mass Fluxes and Gap Sizes. Data From Barnett [1966, 1968].

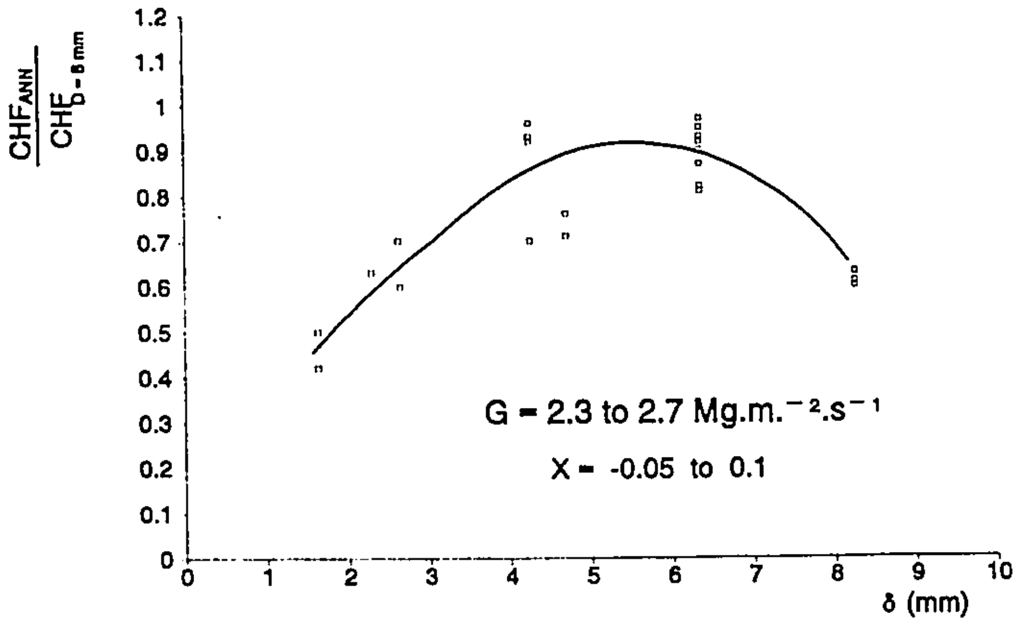

Figure 4.7: CHF Ratio in Annuli and 8-mm Tube Versus Gap Size Over Narrow Range of Quality. Data From Barnett [1966, 1968].

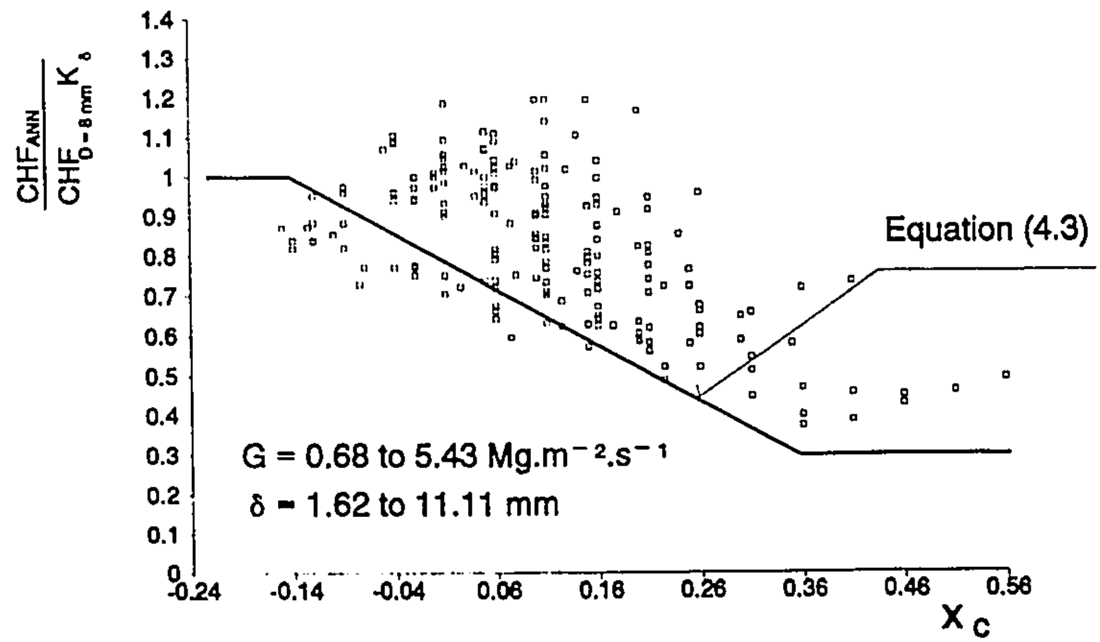

Figure 4.8: Ratio of CHF in Annuli and 8-mm Tube Over Wide Range of Mass Fluxes and Gap Sizes After Gap Correction.

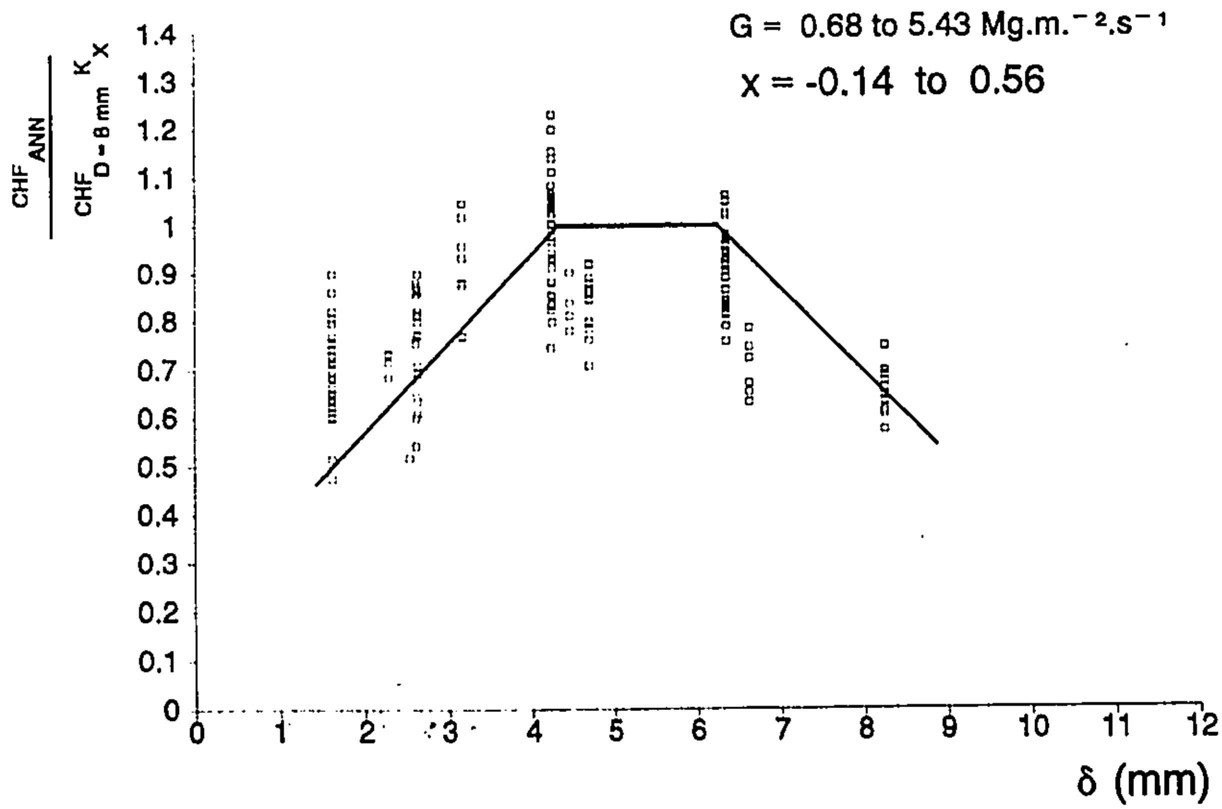

Figure 4.9: CHF Ratio in Annuli and 8-mm Tube versus Gap Size Over Wide range of Qualities, After Quality Correction. Data From Barnett [1966, 1968].

5. ECCENTRIC ANNULI

5.1 General

An examination of the effect of annulus eccentricity on CHF is important because of its similarity to the outer subchannel geometry of CANDU fuel bundles, in particular for bowed- or strained-fuel elements. The important parameters are the minimum gap size and the difference in radii between the heated and unheated surfaces. Table 5.1 summarizes the observed effects in eccentric annuli. Appendix B gives one set of the eccentric annuli CHF data.

5.2 Observed Effects

Tolubinskiy *et al.* [1977] concluded that the CHF decreases with increasing eccentricity. Due to eccentricity, the axial-velocity distribution around the annular cross section is not uniform: the velocity is lower in the narrow gap than in the wide gap. This non-uniformity will in turn cause a temperature difference between the narrow and the wide part of the annulus, hence the CHF will occur first in the narrow gap at a lower heat flux than the concentric case. A second consequence of eccentricity is that the proximity of the walls in the narrow gap makes it difficult for the bubbles to detach from the heating surface. Hence, at low pressure, the narrow gap may become vapour locked, which may result in a Type-I CHF. Moreover, Tolubinskiy concluded, "increasing the equivalent diameter of eccentric annuli always reduces the detrimental effect of eccentricity. Increasing the width of the wider part of the annulus at a constant narrow width (by increasing the equivalent diameter) improves the heat and mass transfer even in the case of subcooled fluid". Tolubinskiy *et al.* [1971, 1977] noted that, the dependence of CHF on flow parameters such as quality, inlet subcooling, pressure, and mass flux, diminishes with increasing eccentricity and practically vanishes with full contact. A correlation derived by Tolubinskiy *et al.* [1977] which considers the effect of eccentricity is given by

$$\frac{CHF_{eccn}}{CHF_{conc}} = 1-0.58\ G^{-0.37\left(\frac{D_{hy}}{D_{he}}\right)^{0.5}}\ L^{0.29\left(\frac{D_{hy}}{D_{he}}\right)}\ \varepsilon^{0.5}\ (1-0.3\ X) \qquad (5.1)$$

where ϵ is the relative eccentricity defined as

$$\varepsilon = \frac{\delta_{conc} - \delta_{min.\ gap}}{\delta_{conc}} = 1 - \frac{\delta_{min.\ gap}}{\delta_{conc}}$$

The data base covers the following range of variables:

$5 \leq P \leq 20$ MPa.

$0.25 \leq G \leq 2.0$ $Mg.m^{-2}.s^{-1}$.

$8 \leq D_{he} \leq 100$ mm.

$1 \leq D_{hy} \leq 5$ mm.

$100 \leq L \leq 2000$ mm.

$0 \leq \epsilon \leq 1$.

$X < X^{o}_{ex}$

X^{o}_{ex} is called the boundary steam quality. This is a constant steam quality at which the CHF is assumed to occur after the DNB type CHF. The existence of this quality is still under investigation by researchers. However, it can be taken that this correlation can be applied at least to subcooled and low quality CHF conditions.

Essentially, Ornatskiy *et al.* [1969c] arrived at the same general conclusion as Tolubinskiy: the CHF decreases with increasing eccentricity at the same local conditions. Figure 5.1 shows the variation of CHF with local subcooling at P = 5 MPa, G = 2.0 $Mg.m^{-2}.s^{-1}$, and for externally heated annuli (concentric gap is 1.5 mm). This figure shows that as the relative eccentricity, ϵ, is increased (i.e., minimum gap size is decreased), the CHF decreases and its dependence on the local subcooling (subcooling at the critical point, h_c-h_f) also diminishes. As the relative eccentricity exceeds 0.66 (i.e., δ_{min} less than 0.5 mm), the CHF becomes almost insensitive to local subcooling. Figure 5.1 also shows results for an 8-mm tube obtained from the CHF look-up Table. Figure 5.2 shows the variation of CHF with relative eccentricity for a fixed local condition: as the relative eccentricity increases, the CHF decreases. Moreover, Ornatskiy *et al.* observed that for $\epsilon \geq 0.66$ (i.e., $\delta_{min} \leq 0.5$ mm), the dependence of CHF on mass flux and pressure became insignificant, and hardly existed for rod tube contact. The quality range in this experiment (Table 5.1) indicates that the CHF type in this experiment is either (II) or (III). Ornatskiy also studied the effect of the position of local eccentricity (i.e., rod bowing). A change in position of local eccentricity from the outlet to the inlet caused a decrease in the CHF. However, because of the very short heated length (15 to 90 mm, see Table 5.1) and the high subcoolings, the observed effects may not be valid for other types of CHF and heated lengths.

Anderson *et al.* [1974] observed a decrease in CHF with an increase in eccentricity, which became more important for higher flows (G greater than 0.5 $Mg.m^{-2}.s^{-1}$). At a mass flux near 0.5 $Mg.m^{-2}.s^{-1}$ the effect of eccentricity was insignificant. As the mass flux increased, the effect of eccentricity increased: 21% reduction is observed at a G = 1.5 $Mg.m^{-2}.s^{-1}$ for a minimum gap of 2.1 mm, compared to the concentric case (δ = 5.1 mm) for the same inlet subcooling. Moreover, Anderson *et al.* concluded that, "the greater the eccentricity, the more uneven the film flow rate. The maximum film flow rate occurs at the maximum gap width. For the highest eccentric displacement (δ = 2.1 mm) the minimum film flow rate occurring at the minimum gap is relatively close to zero". This can be the cause of premature CHF occurrence at the narrow gap, hence the CHF reduction for the eccentric case.

Moeck *et al.* [1966] also observed reductions in CHF as the gap was reduced from 2.6 mm (concentric case) to 0.8 mm. At constant inlet conditions, the CHF decreased by 37, 50 and 60% (compared to the concentric case) for mass flux of 0.68, 1.4 and 4.1 $Mg.m^{-2}.s^{-1}$, respectively. This corresponds to reductions in CHF of 70 to 80% at constant dryout quality. Figure 5.3 illustrates this reduction for mass fluxes of 1.36 $Mg.m^{-2}.s^{-1}$ and 4.07 $Mg.m^{-2}.s^{-1}$, respectively. Also shown in this figure the line for concentric annuli predicted using Equation (4.4). It is also seen that the CHF ratio for this minimum gap of 0.8 mm is approximately constant for this quality range. Therefore, as the quality increases the CHF in eccentric annulus is closer to the concentric case.

Levy *et al.* [1962] (the same results were also reported by Janssen *et al.* [1963]) concluded that, for a minimum gap of 2.4 and 1.5 mm, the CHF results were similar to the concentric case where the gap was 4.2 mm. As the minimum gap was reduced to 0.8 mm, the CHF decreased by only 15% to 30%. Figure 5.4 shows the reduction in CHF for the three eccentric-gap sizes tested, with respect to the concentric case. Figure 5.4 also shows that as quality increases CHF in eccentric annuli for 0.8 mm gap size converges towards the other gap size CHF. The decrease in CHF is somewhat mass-flux dependent: the reduction in CHF at low mass flows is much smaller than at high mass flows. Comparing results obtained by Moeck *et al.* [1966] with results of Levy *et al.* [1962], it is clear from Figure 5.5 that the reductions in CHF as reported by Moeck were much more severe. The difference is thought to be due to the differences in rod diameter: 13.7 mm diameter for Levy as compared to 96 mm for Moeck (Figure 5.5). Hence, both the curvature and the ratio δ_{min}/D_i are quite different for these studies. This cross-section dimension difference was noted by Barnett [1963], who gave this explanation, "a more uneven distribution of liquid occurs in the larger annulus due to the longer flow path around the rod and the relatively narrow part of the gap extending for a greater distance". For a quality range from 9 to 66% and pressure of 7 MPa, the corresponding CHF mechanism in Moeck's experiment is either entrainment-controlled film dryout (Type-IV) or deposition-controlled dryout (Type-V).

Recently, CHF results have been obtained at CRL by Rudzinski [1992] in horizontal bowed annuli. Four gaps have been tested 1.25, 0.708, 0.367 and 0.068 mm (concentric gap was 2.2 mm). Results of these experiments are shown in Figures 5.6 to 5.8. The four plots in Figure 5.6 show the CHF in each gap for different mass fluxes as a function of the outlet quality. It can be concluded that for this range of mass flux (3.0 to 7.0 $Mg.m^{-2}.s^{-1}$) the effect of flow on CHF for each gap size is not very important. Each of the four plots in Figure 5.7 shows the CHF at 9.0 MPa, for a given mass flux and for the series of gaps tested as a function of the outlet quality. It is clear from these plots that the CHF decreases with decreasing gap size. Although the outlet quality range tested was relatively narrow (from -2 to 22 %), it still shows that the decrease is more important for lower quality (near 0%). As the quality increases the CHF for the different gap sizes tends to converge to similar values which also means that the CHF in concentric and eccentric annuli yields similar results at high qualities. It is also seen from these plots that the relative decrease in CHF when changing from 1.25 mm gap to 0.708 mm gap is less important than the relative decrease when reducing the gap size from 0.708 mm to 0.367 mm. However, further reduction in the gap size (from 0.367 to 0.068 mm) did not result in further CHF reduction. Figure 5.7 also shows that the gap size effect is more pronounced for higher mass fluxes (within a range of qualities). Shown as well in Figure 5.7 the concentric annulus prediction using Equation (4.4) which predicts the CHF data for the 1.25 mm gap reasonably well. In Figure 5.8 the CHF has been plotted against gap size for various mass fluxes on a constant quality basis. As noted from the previous figure, the effect on CHF of decreasing the gap size appears to increase as the mass flux increases, with the largest decrease occurring at the higher mass fluxes. Figure 5.9 shows the effect of pressure and gap size on CHF. The effect of increasing pressure and decreasing gap is to reduce the CHF. Unlike the effect of mass flux, the effect of pressure on CHF seems to be the same over the range of minimum gaps tested.

5.3 Effect of Eccentricity - Other Geometries

Tong *et al.* [1967] examined the effect of line contact of the heated rod with the unheated surface using a test section consisting of a heated rod in the centre of an unheated square sleeve. The local qualities tested in this experiment were near saturation (Type-III CHF, bubble clouding). The decrease of CHF in the case of line contact in comparison with the no-contact case was 14% at G=1.36 $Mg.m^{-2}.s^{-1}$, 7% at G=2.72 $Mg.m^{-2}.s^{-1}$ and 2% at G=4.08 $Mg.m^{-2}.s^{-1}$. Increasing the mass flux resulted in more turbulence and hence a better mixing.

5.4 Discussion of the Eccentricity Effect

As for the concentric annuli, the relative decrease in CHF with local quality for eccentric annuli compared to the 8-mm tube is greater for positive qualities than for subcooled conditions. However, comparing the concentric and the eccentric annuli CHF results at the same local conditions shows that, the discrepancy between them decreases with increasing quality and tends to disappear at high qualities (e.g., see Figures 5.4 and 5.7).

One apparent effect due to eccentricity is that the axial-velocity distribution around the annular cross section is not uniform: the velocity is lower in the narrow gap than in the wide gap. For subcooled boiling, this non-uniformity will in turn cause a fluid-temperature difference between the narrow and the wide part of the annulus, hence the CHF will occur first in the narrow gap at a lower heat flux than the concentric case. A second consequence of eccentricity is that the proximity of the walls in the narrow gap lowers the shear stress (e.g., Ouma and Tavoularis [1991a,1991b]) and makes it difficult for the bubbles to detach from the heating surface. Hence, the narrow gap becomes more crowded with bubbles, thus lowering the CHF. This phenomenon is more likely to occur at low pressure and for Type-III CHF (bubble clouding). Moreover, increasing D_{hy} at a constant minimum gap, decreases the effect of eccentricity by improving the heat and mass transfer between the narrow and wide regions.

A comparison between Moeck's *et al.* [1966] and Levy's *et al.* [1962] results suggests that the much stronger negative effect of eccentricity on CHF as observed by Moeck is probably due to the larger radius: for the same minimum gap the higher enthalpy fluid in the narrow gap experiences much better mixing with the fluid in the wider part of the annulus if the radius is small.

Tong *et al.* [1967] concluded that having turbulence promoters, such as rough surfaces, reduces the effect of a line contact with an unheated wall. This effect almost disappears at high mass flux.

A comparison between the conclusions of different studies showed some contradictions in the effect of minimum gap on CHF. For instance Levy's [1962], Anderson's [1974] and Rudzinski's [1992] results showed a larger difference between the concentric and the eccentric CHF results as the mass flux is increased. But, Tolubinskiy [1971, 1977] and Ornatskiy [1969c] concluded that increasing the mass flux brings the eccentric and the concentric CHF results closer to each other. This latter conclusion can be explained physically: increasing the mass flux means more turbulence for a given gap. This increase in turbulence in turn causes more interchange between the narrow and the wide regions, hence the risk of CHF occurring prematurely at the narrow gap is reduced. This however does not explain the opposite effect arrived to by the other studies. It is important to note that the work of Tolubinskiy and Ornatskiy is for very high subcooling (CHF type-II) and for a short test section. On the other hand the work done by the other researchers is for near saturation and relatively high qualities (CHF Type-III or -IV). For these conditions increasing the mass flux might mean more entrainment from the liquid film hence lower CHF. This mechanistic difference of the CHF occurrence might be the cause of the contradictory conclusion reached by the two groups of researchers.

All the studies showed an agreement on the effect of quality on the eccentric CHF results: as quality increases, the CHF in eccentric annuli converges towards the CHF in concentric annuli (although it was shown in Chapter 4 that the CHF in concentric annuli diverges from the 8-mm round tube results as the quality is increased). At high qualities the CHF occurrence is controlled by film dryout (Type-IV, -V or -VI CHF). At these conditions when reducing the gap, the outer surface liquid film may come into contact with the inner surface liquid film thus bridging the complete gap with liquid. This could have the effect of locally enhancing the CHF for the eccentric annuli moving the point of initial CHF occurrence away from the narrow gap region and perhaps making it comparable to the CHF of the concentric annuli. In Chapter 8 the liquid film thickness and the droplet sizes are estimated to determine when this bridging effect might be of importance to CHF occurrence.

5.5 Recommended Prediction Method

The CHF results of Levy *et al.* [1962] and Moeck *et al.* [1966] were compared to the CHF of an 8-mm tube. Figures 5.3 and 5.4 show the results of the comparison. In general, the ratio $CHF_{ann}/CHF_{D=8}$ decreases with quality and eccentricity, as shown by these figures and as concluded in Chapter 4 for the concentric case. From Figure 5.4 it can be seen that the prediction developed in Chapter 4 fits the eccentric annuli results of Levy *et al.* [1962] reasonably well. Figure 5.7 also shows that Equation (4.4) predicts the 1.25 mm minimum gap size CHF data relatively well. However, in Figure 5.3 the results of Moeck *et al.* [1966] are not well predicted by Equation (4.4). Also in Figure 5.7 CHF data for gaps other than 1.25 mm are not well predicted using Equation(4.4), the discrepancies are larger as the gap size is reduced. To derive a prediction method for eccentric annuli the following procedures should be followed:

i- Analyze the effect of each of the dominant parameters controlling the CHF in eccentric annuli. From this review the major parameters identified are: exit quality, mass flux and geometric characteristics of the test section. The effect of pressure is not important except for very low pressures where the bubble size may become comparable to the minimum gap size (see Chapter 8).

ii- Graphically examine the effect and importance of each of the parameter on CHF.

iii- Determine the general trends of the results, and relate the eccentric annuli results to the concentric ones. The objective here is to derive an expression relating CHF_{ecc} to CHF_{conc} having the following general form:

$$\frac{CHF_{ecc}}{CHF_{conc}} = f(X_c, G, geometry) \tag{5.2}$$

Then use the prediction method developed in Chapter 4 to substitute the CHF_{conc} by the CHF in 8-mm tube. Hence the final result will be given as

$$\frac{CHF_{ecc}}{CHF_{D=8mm}} = g(X_c, G, geometry) \tag{5.3}$$

Most of the experimental results found in the literature are presented in graphical form. CHF values need to be extrapolated from the plots which adds another source of errors beside the usual experimental errors. The amount of data found in the literature for eccentric annuli is not sufficient to isolate each effect and present it in a general prediction method.

In Chapter 4, it was found that the quality effect is the dominant one for concentric annuli. As mentioned before, Figures 5.4, 5.6 and 5.7 show that as the quality increases the CHF results in eccentric and concentric annuli converge. This trend is also satisfied by Equation (5.1) where the quality effect is represented by the factor "1- 0.3 X".

The second important parameter is the flow geometry of the test section. In order to fully specify the geometry of an eccentric test section four variables are required: minimum gap, hydraulic diameter, rod diameter and heated length. The heated length is bound to have little effect on the results (that has been assumed by most studies) if $L/D_{hy} \geq 100$ which is satisfied by all studies except for Tolubinskiy's and Ornatskiy's work.

However, Tolubinskiy's correlation showed a strong effect of heated length. The minimum gap size may be the most important geometric variable affecting CHF occurrence in eccentric annuli. However, the gap size is not sufficient by itself to specify the effect of geometry. In fact, Moeck's *et al.* [1966] and Levy's *et al.* [1962] test sections had the same minimum gap but quite different CHF data were obtained from their experiments. In Figure 5.10 several geometric parameters have been used as independent variables in order to find the best parameter that will fit the data. However, the lack of data at similar conditions may be the cause of the large variations in results. In Figure 5.10a, Equation (5.1) has been applied to the different set of results. This correlation showed generally good agreement with the data except for Ornatskiy's *et al.* [1969c] and Moeck's *et al.* [1966] CHF results.

The last parameter that might affect the results is the mass flux. There is no general agreement on the effect of mass flux on the CHF of eccentric annuli. The reasons for some of the differences were discussed in the previous section. Moreover, it is hard to separate the effect of mass flux from that of the quality, since experimentally it is very difficult to get CHF results at low quality and low mass flux, or high quality and high mass flux. Hence, some of the mass flux effects may be due to quality variations. Figures 5.7 and 5.8 show that the increasing mass flux results in a more pronounced difference between the eccentric and the concentric CHF values. However Tolubinskiy's correlation shows as the mass flux is increased the ratio, $\frac{CHF_{eccn.}}{CHF_{conc.}}$, is closer to 1.0 (at the limit when G goes ∞ that ratio goes to unity).

In Equation 5.1 all the important parameters affecting the CHF in eccentric annuli are represented. However, more experimental data are needed in order to validate and specify the limitations of this correlation. In a future work a recommended prediction method that satisfies the observed trends would have some resemblance with Equation 5.1.

Table 5.1: Eccentric Annuli: Compilation of Minimum Gap Effect on CHF

References	Geometry*		Conditions Range			Comments*
	D_i/D_o (mm)	L(mm)	G(Mg/m^2s)	P(MPa)	X_e	
Levy, S. et al. [1962]	13.7/22.2	2591	0.34 to 1.82	6.89	9 to 66%	The minimum gap was reduced from 4.2 mm (concentric case) to 2.4, 1.5 and 0.8 mm. For a minimum gap of 2.4 and 1.5 mm the CHF results were similar to the concentric case. As the minimum gap was reduced to 0.8 mm, the CHF decreased by 15 to 30%.
Janssen, E. et al. [1963]	13.7/22.2, 9.5/22.2, 9.5/31.7, 9.5/18.0, 9.5/14.1, 12.7/25.4, 12.7/19.1	2591, 2743, 1829, 1778 914 & 736	0.2 to 8.4	4.1 to 10	0 to 61.5%	Subcooled inlet conditions. Minimum gap sizes were 2.4, 1.5, 0.8, & 0.0 mm. For minimum gap of 2.4 and 1.5 mm, the CHF was almost the same as in the concentric case. When the gap was reduced to 0.8 mm, the CHF decreased by at least 30% for low subcooling. Results were difficult to interpret as the flow is not kept constant. Further decrease in the minimum gap size resulted in reduction of CHF, and at zero clearance the reduction in CHF was from 37 to 65%, depending on the mass flux. CHF results from this study for minimum gap of 0.8 mm were identical to CHF results from Levy [1962] for the same gap.
Bennett, A.W. et al. [1964]	9.5/15.9	736.6	2.0	1.38 to 3.45	24.1 to 45.5	The minimum gap size was 0.9 mm at the level of the upper rod supports (bowed rod). The bowed rod CHF results and the concentric rod CHF results show good agreement.
Moeck, E.O. et al. [1966]	76.3/79.6, 96.5/99.7 & 96.5/101.8	1882.6	0.678 to 6.78	6.89	-20 to 71%	Minimum gap size varied from 2.6 mm (concentric case) to 0.8 mm. The eccentric annulus gave CHF values lower than the concentric annulus (60% reduction for G=4.1 Mg/m^2s). The reduction in CHF was more severe than that reported by Levy [1962] for minimum gap of 0.8 and same local conditions (70 to 80% instead of 30% reported by Levy).

continued...

Table 5.1 (continued)

References	Geometry*		Conditions Range			Comments*
	D_i/D_o (mm)	L(mm)	G(Mg/m²s)	P(MPa)	X_c	
Ornatskiy, A.P. et al. [1969c]	Average gap 1.5 mm	15, 30, 45, 60 & 90	0.5 to 3.0	9.81 to 20.05	-60 to 0%	External heating. The relative eccentricity, ϵ, values were 0.13, 0.33, 0.48, 0.66, and 0.80, which correspond to these minimum eccentric gap, δ_{min}, 1.3, 1.0, 0.78, 0.51, and 0.3 mm, respectively. The CHF decreased with increasing eccentricity. The influence of the local parameters (quality, pressure and mass flux) on the CHF decreased with increasing eccentricity and hardly exist for near rod/tube contact (at ϵ = 0.66 & 0.80). The change of location of the local eccentricity (bowing of rod) from the outlet to the inlet led to a decrease in the CHF.
Bowditch and Lee [1973]	15.9/22.7	3660	0.69 to 3.4	6.9	-11 to 43%	Eccentric rod. Minimum gap size was 1.83 mm. Ceramic ramp was used to simulate rod bow. Rod contact with the ramp occurred at either 2030 or 3250 mm from the inlet end of the heated length. Presence of the ceramic ramp contacting the heater rod did not have a detrimental effect on CHF, until the local heat flux at contact position reaches 1.6 MW.m².
Anderson, P.S. et al. [1974]	17/27.2	3500	0.5 to 1.5	7.0	>19%	Minimum gap varied between 5.1 and 2.1 mm. Eccentricity effect on CHF became more important for higher flows (G > 0.5 Mg/ m²s). The effect of eccentricity increases with increasing mass flux. At G ≈ 0.5 Mg/ m²s, the effect of eccentricity was insignificant. The film flow rate was minimum in the narrow gap and maximum in the wide region.
Tolubinskiy, V,I et al. [1971]	9/13	50 to 100, 200 & 400	0.25, 0.50 & 1.0	2.46 to 19.6	-220 to 20%	Gap varied from 2 mm for the concentric case to contact over the whole length. CHF occurred first in the narrow gap side. The CHF decreased with increasing eccentricity and its dependence on local conditions quality, pressure and mass flux also diminished. This dependence practically vanished with contact.

continued...

Table 5.1 (concluded)

References	Geometry*		Conditions Range			Comments*
	D_i/D_o (mm)	L(mm)	G(Mg/m²s)	P(MPa)	X_e	
CRL results [1992]	13.5/17.9	1500	3.0, 4.0, 5.0, 6.0 & 7.0	7.0 & 9.0	-2.3 to 21.1%	Horizontal channel. The rod eccentricity reaches a maximum at the exit of the test section. The minimum gaps obtained at the channel exit were 1.25, 0.708, 0.367 and 0.068 mm. The 0.367 mm and 0.068 mm gap gave very close CHF results. The results for the different gaps converges to each other as the quality increases. The largest reduction in CHF with eccentricity was observed specially for the lower qualities.
Tolubinskiy, V,I <u>et al.</u> [1977]	8/9 to 8/13	100 to 2000	0.25 to 2.0	5 to 20	--200 to -20%	Eccentricity varied from zero (concentric position) to contact. The CHF decreased with increasing eccentricity. The relative decrease (compared to the concentric case) was greater for positive qualities than for subcooled conditions (better mixing). Eccentricity produced a reduction of velocity in narrow part, resulting in a local decrease in the CHF. Changes of curvature between the inner and the outer wall might be responsible for differences in CHF between these two surfaces.

* D_i, D_o, and L are the internal diameter, external diameter and the heated length of the annulus, respectively.

* All these references are for vertical upflow of water and uniform AFD with unheated outside wall, unless otherwise specified.

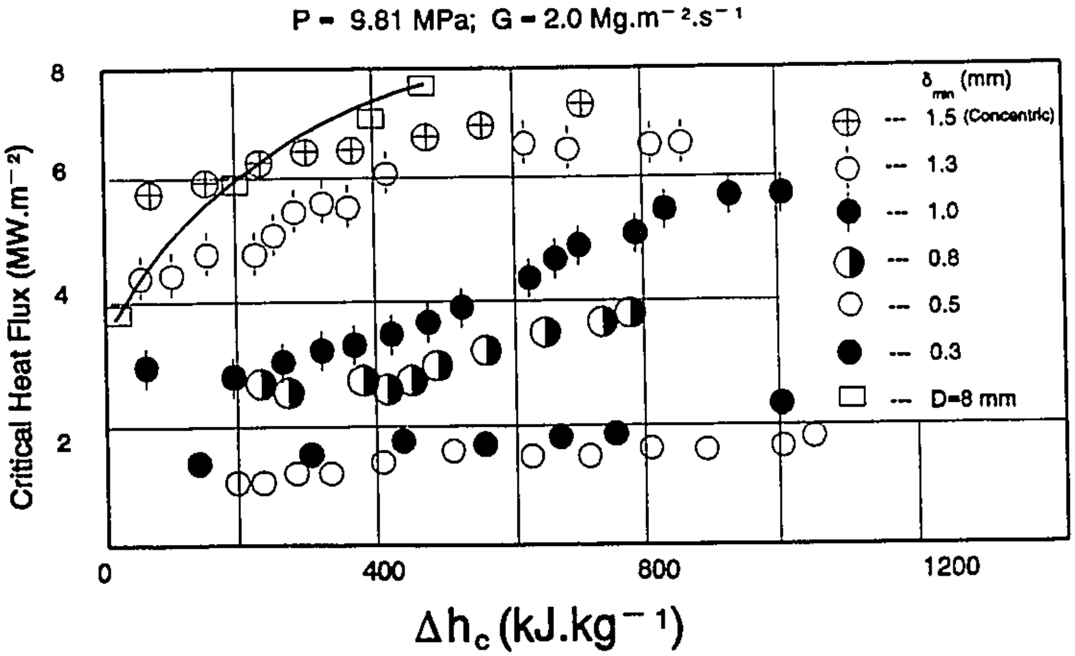

Figure 5.1: Effect of Minimum Eccentric Gap Size on CHF. D = 8 mm Correspond to Values from the CHF Table for 8-mm Tube. From Ornatskiy *et al.* [1969c].

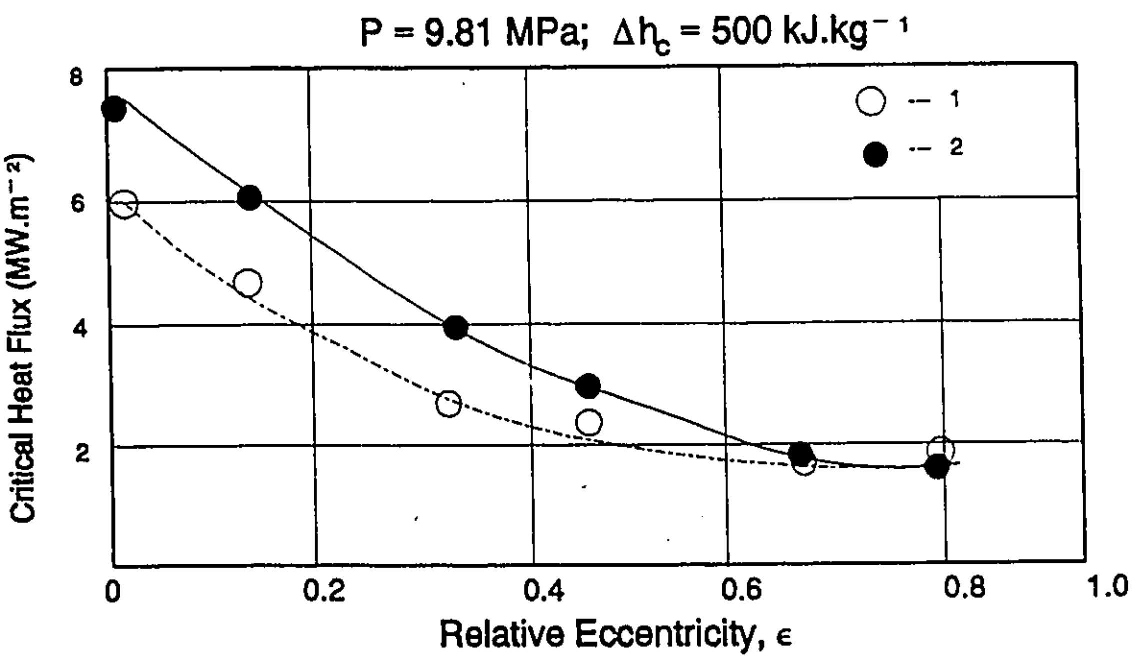

Figure 5.2: CHF as a function of the relative eccentricity, ϵ. 1- G = 1.0 $Mg.m^{-2}.s^{-1}$; 2- G = 2.0 $Mg.m^{-2}.s^{-1}$. From Ornatskiy *et al.* [1969c].

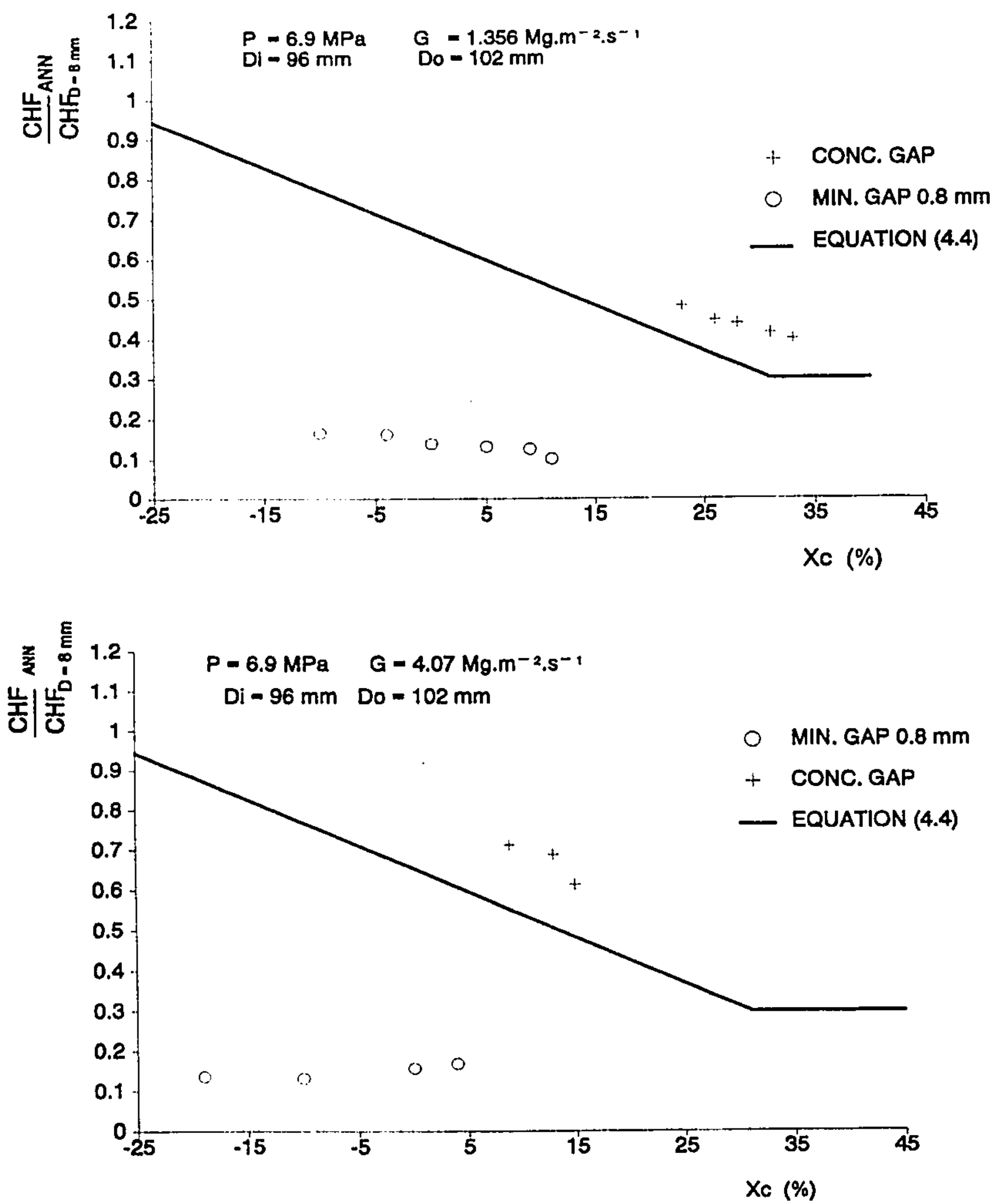

Figure 5.3: Effect of Eccentric Gap Size on CHF in Annuli. Data From Moeck *et al.* (1966).

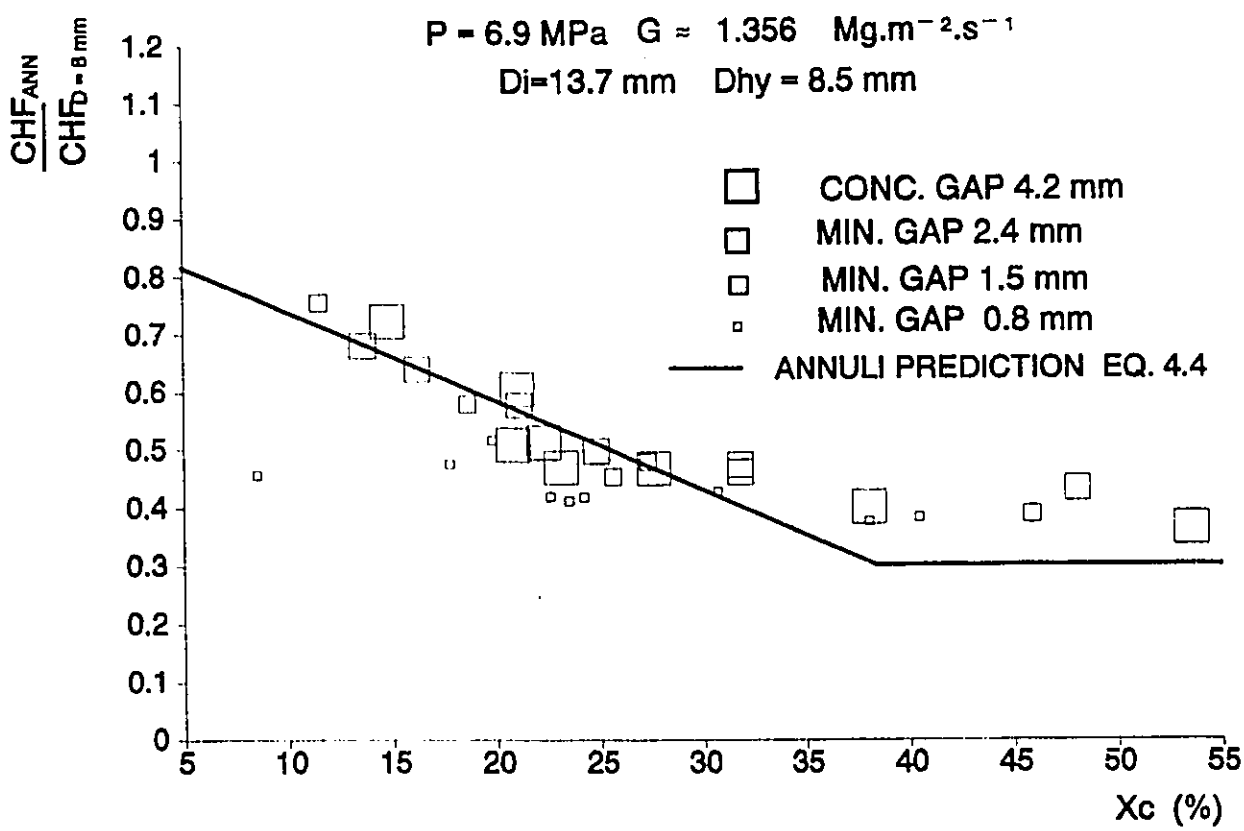

Figure 5.4: Effect of Eccentric Gap on the CHF in Annuli. Data From Levy *et al.* [1962].

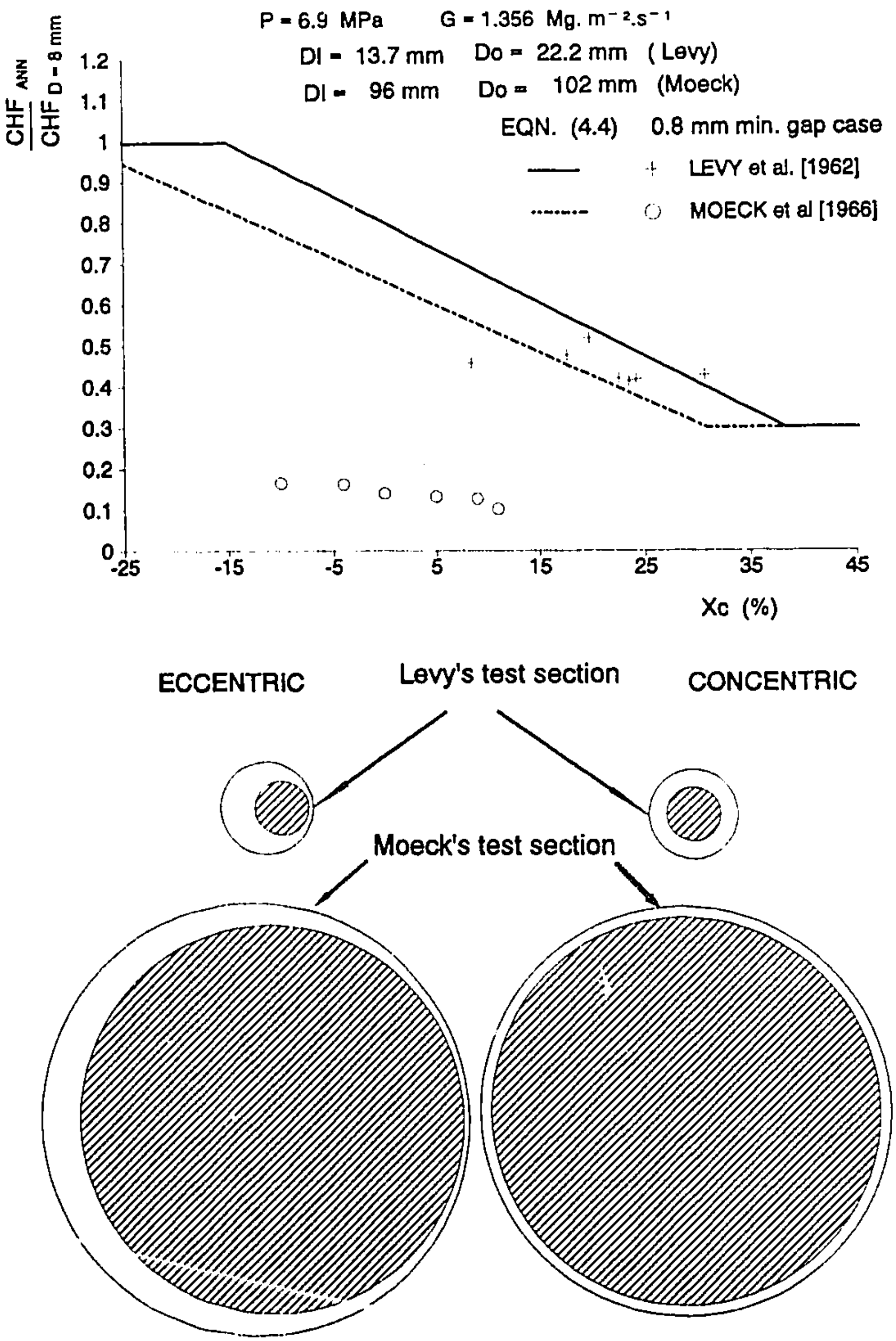

Figure 5.5: Comparison Between Moeck's and Levy's CHF Results and Test Sections (the Same Scale is Used to Draw Both Test Sections).

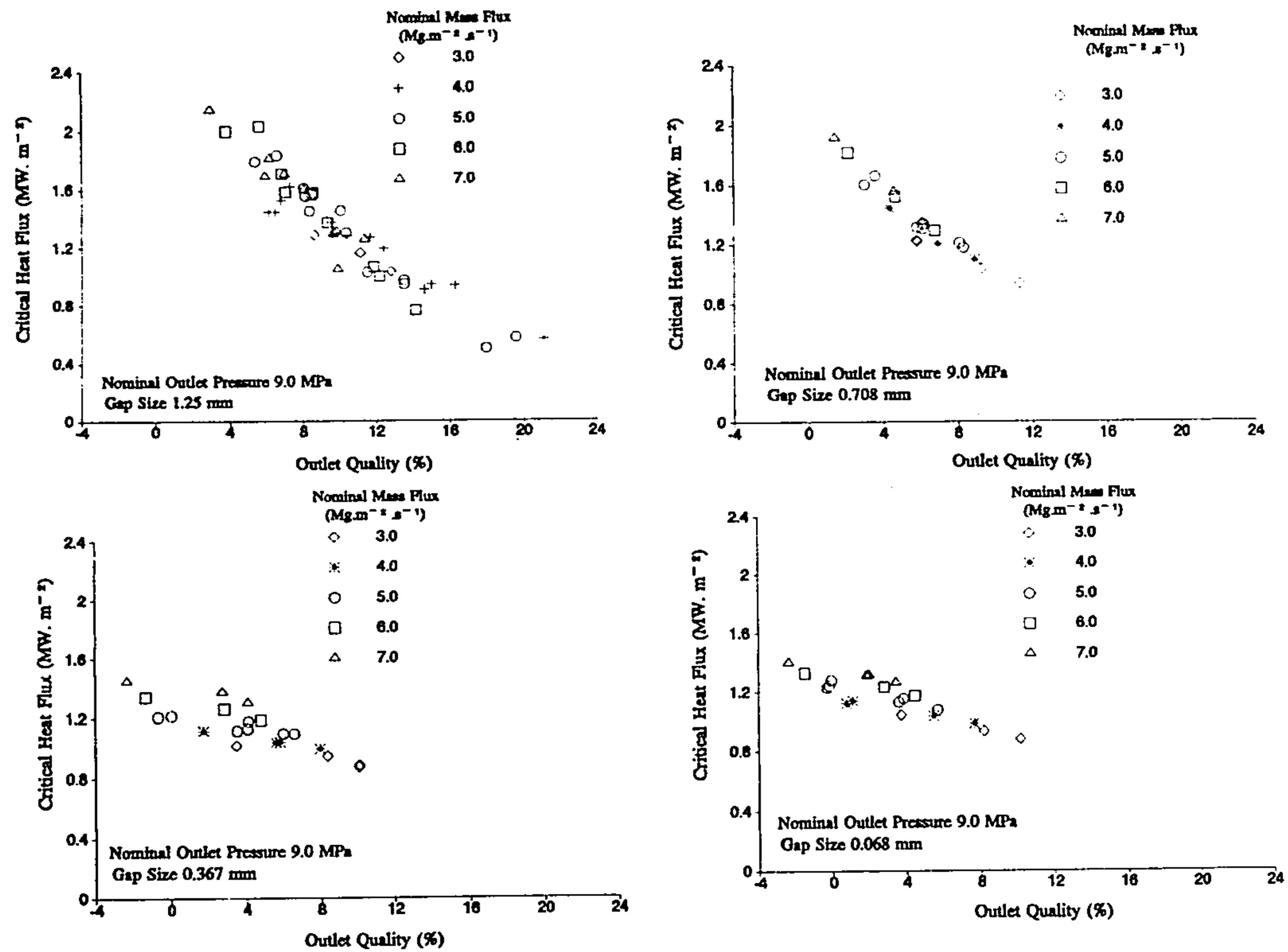

Figure 5.6: Effect of Mass Flux and Critical Quality on CHF. CHF Data From Rudzinski [1992].

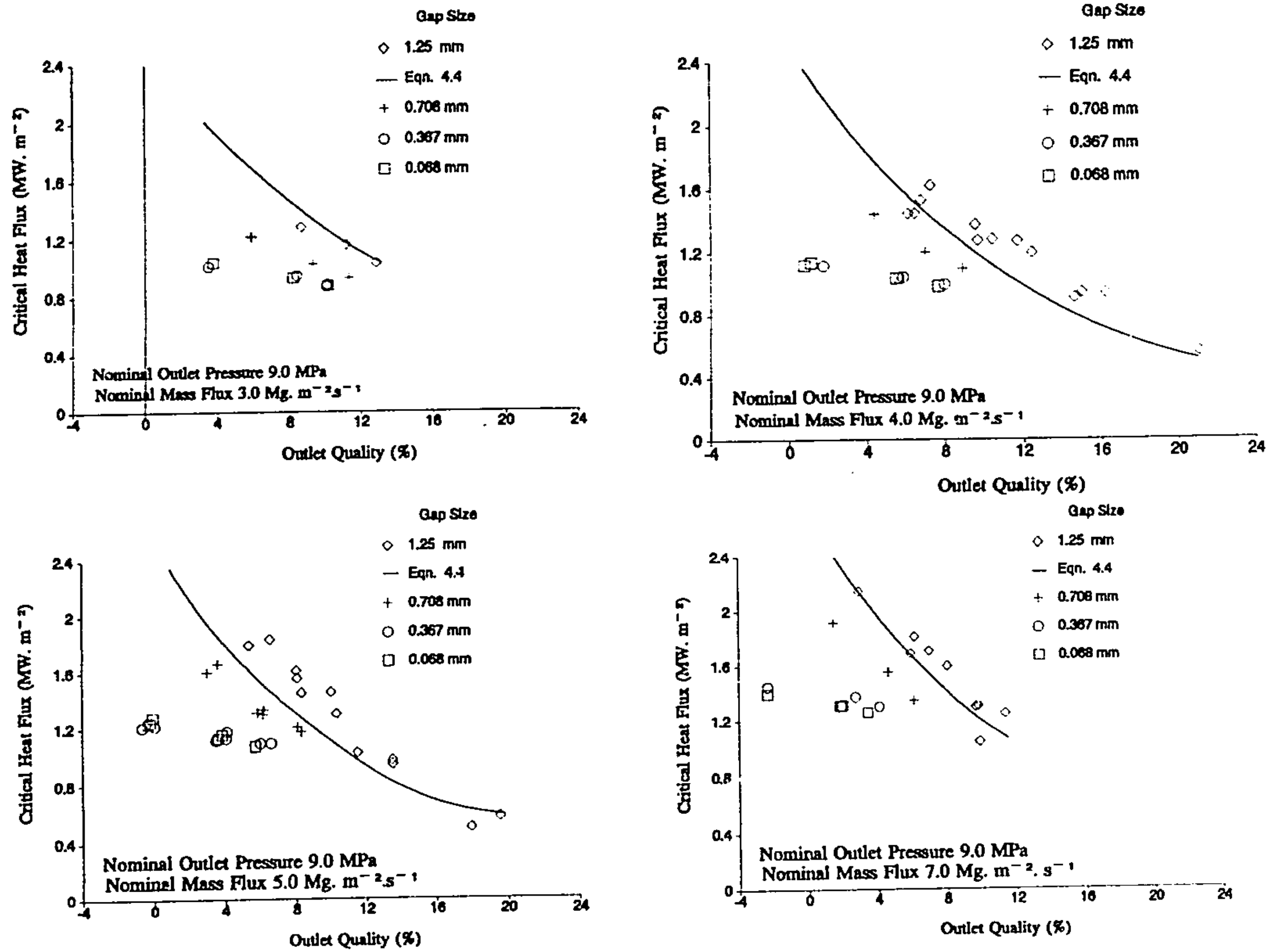

Figure 5.7: Effect of Minimum Gap Size and Critical Quality on CHF. CHF Data From Rudzinski [1992].

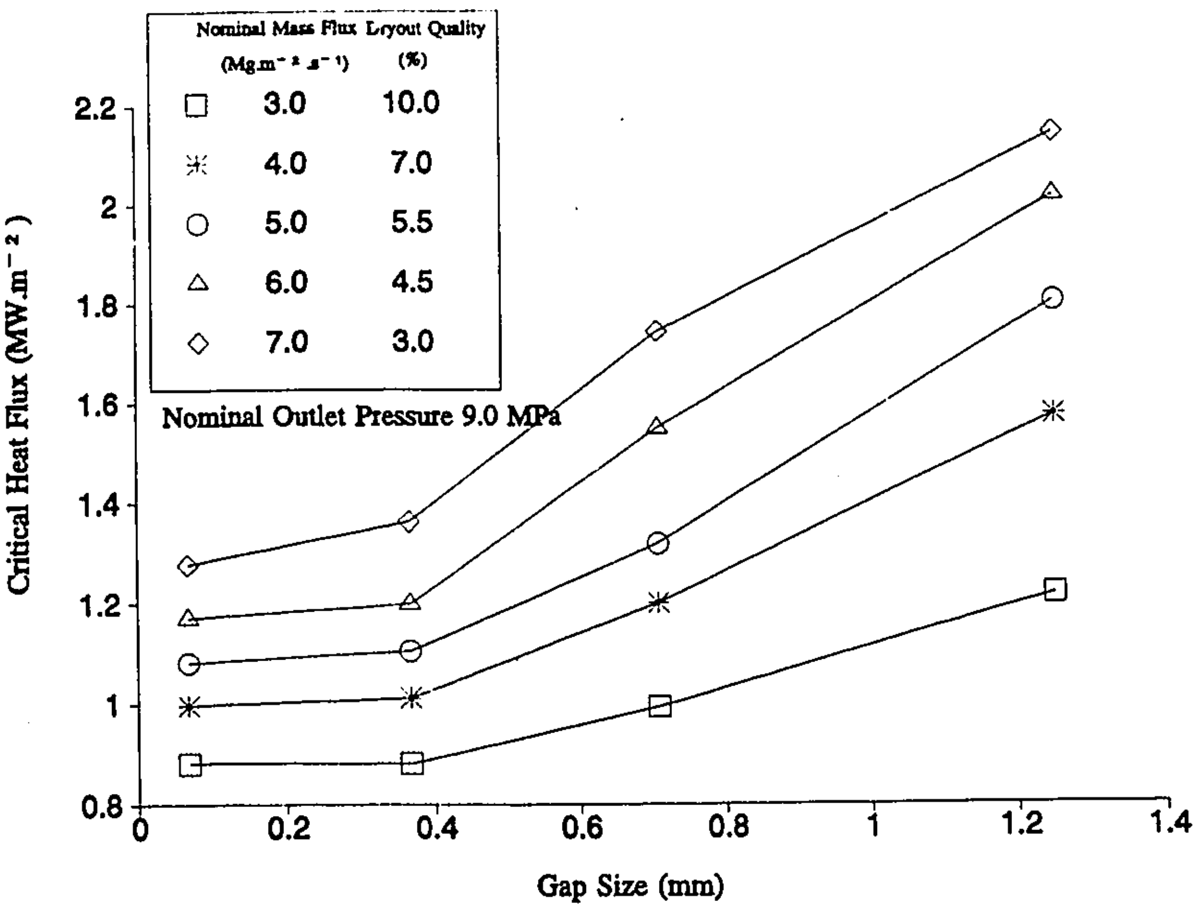

Figure 5.8: Effect of Minimum Gap Size and Mass Flux on CHF. CHF Data From Rudzinski [1992].

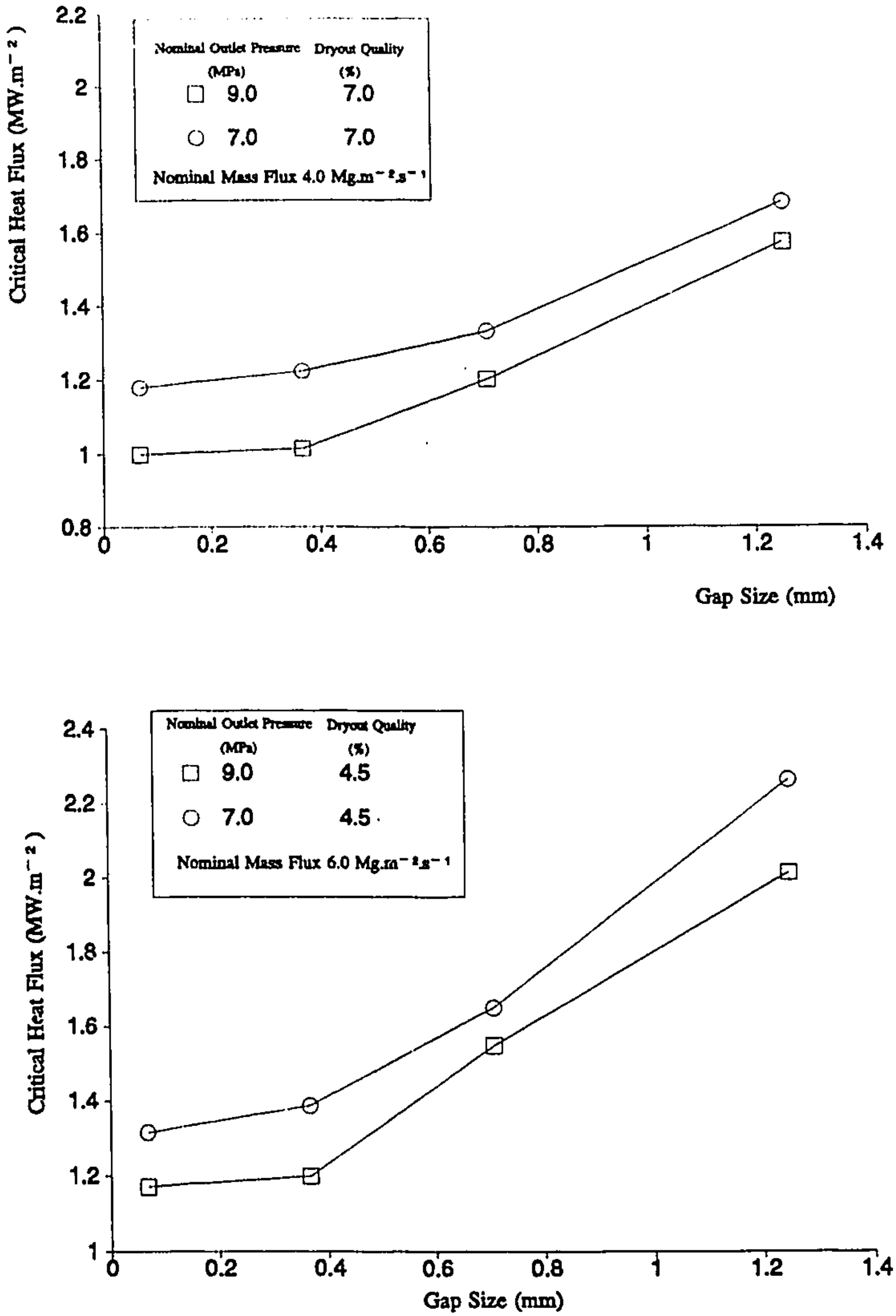

Figure 5.9: Effect of Minimum Gap Size and Pressure on CHF. CHF Data From Rudzinski [1992].

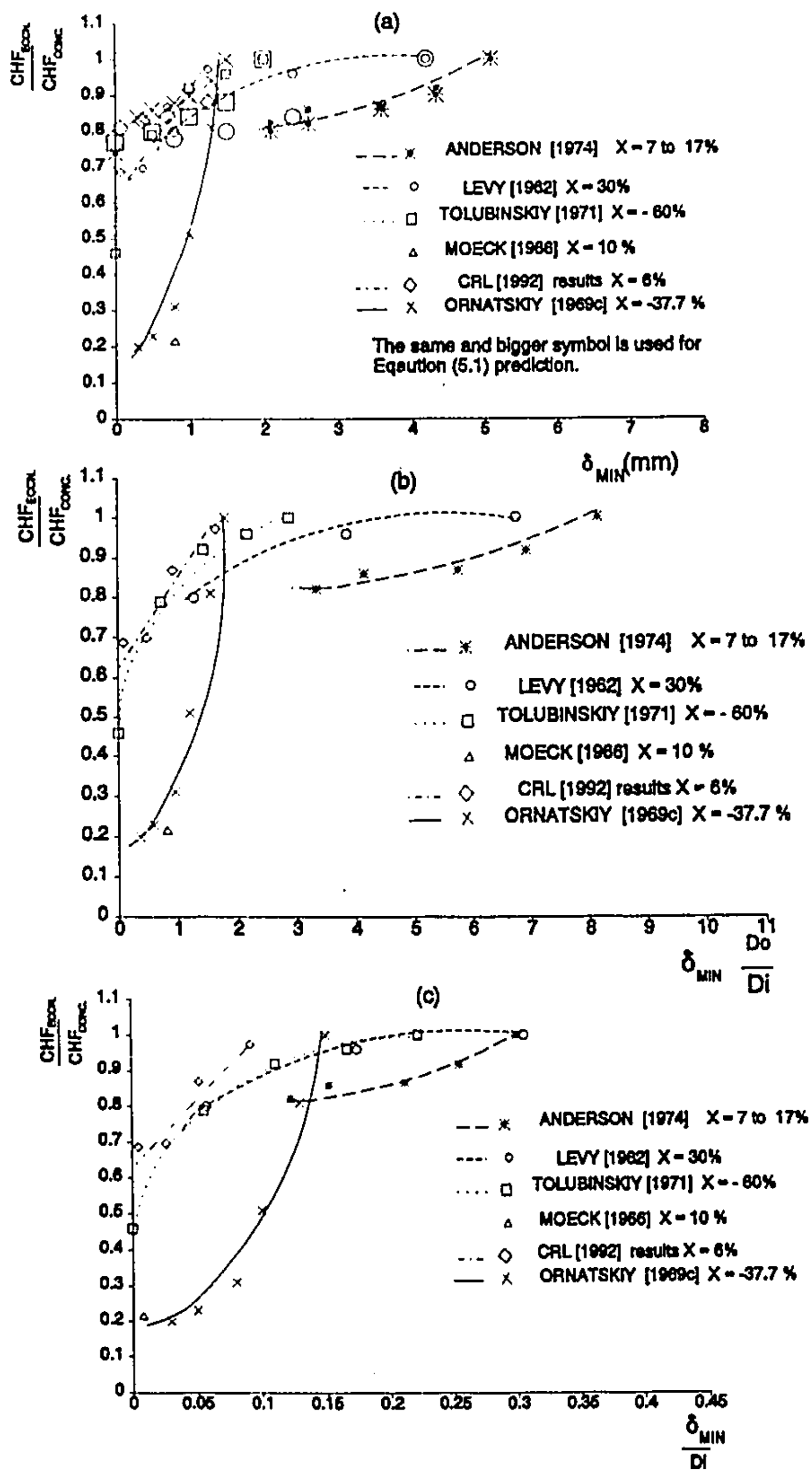

Figure 5.10: Some Geometric Parameters Considered and Their Effect on CHF.

6. OBSERVED GEOMETRIC EFFECTS: OTHER CROSS SECTIONS

6.1 Rectangular Channels

A summary of the work found in the literature for this geometry is presented in Table 6.1. Appendix C presents some of the rectangular channel CHF results.

De Bortoli *et al.* [1958] presented CHF data for gaps of 1.27 to 2.56 mm. Both the long sides of the rectangular channel were heated. A comparison with tube CHF data having the same inlet condition and L/D_{hy} shows that the CHF for round tubes is as much as 45% lower than for rectangular channels. The comparison would have been more useful if it had been based on the same local conditions. Pexton [1961] re-analyzed the previous data and reached similar conclusions. He also concluded that the CHF appears to increase with decreasing D_{hy} at constant local conditions.

Jacket *et al.* [1958] obtained CHF results in a rectangular channel heated from both long sides. The heated width (22.3 mm) was slightly less than the channel width (25.4 mm) to eliminate corner effects. There was good agreement between CHF results for rectangular channel (2.5 mm gap) with those of a round tube for the same local quality and equivalent diameter (D_{hy} and D_{he} were approximately equal).

Levy *et al.* [1959] considered the case of a rectangular channel where the complete perimeter was heated. As expected, overheating occurred at the corners of the test section where the CHF condition occurred at a value of about one-third of those obtained in a circular tube.

Gambill *et al.* [1961] reported that Kafengauz and Bauarov showed no effects of gap size on CHF up to a gap size that was comparable to the maximum bubble diameter. An assessment of the bubble sizes is performed in Chapter 8 to determine the gap size at which blockage of the cross section by bubbles might occur.

Chernobay [1970] investigated the CHF of a rectangular channel at very high mass velocities (G = 5 to 28 $Mg.m^{-2}.s^{-1}$) by varying the fraction of perimeter with maximum heat release from 16.7% to 100%. Chernobay concluded that the CHF values of uniformly heated rectangular channel (D_{hy}=D_{he}=2.4 mm) are noticeably lower than those of a 2-mm ID round tube for a constant inlet subcooling. This normally could be due to the corner effect, but this effect is thought to be less important at very high mass flux values, where mixing is much more effective. Moreover, the CHF increases as the fraction of perimeter with maximum heat release is decreased at constant inlet subcooling. The highest CHF values are obtained when only 17% of the perimeter is exposed to maximum heat release. Results suggest that, as the fraction of the perimeter with maximum heat release decreases, the CHF values for a rectangular channel approach those of a round tube.

Zeigarnik *et al.* [1981] (reporting on Zenkevich's *et al.* findings) concluded that the CHF for their rectangular channel (all sides heated) was 20% lower than that of an equivalent round tube. This was thought to be due to poor mixing at the corners, resulting in local over-heating. Zeigarnik also conducted an experiment in a horizontal channel with one side heating (D_{hy}=3.6 mm, D_{he}=7 mm) within the pressure range of 0.5 to 3 MPa. CHF results obtained from a uniformly heated, 4-mm diameter, round tube were in good agreement with the rectangular-channel results. At these high flow rates and high local subcoolings (see Table 6.2), the bubbles were extremely small and the flow was quite homogeneous. Hence, the differences in phase distribution and CHF between tubes and rectangular channels are expected to be small.

6.2 Irregular-Shaped Flow Geometries

Table 6.2 presents the related CHF studies on irregular-shaped channels or subchannels.

Rogers [1966] presented CHF results in two-element test section which simulated a portion of a 19-element reactor fuel bundle. It was found that CHF Type-I or -II (Departure from nucleate boiling) occurs locally in the gap region (hottest region) in the lee of a helical spacer near the downstream end of the test section.

Green *et al.* [1969] performed CHF tests for water on a "dumb-bell"-shaped channel (Figure 6.1), which consisted of two subchannels interconnected via a narrow gap. Their experiment covered the following range of conditions (Appendix C presents all the experimental results of Green *et al.* [1969]):

Pressure	:	8.3, 11.0 and 13.8 MPa
Mass Flux	:	0.339 to 5.425 $Mg.m^{-2}.s^{-1}$
Inlet Temperature	:	93 to 316°C

Two gap sizes (0.76 and 0.38 mm) were tested to simulate different rod-to-rod spacings of a nuclear fuel bundle. At low mass fluxes ($G < 0.7$ $Mg.m^{-2}.s^{-1}$), dryout was detected simultaneously at the gap and at the subchannel for the large gap size (0.76 mm) at all pressures, and for the small gap size (0.38 mm) at a pressure of 8.2 MPa only. For other conditions, dryout appeared only in the gap region. A comparison, presented in Figure 6.2, of these CHF data (dumb-bell-shaped channels) was made against the CHF data of De Bortoli et al. [1958], who tested two, 685.8-mm long, rectangular channels of dimensions 1.50x25.4 mm and 2.46x25.4 mm with heating along the 25.4 mm sides only. In general, the CHF for the dumb-bell-shaped channels agreed rather well with that for the rectangular channels at the same dryout condition. Hence, Green *et al.* concluded that the effect of channel spacing on CHF was negligible for gap sizes between 0.76 to 2.46 mm. However, this would not be the case if the two lobes of the dumb-bell were of different sizes. Then, enthalpy imbalance would become important and should be considered.

The CHF values of the look-up table for the same dryout conditions are also indicated in Figure 6.2 for comparison. Since the values of both the hydraulic and the heated diameter for these channels are much less than 8 mm, the table CHF values were corrected by

$$\frac{CHF_D}{CHF_{D=8}} = \left(\frac{8}{D}\right)^{1/3} \qquad (6.1)$$

A value of 3.8 mm was used as the diameter in Equation (6.1). It represents the hydraulic diameter of the dumb-bell-shaped channel with a 0.76 mm gap as compared to the values of 2.83 and 4.49 mm for the rectangular channels having 1.50 and 2.46 mm in height, respectively. Note that the hydraulic diameter cannot be calculated for the dumb-bell-shaped channel with a 0.38 mm gap, because the dimensions were not presented by Green et al. [1969]. The predictions based on the look-up table agree with the experimental data of these channels. This is rather surprising because the narrow gap is expected to affect the dryout mechanism significantly and causes a reduction in CHF. Apparently, the gap effect has some influence at high-flow conditions where the CHF is lower for these channels than for a tube.

Youk and Dimmick [1985] obtained CHF results in three different subchannel-shaped test sections: round, triangular and rectangular. They concluded that the effect of shape on CHF is important in the subcooled region (Type-II or Type-III CHF), but becomes less important as the quality increases and almost disappears in the high-quality region. Compared against the predictions of the W-3 and the Biasi correlations, the CHF results for the round-tube geometry were within a 5% error margin, but those for the rectangular and the triangular channels were lower by as much as 40% and 20%, respectively. Youk and Dimmick indicated that the reduction in CHF for both the rectangular and triangular channels is caused by a premature dryout due to local overheating in the presence of stagnant corners. A similar trend has been shown in the section 6.1 for rectangular channels.

Snoek [1988] performed an experiment to measure the CHF in an annular geometry. The test section consisted of a 1.19-cm ID Inconel tube and a 3-part triangular-shaped insert forming three subchannels interconnected by narrow gaps. Figure 6.3 shows schematically the configuration of this test section. The insert was placed either concentrically or eccentrically inside the tube. For the concentric configuration, the flow area of all subchannels and the size of all gaps are the same. The gap size is 1.76 mm. For the eccentric configuration, the flow area for two subchannels is the same, but it is smaller for the third subchannel. The small gap size is 1.0 mm. The total applied power was divided, with about 2/3 distributed to the tube and 1/3 to the insert, to ensure dryout occurred at the outer tube first. This resulted in a heat-flux ratio of 0.72:1 between the insert and the outer tube. No CHF instrumentation was provided for the inner surface (the assumption was that all surfaces would experience CHF at approximately the same heat flux level; a lower CHF for the inner surface as observed for the annular geometry was not considered). For the configuration with 3 equal subchannels, dryout was initially detected in the gap region between the subchannels at low-flow conditions, but in the subchannel region at high-flow conditions. Only a slight increase in power, however, is required to spread the dryout front to the subchannel, and gap respectively. The experimental results have indicated that CHF is not significantly affected by mass flux (except below 2 $Mg.m^{-2}.s^{-1}$) for the same dryout quality (Figure 6.4). This is rather different from the results obtained in a tube (Leung *et al.* [1990]): the tube CHF increases consistently with mass flux for the range of 3 to 10 $Mg.m^{-2}.s^{-1}$ at a dryout quality close to 0.33. For the case with 3 unequal subchannels, dryout is initiated in the small subchannel and small gap, and subsequently spreads to the larger subchannel and larger gap. The measured CHF is lower than that obtained in an equal-subchannel geometry for the same dryout condition. This reduction in CHF is consistent with an imbalance in flow and enthalpy between the subchannels.

6.3 Bundle Geometries

6.3.1 General

Midvidy [1976] reviewed the effect of element bowing and bundle eccentricity on CHF in bundle geometries. This review was recently updated by Rudzinski [1991]. Table 6.3 summarizes the observations and specifies the experimental range of conditions.

6.3.2 Tube-Equivalent Approach

An equivalent-tube approach is often used in the thermalhydraulic analysis of multi-rod bundle geometries. However, this approach is complicated by the fact that two possible values of equivalent diameter can be defined in a bundle: heated-equivalent and hydraulic-equivalent diameter. While a heated-equivalent diameter may simulate a correct rise in enthalpy, a hydraulic-equivalent diameter accounts more effectively for the flow or phase distribution for adiabatic flow. However, no matter how the equivalent diameter is defined it completely ignores effects of enthalpy imbalance. Moreover, these equivalent diameters when applied to annuli or bundles do not seem to simulate the CHF behaviour in tubes, which was described in Chapter 3. This is clearly illustrated by the experiments in eccentric annuli where a change in eccentricity affects the CHF without changing either D_{he} or D_{hy}. This is shown in the experiments of Moeck *et al.* [1966] and Janssen *et al.* [1963], who measured the CHF in annuli with a varying hydraulic-equivalent diameter (also the heated-equivalent diameter changes). They observed an increase in CHF with increasing hydraulic-equivalent diameter from 5.3 to 8.9

mm, but a decrease in CHF when the hydraulic-equivalent diameter was further increased to 22.2 mm as shown in Figure 4.1 of Chapter 4. The same trend can also be noticed if the analysis is based on the heated-equivalent diameter (i.e., CHF increased when the heated-equivalent diameter increased from 6.4 to 20.3 mm, but decreased with a further increase to 55.9 mm in heated-equivalent diameter). Neither of these trends agree with the observed diameter effect on CHF in tubes.

Heron *et al.* [1969] measured the effect of rod spacing on CHF in 7-rod bundles. They observed a significant change in CHF as the rod spacing varied. Lower CHF values corresponded to small gaps between rods. Since both the heated- and the hydraulic-equivalent diameters remained the same for various rod spacings, they concluded that equivalent-diameter approach does not adequately represent CHF in a bundle geometry. Other factors, such as rod spacing, have to be accounted for in CHF predictions for bundles.

6.3.3 Effect of Eccentricity and Element to Pressure-Tube Bowing

Midvidy [1976] concluded that the effect of eccentricity on a multi-element assemblies depended on the location of CHF when the assemblies are positioned concentrically in the flow tube. He noted that eccentricity reduced the cross-sectional average CHF when dryout occurred on an outer rod, but it had little effect when the dryout occurred on an inner rod.

Moeck *et al.* [1966], Tong *et al.* [1967], Lund [1975], Israel *et al.* [1969], Tolubinskiy *et al.* [1971], Nagino *et al.* [1978] and Markowski *et al.*

[1977] investigated the effect of rod bowing on CHF and concluded that bowing the heater did affect the CHF.

Howard [1963] performed experiments on a heater rod bowed to the point of making contact with the channel wall. This resulted in a CHF decrease by a factor of two or more from the values for the concentric position. Israel *et al.* [1969] also concluded that the CHF data obtained with a heater rod bowed towards the outer channel wall exhibit a substantial decrease from the concentric rod bundle.

In contrast with the previous studies, Heron *et al.* [1969], Macduff and Fighetti [1983], Nakajima *et al.* [1977], Hill *et al.* [1975], Groeneveld and Merilo [1974], Green *et al.* [1969], and Nixon *et al.* [1975] experiments indicated little or no effect of heater bowing on CHF.

Groeneveld and Merilo [1974] carried out experiments in three-elements rod bundle with Freon-12 as a coolant. One of the heater rods could be externally bowed towards the shroud reaching gaps between 1 and 0.06 mm. Their results indicated that the heater rod bowing had only a slight effect on the CHF.

Figure 6.5 shows the six configurations of the seven elements in the fuel bundle tested by Heron *et al.* [1969]. Figure 6.6 shows that the maximum decrease in CHF is obtained when having configuration A (all rods are touching). Little effect on CHF is observed when the gap between the outer rods and the shroud is reduced to a small values up to contact (configurations

E and F). This behaviour could be attributed to the enthalpy imbalance: little or no enthalpy imbalance would be expected in geometries E and F, but significant enthalpy imbalance would occur in geometries A and B, with less in C and D.

6.3.4 Effect of Element-Element Bowing and Element Spacing

Nagino *et al.* [1978] conducted CHF experiment (DNB type) with a sixteen-element rod bundle. One of central heater rods was bowed into contact with another rod. Their results indicated that at 10.5 and 12.7 MPa there was no effect of rod bowing on CHF, while at high pressure (14.8 and 16.9 MPa) there was a considerable decrease in CHF.

Lund [1975] carried out experiments at atmospheric pressure and for DNB type CHF in a five-by-five square rod array. He concluded that the DNB type CHF depends mainly on the local hydrodynamic conditions and it decreases as the rod spacing decreases.

Markowski *et al.* [1977] also obtained CHF data on a five-by-five square rod array for several bowing configurations. They reduced either the gap between two heated rods or between a heated and unheated rod. CHF data obtained with a heated rod bowed towards another heated rod indicate that the CHF is adversely affected only if the bowing is important (if the gap is reduced by more than 50% which implies that the inter-elements gap becomes less than 1.65 mm). They also concluded that moderate bowing of heated rods does not result in significant CHF decrease. However, bowing of an unheated rod towards a heated one has no effect on CHF, even if the unheated rod is bowed to contact adjacent heated rods.

Similarly, Macduff and Fighetti [1983] studied the effect of rod bowing in a five-by-five square rod array. They reduced the gap between two centrally located high-powered rods by 71% (the inter-elements gap was reduced to from 3.46 mm to 1 mm). Their results indicated that a pressure of 16.6 MPa, the effect on CHF was very little (about 5%) and no effect at 13.8 MPa.

Hill *et al.* [1975] performed CHF tests in a four-by-four square rod array, where one of the central heated rods was bowed into contact with the adjacent rods. They also concluded that a bowing effect is noticed only above a certain pressure (for their experiment higher than 12.4 MPa).

Nakajima *et al.* [1977] carried out CHF experiments in a 36-rod bundle to determine the effect of rod bowing. The minimum gap between the outer and the inner rod was reduced from 2.1 mm (nominal value) to 0 mm. Their results showed that rod bowing had only a slight effect on CHF over the range of conditions tested.

Nixon *et al.* [1975] tested a full-scale eight-by-eight rod bundle. They found that the effect of reduced gap and rod bowing had little or no effect on CHF over the conditions tested.

Analysis of the results of the reviewed investigations shows two conflicting trends on the effect of gap and rod bowing on CHF: (i) bowing of the heater rod has an effect on CHF, (ii) bowing of the heater has no effect on CHF. It seems that the effect of bowing is very much dependent on flow conditions (e.g., pressure) which might explain the contradiction. Also, from this study bowing a heated rod towards another heated rod is more likely to cause reduction in CHF than if the rod was bowed to the outer shroud. The lack of data relevant to CANDU conditions of interest and the conflicting results found in the literature indicates that further study is needed to reach better understanding of this effect. It would be extremely difficult to account for the effect of gap on CHF in rod bundles by a single empirical correlation. However, in Chapter 9 the gap effect on CHF is accounted for by introducing a gap correction factor. This factor would then be combined with an existing CHF correlation to predict the CHF for a bowed element in a subchannel code environment. The data obtained in the bowed-element experiments would be used to develop the gap correction factor, while the table look-up CHF prediction method presented by Groeneveld *et al.* [1986a] would be used as the reference correlation.

Table 6.1: Summary of Observed Geometric Effects in Rectangular Channels

References	Geometry		Conditions Range			Comments*
	Cross-section(mm)	L(mm)	G(Mg/m²s)	P(MPa)	X_e	
De Bortoli *et al.* [1958]	25.4x1.27, 25.4x2.56, 25.4x2.46, 25.4x1.50 & 25.4x1.40	152 to 685	0.0272 to 6.5	4.15 to 13.8	1.5 to 98.3%	The heated width was 22.8 mm. For the same mass velocity, inlet subcooling, pressure and L/D_h, the CHF for round tubes was as much as 45% lower than the rectangular channels. Comparisons should have been made for equal L/D_h in order to have the same local conditions.
Jacket, H.S. *et al.* [1958]	25.4x1.27, 25.4x1.40& 25.4x2.46	306 & 686	0.23 to 4.46	13.8	0.9 to 100%	The heated width was 22.3 mm (both sides were heated). CHF results were plotted versus mass velocity and compared with 4.75 mm round-tube data ($D_h = D_h = 2$ S where S is the channel spacing). Plots showed good agreement between round tube CHF values and rectangular results for the same mass flux inlet subcooling and D_h.
Levy *et al.* [1959]	63.5x2.54	457.2 & 914.4	1.63 to 14.4	0.448 to 1.379	ΔT_{sub} 50–111°C	Heating around the entire perimeter. Downward water flow. The CHF condition with steam blanketing occurred first at the corners of the channel and gave values considerably lower than those of the round tube.
Gambill and Bundy [1961]	26.9x1.09 & 25.4x1.45	305 and 477	2.72 to 23.1	1.1 to 3.93	ΔT_{sub} 14.5–36°C	The heated width was 25.4 mm. Downward water flow. Gambill reported that Kafengauz and Bauarov showed strong effects of gap size on CHF provided gap size is similar to maximum bubble size.
Tippets, F.E. [1962]	53.3x12.7 & 53.3x6.3	1493.94	0.244 to 1.953	6.9	3.3 to 67.8%	The heated width was 53.3 mm. First both long sides were heated and then just one side (D_h=25.4 or 50.8 mm). For fixed inlet subcooling the CHF increased as D_h increased. For fixed exit quality the CHF decreases as Dhe increases.

continued...

Table 6.1 (concluded)

References	Geometry		Conditions Range			Comments*
	Cross-section(mm)	L(mm)	G(Mg/m²s)	P(MPa)	X_i	
Chernobay, V.A. [1970]	3.6x1.8	70	7 to 40	4.9	sub. 40 to 150 K	Non-uniformly heated rectangular channel over the perimeter. For uniform heating, CHF values were lower than for round tubes. The CHF in rectangular channel increased with increasing heating non-uniformity: when heating one side only (1.8 mm) CHF results were close to round tube CHF data with uniform heating and equivalent hydraulic diameter.
Zeigarnik *et al.* [1981]	3.5x3.75 D_h=3.62 D_w= 14	200	4 to 25	0.5 to 3	Sub. 20 to 160°C	Horizontal test section with one-side heating (3.75 mm). Within the investigated range the dependence of CHF on mass flux and inlet subcooling proved to be similar for a rectangular channel with one side heating and a round tube with uniform heating and equivalent hydraulic diameter.

* All these references are for vertical upflow of water and uniform AFD, unless otherwise specified.

Table 6.2: Effect of Shape

References	Geometry*		Conditions Range			Comments+
	D_{hy} (mm)	L (mm)	G ($Mg.m^{-2}s^{-1}$)	P(MPa)	X_e	
Collier, J.G. _et al._ [1964]	Annulus type with irregular outer surface	610	0.11 to 0.30		10 to 80%	Two-phase inlet. Gap sizes of 5.08 and 1.7 mm were used between the inner core and the outer copper-rod profile. Heating both surfaces of the duct (increasing the outer-surface heat flux) resulted in an increase of the CHF as compared to heating only the inner surface.
Green, S.J. _et al._ [1969]	Dumb-bell-shaped flow channel (Fig. 6.1)	1219	0.33 to 3.6	8.3 to 13.8	-17 to 93%	Minimum gaps were 0.762 and 0.381 mm. The test results indicated that there was negligible effect of the channel spacing on the CHF. Results were in agreement with data obtained for rectangular channel with spacing of 1.27 and 2.46 mm (Fig. 6.2).
Youk and Dimmick [1985]	6.91 for the circular and rectangular channels, and 6.64 mm for the triangular one	550	1 to 6	1.25 & 1.08	-20 to 20%	Freon-12 was the cooling fluid. Test-section cross section were circular, triangular and rectangular. In the subcooled region, the CHF was reduced up to 38% in non-circular geometries. The shape effect almost disappeared in the high-quality region. The CHF always occurred first at the corners. For Type-II or -III CHF (DNB), the shape effect has to be considered.
Snoek, C.W. [1988]	5.1 for the channel. The outer-tube diameter is 11.9	1500	1 to 7	9.6	10 to 80%	Subchannel configurations were formed by placing a triangular insert inside a vertical tube (Fig. 6.3). About 67% of the total power was dissipated in the outer tube, to ensure that dryout would occur at the outer surface. For constant quality, the CHF increased with a decrease of flow, especially at high qualities and low flow rate. Using the equal-subchannel data, a formulation was developed to correct the predicted CHF value from the CHF look-up table, using different constants for the gap and subchannel geometry.

* D_{hy} and L are the hydraulic-equivalent diameter and the heated length of the channel, respectively.
\+ All these references are for vertical upflow of water and uniform AFD with internal heating, external heating or dual heating, unless otherwise specified.

Table 6.3: Summary of the Effect of Element to Element Gap on CHF. From Rudzinski [1991].

References	Assembly Geometry					Operating Conditions			Remarks
	No. of Elements	Element Spacing (mm)	Flow Tube Diameter (mm)	Element O.D. (mm)	P/T Element Gap (mm)	G ($Mg/m^2 s$)	P (MPa)	X_e	
Kobori [1976]	28	1.75-2.2	117.8	16.25-16.81	1.2	0.03-3.0	6.87	10 to 65%	Vertical Orientation. Full-Scale Bundle tests. Small eccentricity markedly lowered CHF.
Midvidy [1976]	-	-	-	-	-	-	-	-	Literature review of CHF in rod bundles.
Israel *et al.* [1969]	16	3.3	73.7 x 73.7	14.3	3.3,1.5 2 & 2.3	0.7-2.44	6.9	-.5 to 33%	Vertical Orientation. Rod bundle skewed to one corner of a square flow channel. Test results indicated that reduced rod-to-shroud gap reduces CHF.
Nixon *et al.* [1975]	64	3.71, 2.54 & 1.45	-	-	-	0.34-1.7	6.9	-	Vertical Orientation. Square flow channel. Gap between rods reduced. Found no effect of reducing gap on CHF.
Hill *et al.* [1975]	16	3.38	-	10.72	-	1.9-4.8	10.4 to 16.5	-6 to 20%	Vertical Orientation. Square flow channel. Rod to rod bowed to contact. CHF decreased with decreasing gap size, but only when pressure greater than 15 MPa.
Nakajima *et al.* [1977]	36	2.1-0	117.8	14.72 & 9.74	-	1.3 to 2.6	7.0	30 to 60%	Vertical Orientation. Bundle eccentrically located in flow channel. The minimum gap between the outer and inner rods was reduced variously to 1.6 mm, 1.0 mm and zero. Tests indicated that element bowing decreased CHF slightly -1 to 2%.
Lund [1975]	25	2.51	83.82 x 83.82	13.75	2.52	2.5-6.3	0.09-0.13	Subcooled	Vertical Orientation. Down flow of water in a square channel. Corner rod bowed towards inner rod. The authors concluded that CHF is reduced at small rod spacings.

continued...

Table 6.3 (concluded)

References	Assembly Geometry					Operating Conditions			Remarks
	No. of Elements	Element Spacing (mm)	Flow Tube Diameter (mm)	Element O.D. (mm)	P/T Element Gap (mm)	G (Mg/m^2 s)	P (MPa)	X_e	
Macduff and Fighetti [1983]	24+1	3.46	65.1 x 65.1	9.14	2.79	2.0-4.1	13.8-16.5	-	Vertical Orientation. Square flow channel. Gap between two central rods reduced to 71% of nominal. Reducing the gap to 50% of nominal had no effect on CHF. Reducing the gap to 71% of nominal had a small effect on CHF.
Heron et al. [1969]	7	0-6.3	60.45	15.88	0.14-6.41	0.88-2.6	1.1	-20 to 50%	Vertical Orientation. Used Freon-12 as coolant. Decreasing the gap between elements decreased CHF. Results are difficult to interpret since both rod-to-shroud gap as well as rod-to-rod gap were varied in each experiment.
Nagino et al. [1978]	16	3.4	-	10.7	-	2.0-4.7	10.5-17.0	-35 to 15%	Vertical Orientation. Center rod bowed into contact with either two heater rods, one heater rod, or a cold rod. No effect of rod bow to contact until pressures greater than 15 MPa.
Groeneveld and Merilo [1974]	3	1.02	33.27	13.97	1.02-0.06	0.81-3.0	1.1	10 to 85%	Vertical Orientation. Used Freon-12 as coolant. Bowing heated rod towards unheated shroud had little effect on CHF.
Green et al. [1969]	1	0.76 & 0.38	-	8.60	-	0.33-3.6	8.3-13.8	--10 to -98%	Vertical Orientation. Dumbbell-shaped test section made from a round tube. Found negligible effect of reducing gap from 0.76 mm to 0.3 mm.
Markowski et al. [1977]	21	3.55, 1.65 & 0	79.96 x 79.96	11.18	3.43	1.36-4.07	12.1-16.5	-16 to 20%	Vertical Orientation. Heated rods bowed to contact. CHF decreased when gap between heated rods reduced by more than 50%. Bowing an unheated rod into contact with heated rod had no effect on CHF.

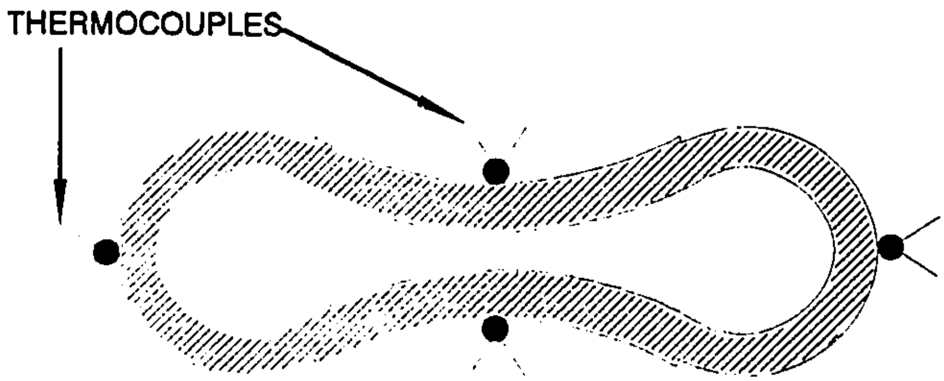

Figure 6.1: Dumb-Bell-Shaped Channel Tested by Green *et al.* [1969].

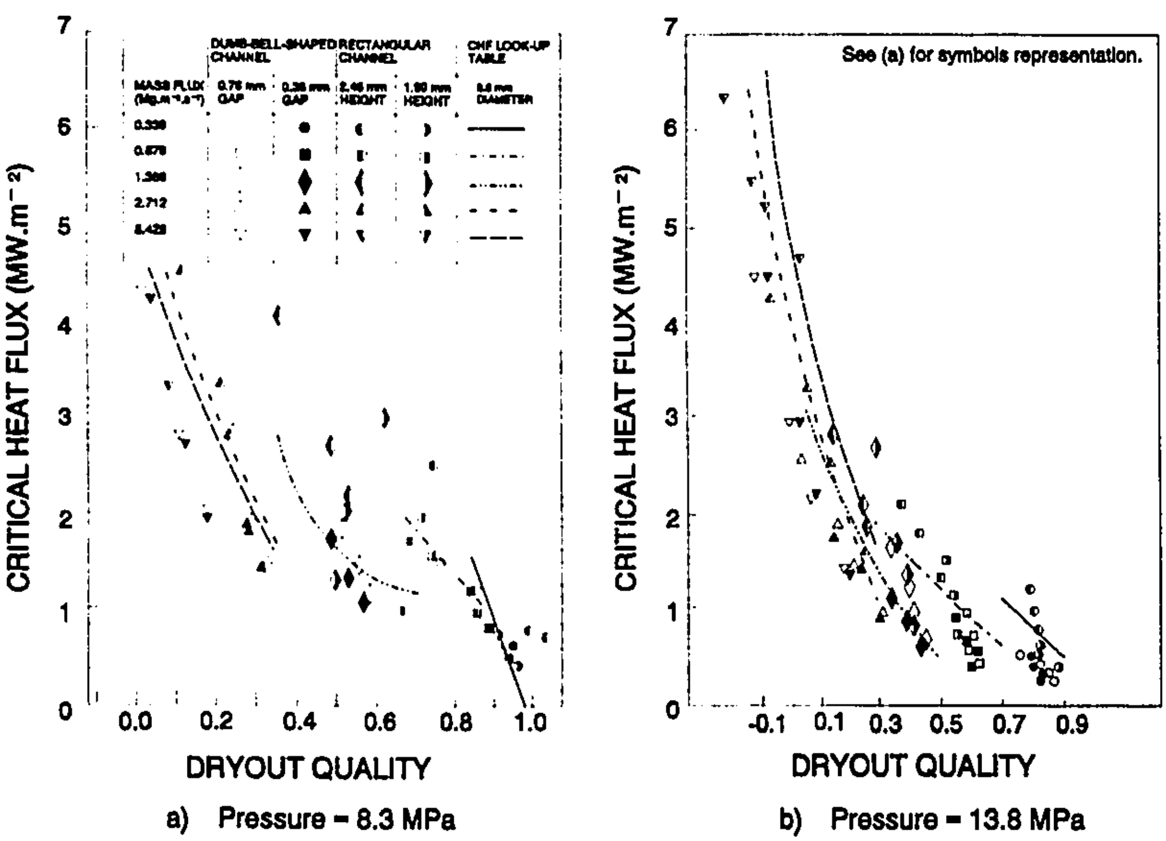

Figure 6.2: Comparison of CHF Data Between the Dumb-bell Shaped and Rectangular Channels.

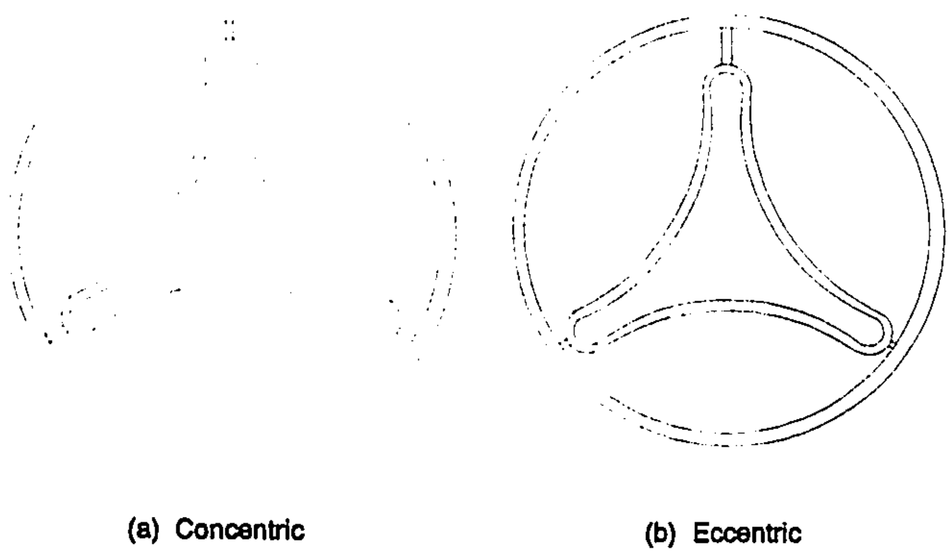

Figure 6.3: Subchannel-Shaped Channel Tested by Snoek [1988].

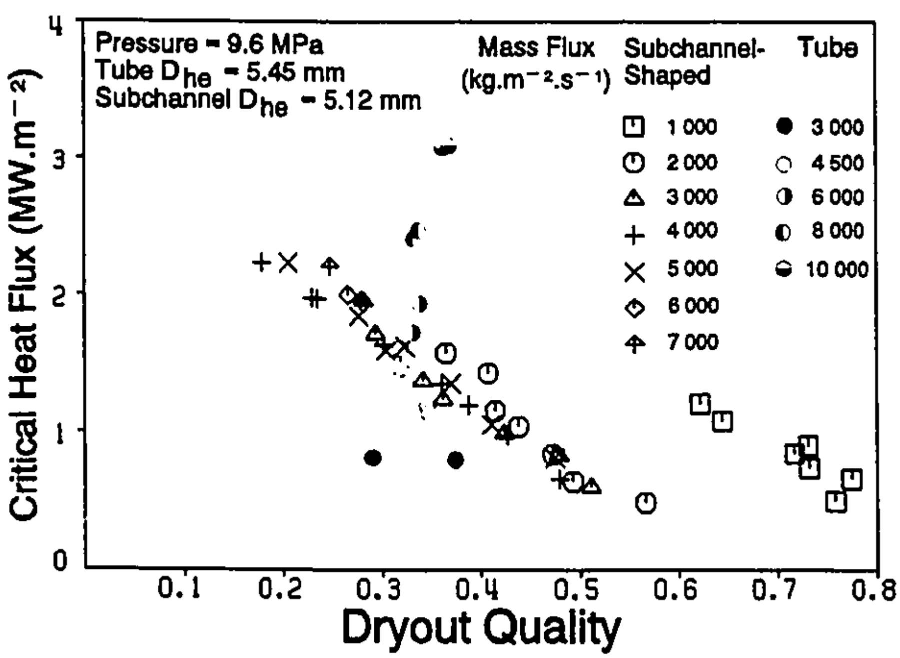

Figure 6.4: Comparison of CHF Data Between the Subchannel-Shaped and Tube Geometries.

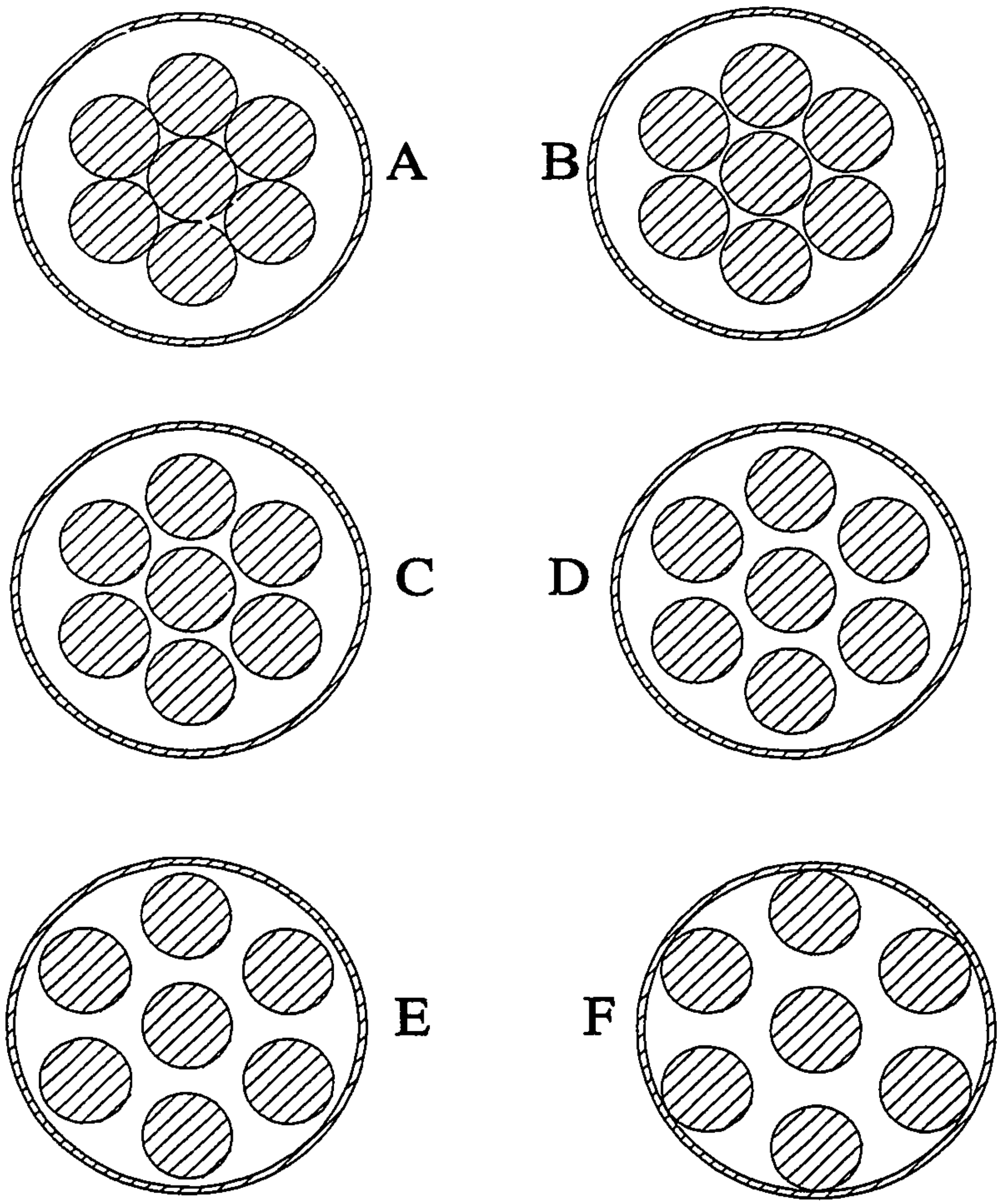

Figure 6.5: Arrangement of Rods in the Configurations Tested by Heron *et al.* [1969]

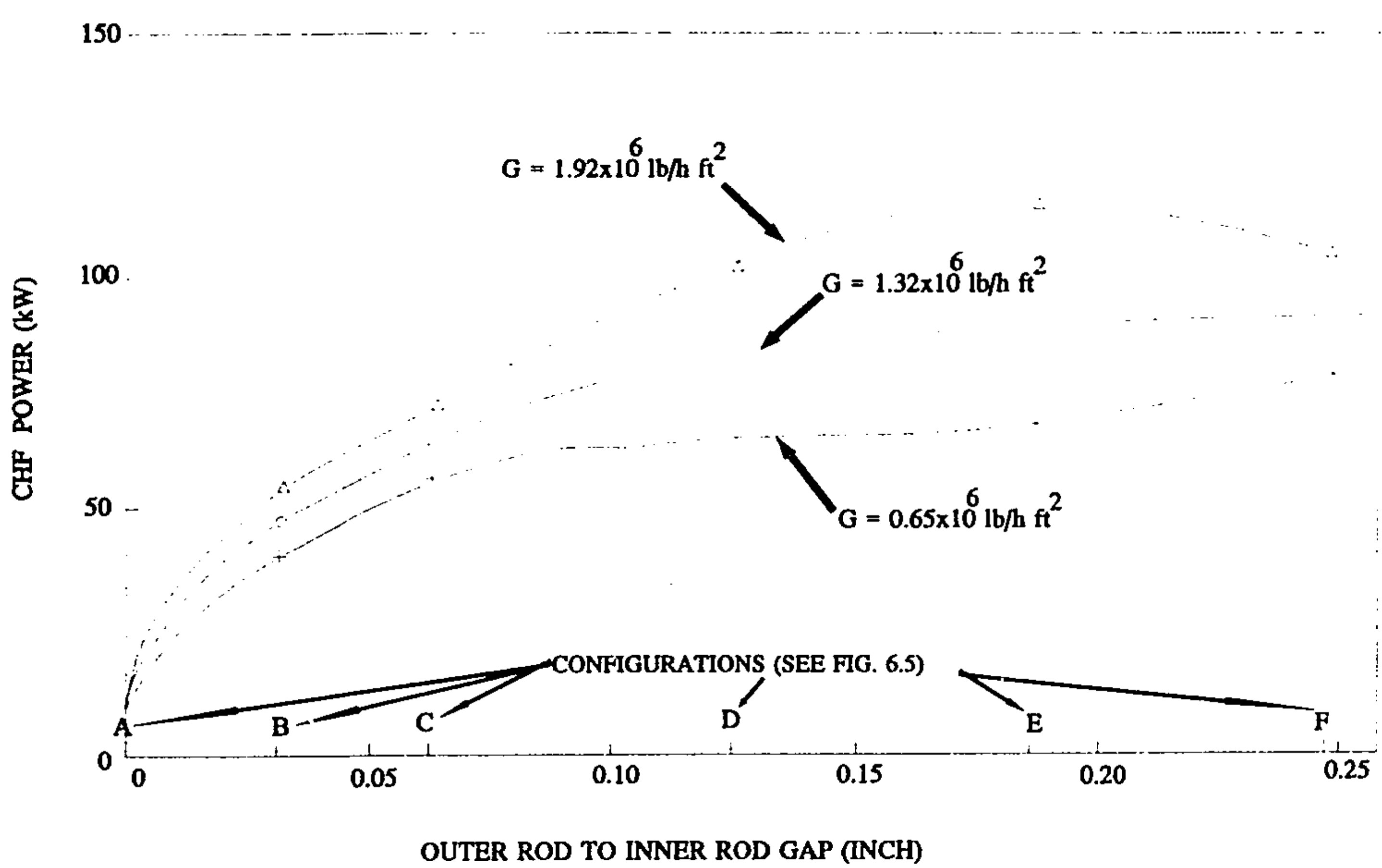

Figure 6.6: Effect of Gap Between Rods on CHF for $\Delta hi = 0$. From Heron et al. [1969]

7. EFFECT OF HEAT FLUX ON ADJACENT SURFACE

7.1 Bilaterally Heated Annuli

The effect of changing the ratio of inner-rod/outer-tube heat flux on the CHF has been studied by several investigators: their results are summarized in Table 7.1. Some Experimental results for concentric bilaterally heated annuli are tabulated in Appendix D.

Becker and Letzter [1975] performed the most detailed investigation on the effect of bilateral heating in annuli. They varied the ratio of outer tube to the inner rod heat flux, R, gradually from 0 to 4 for a constant inlet temperature. For low ratios, the CHF always occurred first on the inner surface. Simultaneous occurrence of CHF was observed to occur for a ratio somewhere between 1.5 and 2.75 (depending on the flow conditions); this corresponds to a maximum in critical quality. At higher heat-flux ratios, the CHF eventually moves to the outer wall. Their study applies only to Type-IV and Type-V CHF (i.e., entrainment-controlled and deposition-controlled CHF). The results of a more detailed analysis of Becker's results are shown in Figures 7.1 to 7.3. These figures show the effect on CHF of gradually changing the heat-flux ratio, R. For lower ratios, when CHF occurs on the inner surface, the CHF is close to that of an internally heated annulus (the solid line corresponds to the prediction for internally heated annuli). A trend of increasing CHF above that of an internally heated annulus can also be noticed, especially for higher heat-flux ratios. A significant jump in CHF occurs for a ratio between 1.5 and 2.75, corresponding to the simultaneous occurrence of CHF on both surfaces. The critical quality also reaches a maximum value (during the experiment, the inlet subcooling remains constant). For higher heat-flux ratios, the CHF occurs only on the outer surface at a value much closer to that of a tube.

Becker and Hernborg [1964] performed experiments on a 608 mm long, bilaterally heated concentric annulus. The results of this experiment were presented by Becker *et al.* [1965]. The analysis of the results showed that, when applying equal heat fluxes on both walls of the annulus, CHF always occurred at the inner wall. When the annulus was heated internally only, the data showed lower CHF values compared to bilateral heating. For external heating, the data were higher than for internal heating, and somewhat comparable to round tube CHF results. For bilateral heating, it was found that the outer surface heat flux can be from 30% to 70 % higher than the inner surface heat flux before the CHF moves to the outer surface. The interpretation given for the preferential occurrence of the CHF on the inner surface is based on the asymmetric distribution of the flow. They assumed that the same asymmetry present in single-phase turbulent flow, is also valid for two-phase flow: the maximum velocity occurs closer to the inner surface than the outer surface. The shear stress ratio is obtained from a force balance

$$\frac{\tau_i}{\tau_o} = \frac{r_o}{r_i}\left(\frac{r_m^2-r_i^2}{r_o^2-r_m^2}\right) \tag{7.1}$$

where r_m is the radius of maximum velocity given by

$$r_m^2 = \frac{r_o^2-r_i^2}{2\ln\left(\frac{r_o}{r_i}\right)} \tag{7.2}$$

Substituting the annulus dimensions for this experiment gives r_m = 6.74 mm and τ_i/τ_o=1.21. From this ratio it is seen that the interfacial shear stress on the liquid film flowing at the inner wall is higher than the one for the outer wall (this has been also observed by Rogers [1966]). Since, the range of the quality corresponding to this experiment is for Type-IV or Type-V CHF (film dryout), then a higher shear stress results in an increase of the entrainment rate and a faster film dryout. This interpretation cannot be used in the case of Type-II or -III CHF, where a higher interfacial shear stress results in a better bubble transport between the wall and core region, which would enhance the CHF.

From the experimental results of Becker *et al.* [1965] an attempt is made to separate the curvature effect. Figures 7.7 and 7.8 show the differences between CHF occurring at the outer surface and the inner surface for external heating and internal heating respectively. From the two figures it can be seen that the CHF for internally heated surface occurs at lower quality than the CHF for externally heated surface for the same inlet conditions. For the same exit quality the CHF at the inner surface is lower than the outer surface CHF as mentioned before. This difference seems to vanish at high pressure (14 MPa) and mass flux, where the CHF for both surfaces occur at approximately the same exit quality. This implies that the effect of curvature for high pressure and mass flux is less important; at these conditions the flow can be considered to be homogeneous and the CHF mechanism becomes different from the other conditions. This effect of curvature on CHF can be interpreted as follows: Whalley [1989] mentioned that the entrained droplets travel in straight line in the radial direction, from the point where they are entrained to the point where they are deposited (the actual behaviour is more complex, since this assumes that the entrained drop does not hit another drop, or is not affected by turbulence). In case of annuli a droplet entrained from the inner surface (convex) cannot be deposited at the same surface, it will necessarily hit the facing surface (concave) or remain entrained. However, a droplet entrained from the outer surface can be deposited at either surface. Hence, for the annular flow regime (CHF Type-IV and -V) the liquid film will be depleted faster for a convex heated surface (i.e., lower CHF for the internal surface of the annuli). This also explains the fact that the discrepancy between the CHF occurring at the outer surface and the inner surface of the annuli is less severe at low quality and subcooled conditions, where this interpretation is no longer valid because of the difference in the CHF mechanistic description at these conditions.

Jensen and Mannov [1974] also studied bilaterally heated annuli and observed similar trends as Becker and Letzter: the heat flux at the outer surface is higher than at the inner surface when the CHF moves to the outer surface. The maximum dryout quality and hence dryout power corresponds to the simultaneous occurrence of CHF (which occurs when approximately 70% of power is dissipated from the outer surface). Their results are plotted in Figure 7.4 as the critical quality versus the outer tube power fraction.

Kirrilov and Smogalev [1974] presented two plots for different mass fluxes showing the effect of bilateral heating: Figure 7.5 demonstrates an increase in inner-surface CHF due to the presence of a heat flux at the outer surface. Figure 7.5 also shows that, as the outer-surface heat flux is increased, the CHF which was initially below the annuli prediction (solid line) increases towards this prediction line and may exceed it at high qualities. Moreover, increasing the mass flux and/or decreasing the quality results in a decrease of the effect of the outer-surface heat flux on CHF. Kirillov and Smogalev's data apply primarily to Type-IV CHF (entrainment controlled).

Tolubinskiy *et al.* [1973b] investigated the effect of bilateral heating at high pressures (15-20 MPa) and high subcoolings. They concluded that the presence of a heat flux at the outer surface does not affect the CHF at the inner surface, and that the CHF on the inner surface is higher than the CHF on the outer surface. These results disagree with Becker's, Jensen's, and Kirillov's results, which is not surprising as the flow conditions are also quite different. The same correlation (Equation 7.1) for the shear stress ratio as given by Becker and Hernborg is given by Tolubinskiy *et al.* [1973a]. He also concluded that, the radius corresponding to maximum velocity in an annulus, r_m, is shifted to the inner wall and also given by Equation (7.2). Moreover, Tolubinskiy assumed that:

$$\frac{CHF_i}{CHF_o} = \left(\frac{\tau_i}{\tau_o}\right)^n \tag{7.3}$$

also assuming n=1 they reached the conclusion that the CHF at the inner wall is higher than at the outer wall. A different value of the exponent n (0.5) has been assigned by Tolubinskiy *et al.* [1970a]. Though this conclusion supports the results of Tolubinskiy [1973b], it contradicts most of the other studies.

Alekseev *et al.* [1965] stated that, for pressures between 9.81 and 14.72 MPa and for the same local conditions, the CHF for an annular channel heated from both surfaces was higher than for the case of one-side heating.

Ornatskiy *et al.* [1969] reached contradictory results: the CHF at the outer surface is independent of the heat flux applied to the inner surface, even when the inner heat flux surpasses the outer one. Results are well correlated (within ± 15%) using an expression derived for the case of external heating by Ornatskiy *et al.* [1966]. However, Ornatskiy only considered highly subcooled CHF data at pressures greater than 17 MPa.

7.2 Rectangular Channel

Tippets [1963] performed experiments in a rectangular channel where either one or both long sides were heated. Collier [1981] plotted Tippets' data as shown Figure 7.6 to which the CHF table values for the heated equivalent diameter, hydraulic equivalent diameter and the 8-mm tube were added. Note that (i) heating the opposite surface increases the CHF for D_{hy} = 20.6 mm (or 12.7 mm spacing), (ii) decreasing the gap to 6.35 mm increases the CHF noticeably for both long surfaces heated, and (iii) overall the CHF table values for the 8-mm tube without any diameter correction fit better the rectangular CHF data than the CHF table values corrected to the D_{he} or D_{hy} using Equation (6.1).

7.3 Other Geometries

Collier *et al.* [1964] observed effects on CHF of the proximity of an adjacent heated surfaces, in a cross section consisting of a centrally heated rod surrounded by an outer-surface which simulated several other adjacent rods. Two sizes of spacings were considered: 1.7 and 5 mm gaps. An increase in the outer surface heat flux resulted in an increase of the rod CHF for constant exit quality. However, the effect of bilateral heating appeared less strong for the smaller gap size. Also, the CHF values were lower for the smaller gaps. According to Collier, this increase in CHF with outside-surface heating results only from an increase in film-flow rate by extra deposition or less entrainment. Two explanations are offered in terms of the nucleate-boiling entrainment mechanism described by Hewitt *et al.* [1963]. First, Collier suggested that "the introduction of the additional heating on the quadrants causes the quality to rise more rapidly along the channel and would lead to the suppression of some of the active sites on the centre rod. Consequently, less liquid would be lost from the rod and the burnout heat flux increased." The second explanation is that droplets ejected from the outside surface hit the centre rod, and hence the film flow rate on the rod will increase.

The effect of an unheated wall on CHF was studied by Tong *et al.* [1967] using a heated rod inside a square flow channel with subcooled and low-quality steam-water flows. Their results showed that the proximity of an unheated wall as well as a rod in line contact with an unheated wall decreased the CHF. This decrease in CHF decreased as the mass flux increased and became minimal at mass fluxes greater than 4.1 $Mg.m^{-2}.s^{-1}$. To account for the effect of the unheated wall, a modification factor as a function of D_{he} and local quality was developed.

Tong [1972] has related the CHF for an annulus with that of a tube as predicted using the W-3 correlation:

$$\frac{CHF_{unheated\ wall}}{CHF_{W-3,D_{he}}}=1.0-(1-\frac{D_{hy}}{D_{he}})\ [13.76-1.372\ e^{1.78x} -4.732(\frac{G}{10^6})^{-0.0535}-0.0619(\frac{P}{10^3})^{0.14}-8.509D_{he}^{0.107}] \tag{7.4}$$

where $CHF_{W-3,Dhe}$ is calculated with the W-3 correlation based on D_{he} rather than D_{hy}. The correlation uses British units. The range of data used to develop this correlation is given by:

$X_c \leq 0.1$

$1.356 \leq G \leq 6.78$ $Mg.m^{-2}.s^{-1}$ ($1.0 \leq G \leq 5.0$ $lb.h^{-1}.ft^{-2}$)

$6.895 \leq P \leq 15.858$ MPa ($1000 \leq P \leq 2300$ psia)

$L \geq 254$ mm and $\delta \geq 2.54$ mm ($L \geq 10$ in and $\delta \geq 0.1$ in)

Because of the relatively narrow range of qualities this correlation cannot be used generally, and thus has a limited range of applicability. According to Tong [1972] the presence of an unheated wall causes a build up of a cold liquid film on the unheated wall. He concluded that " the cold film is considered wasted or bypassed. Thus, the CHF in a tubular flow channel with one side of unheated wall is usually lower than that in a channel with all sides of heated wall at a same bulk exit enthalpy".

7.4 Discussion

An explanation of the higher CHF on the outer surface of an annulus has been offered by Becker and Hernborg [1964]. They suggested that the asymmetric velocity distribution for single-phase flow is also the case for two-phase flow. This asymmetry results in a higher interfacial shear stress on the liquid flowing at the inner-wall. The higher shear stress at the inner wall increases the rate of entrainment, leading to a faster dryout of the inner liquid film compared to the outer one. This phenomenon is less important for lower qualities, where the CHF is usually closer to that of a directly heated tube.

An explanation for the observations made by Tolubinskiy [1973b] (higher CHF on the inner surface than on the outer one and absence of any noticeable effect of outer surface heating on the inner surface CHF occurrence), can be attributed to differences in flow conditions. The proposed explanation in terms of entrainment behaviour offered by Becker and Hernborg obviously does not apply to subcooled conditions, but the increase in inner wall shear stress for subcooled boiling will result in better mixing and bubble removal from the inner surface, thus increasing the CHF for that surface.

In general, in the case of annuli, the CHF occurs preferentially on the inner surface at a heat-flux level well below that of a tube. Also, the presence of an outer-surface heat flux generally increases the inner-surface CHF: Collier [1964], Alekseev [1965], Tong [1972] and Kirillov [1974] reported such an increase, although Tolubinskiy reported no noticeable effect. It may be that this increase becomes less noticeable for higher flows, higher pressures and low qualities.

In Tippets' [1963] experiment with rectangular channels, high-speed motion pictures showed that the film thickness at the unheated wall was larger than the heated one. The liquid film appeared to be much less agitated at the unheated wall than at the heated wall. As the CHF condition approached, there was an increase of the film agitation at the heated wall.

At high flow rates, high pressures and high local subcoolings, bubbles are extremely small and the flow is more homogeneous. Hence, the differences in phase distribution and CHF between various geometries (tubes, rectangular channels and subchannels) whether heated from one-side or bilaterally, should be small.

Table 7.1: Effect of Bilateral Heating

References	Geometry*		Conditions Range			Comments*
	D_i/D_o (mm)	L(mm)	G(Mg/m²s)	P(MPa)	X_c	
Collier, J.G. et al. [1964]	Annulus type with irregular outer surface	610	0.11 to 0.30		10 to 83%	Two-phase inlet. Gap sizes of 5.08 and 1.7 mm were used between the inner core and the outer copper rod profile. Heating both inner and outer surfaces resulted in an augmentation of the inner surface CHF, compared to heating only the inner surface.
Becker and Hernborg [1964]	9.92/17.42	608	0.071 to 0.961	0.85 to 3.7	10 to 91%	In the case of equal heat flux on both walls, CHF occurred in the inner wall and the CHF results were the closest to those of a round tube. For internal heating only, lower CHF values were obtained. CHF results were closer to round tubes for external heating only. The outer wall heat flux was 30 to 70% above the inner wall one before the CHF changed position from the inner to the outer wall. The highest critical qualities were obtained when CHF occurred simultaneously on both surfaces.
Becker, K.M. et al. [1965]	9.92/17.42, 10.05/17.42 & 9.96/24.95	608 & 1216	0.050 to 0.966	0.85 to 3.7	10 to 91%	The report contains CHF data obtained for flow in vertical round tubes, annuli and 7-rod clusters. The annuli data were obtained for external heating only, internal heating only and bilateral heating. Becker and Hernborg [1964] used part of the annuli data presented in this report.
Alekseev, G.V. et al. [1965]	12.0/15.0	200	3.92 to 19.62	up 3.3		The CHF values in an annular duct with heating on both sides were higher than the CHF values for one-side heating at constant local conditions. The CHF at the inner surface increased as the heat flux from the opposite surface rose.
Tong, L.S. et al. [1967]	Rod dia. 10.0 Square sleeve: 15.0x15.0, 15.0x17.0 & 15.0x18.0	724	1.36 to 4.88	13.8	-18.1 to 5.4%	CHF Type-III. The test section consisted of a heater rod in the centre of square sleeve. Tong concluded that the decrease in CHF due to proximity of unheated wall is reduced by introducing turbulence promoters (e.g., roughness). Tong also reported that the CHF decreased when the rod was in line contact with the sleeve. However, this decrease became less important for higher mass flux.

continued...

Table 7.1 (concluded)

References	Geometry*		Conditions Range			Comments•
	D_i/D_o (mm)	L(mm)	G(Mg/m²s)	P(MPa)	X_c	
Ornatskiy, A.P. et al. [1969b]	10.0/12.0, 10.0/13.0 & 10.0/14.0	140	0.5, 1.0, 2.0 & 3.0	17.2, 18.6, 20.2 & 21.6	-60 to 10%	CHF results at the external surface were independent of the heat flux applied to the inner surface (even when the inner heat flux exceeded the outer surface heat flux). Within the given range of parameters, results were satisfactorily correlated using an expression developed by Ornatskiy et al. [1966] for externally heated annuli (within ± 15%).
Tolubinskiy, V.I. et al. [1973b]	9.0/13.0	100 to 400	0.5 to 1	15 to 20	sub. to 30%	The outer-surface heat flux did not affect the inner surface CHF within these conditions!
Kirillov and Smogalev [1974]	7.1/12.5		1.1 & 2.2	5.0	5 to 30%	Two correlations were developed for annuli: one for internal heating and the second for bilateral heating. For the same local conditions, heating the outer surface resulted in an increase of the inner-surface CHF.
Jensen and Mannov [1974]	17.0/26.0	3500	0.6, 0.8, 1.0, 1.2 & 1.4	6.9	20 to 90%	Results were plotted as X_c versus the outside wall power to the total power ratio. Graphs showed the same trend as the ones obtained by Becker [1975]: for equal heat flux, the CHF occurred at the inner surface. The highest critical quality was obtained when the CHF occurred simultaneously at both surfaces.
Becker and Letzter [1975]	12.0/21.3	3000	0.25 to 4.0	3, 5, 7, 10 & 14	10 to 100%	For equal heat flux, the CHF condition occurred at the inner surface. The heat flux applied to the outer surface could be increased substantially before the CHF occurred at the outer wall (up to 2.39 times higher than the inner wall heat flux). When the CHF occurred simultaneously on both surfaces, the highest critical quality was obtained.

* D_i, D_o, and L are the internal diameter, external diameter and the heated length of the annulus respectively.

• All these references are for vertical upflow of water and uniform AFD with internal heating, external heating or dual heating, unless otherwise specified.

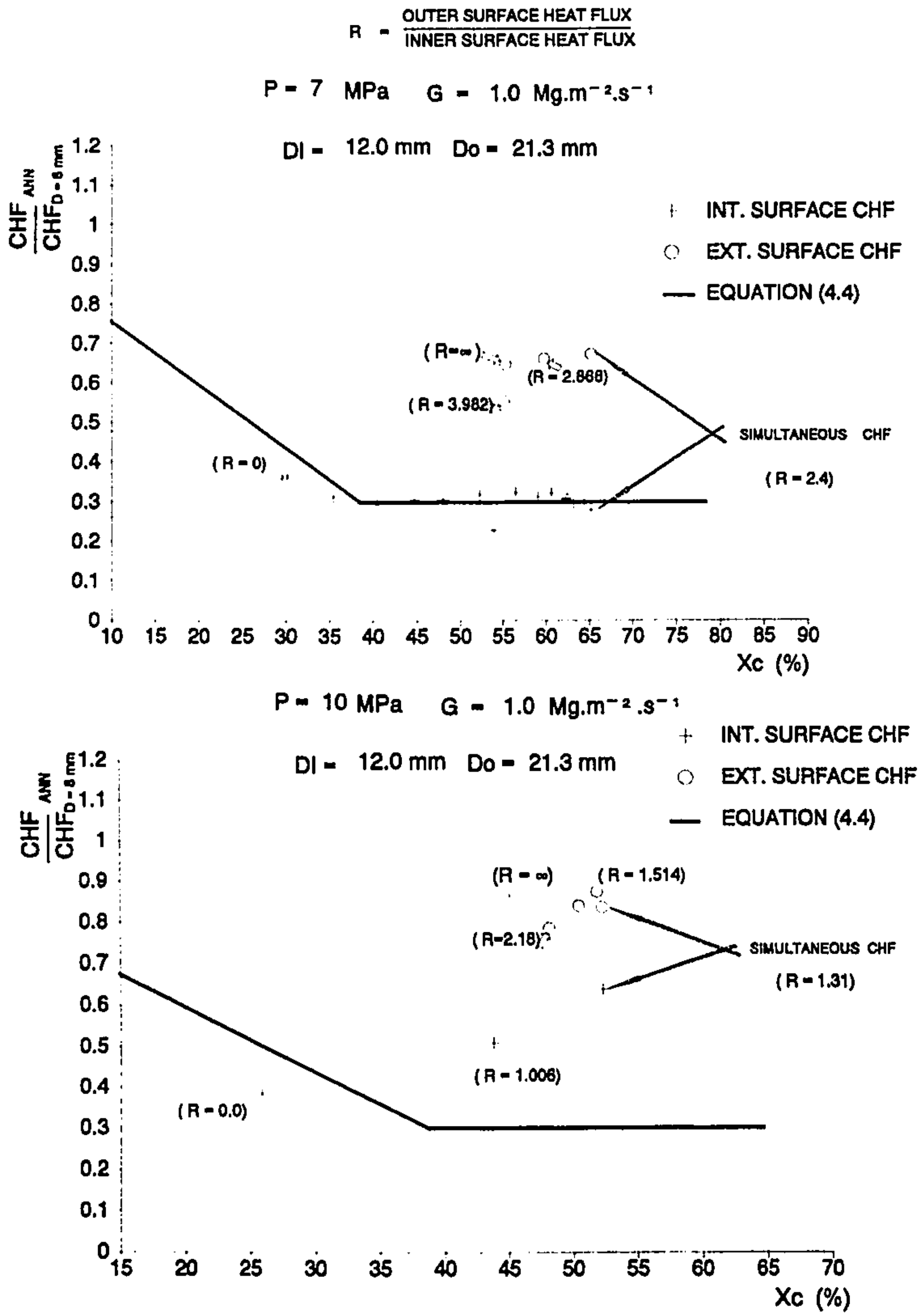

Figure 7.1: Effect of Bilateral Heating on CHF in Annuli (I). Data From Becker and Letzter [1975].

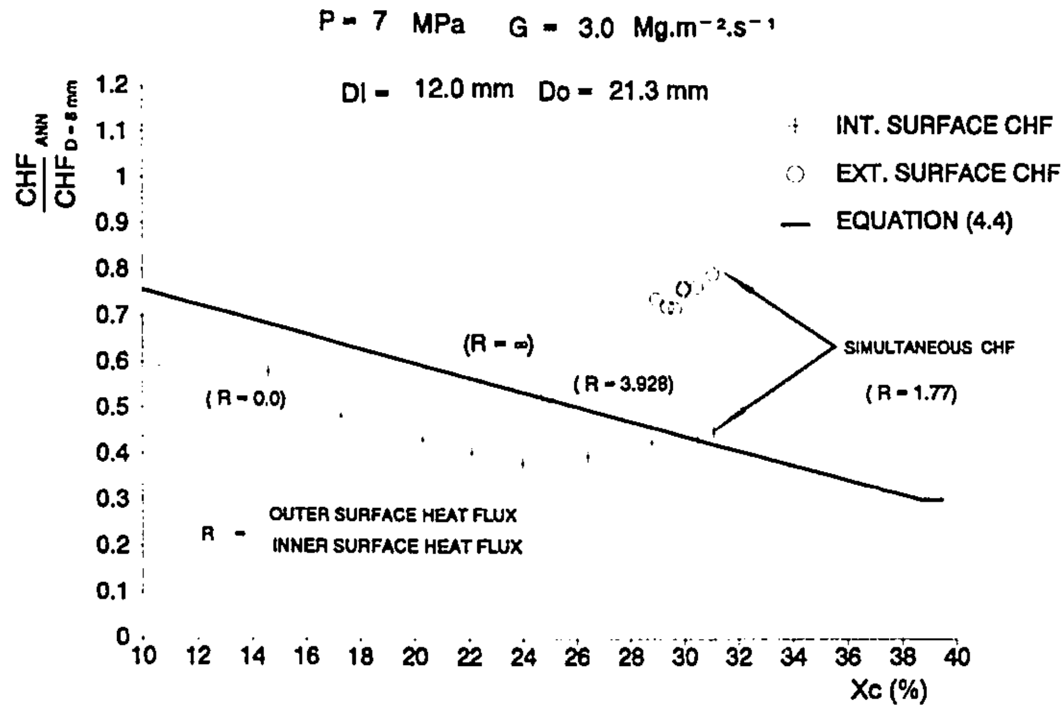

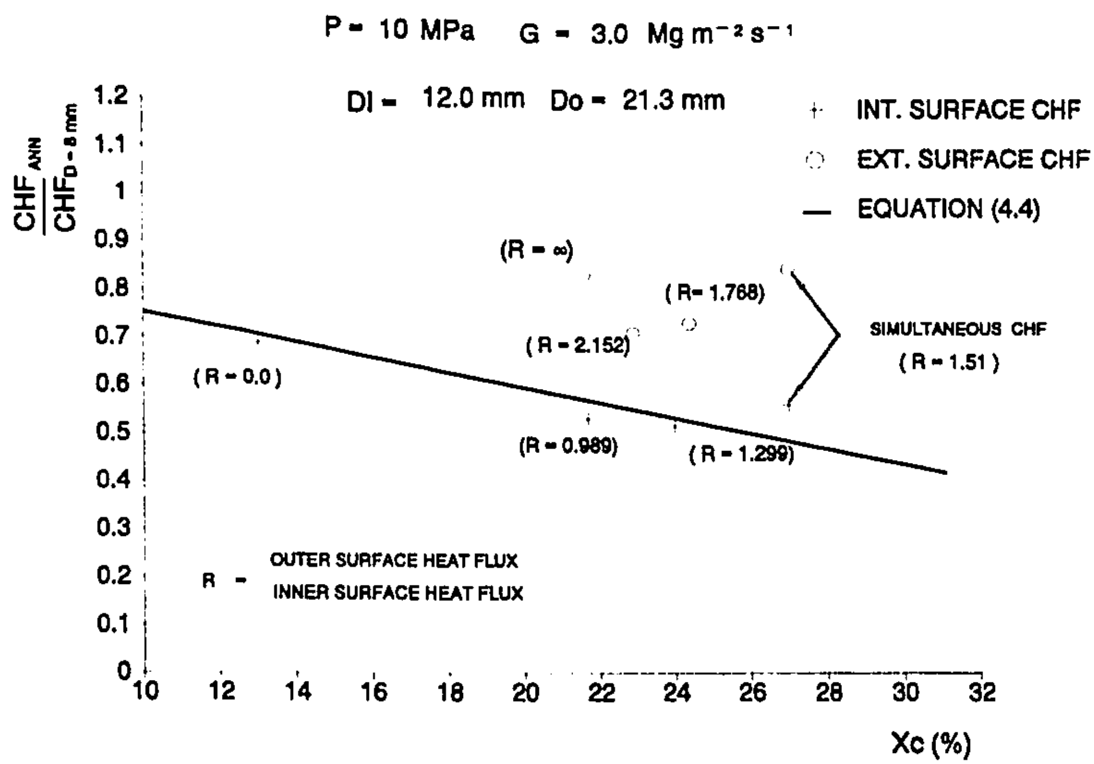

Figure 7.2: Effect of Bilateral Heating on CHF in Annuli (II). Data From Becker and Letzter [1975].

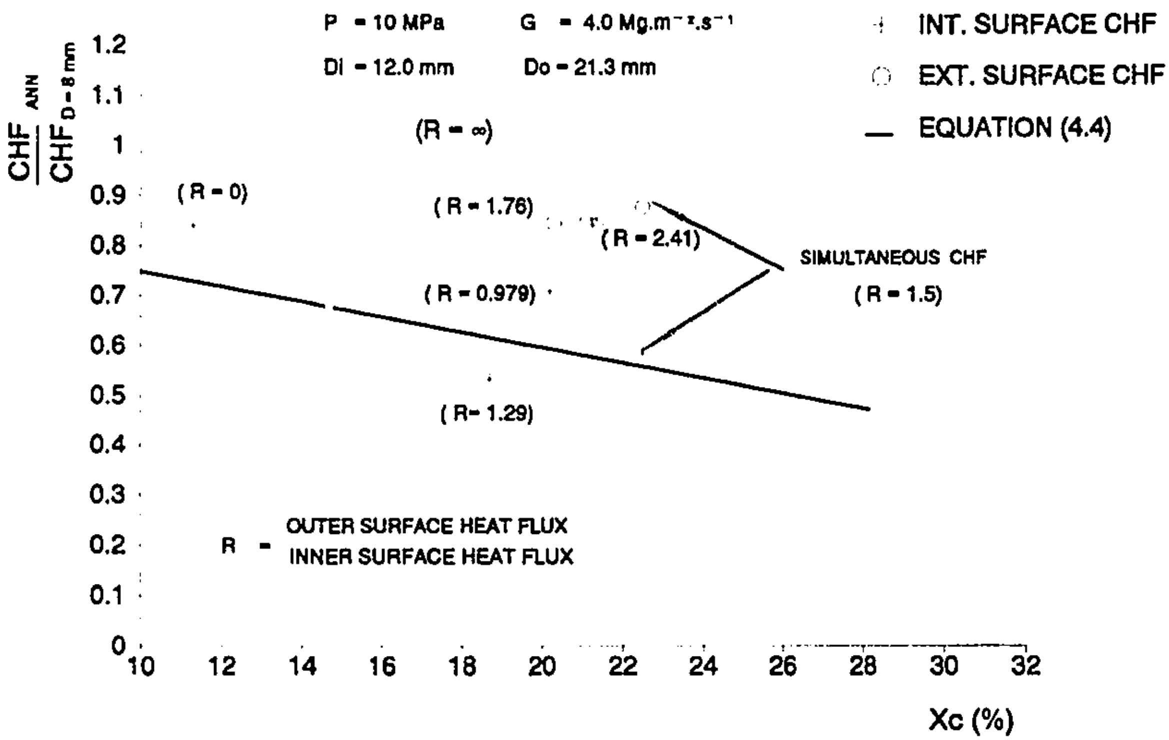

Figure 7.3: Effect of Bilateral Heating on CHF in Annuli (III). Data From Becker and Letzter [1975].

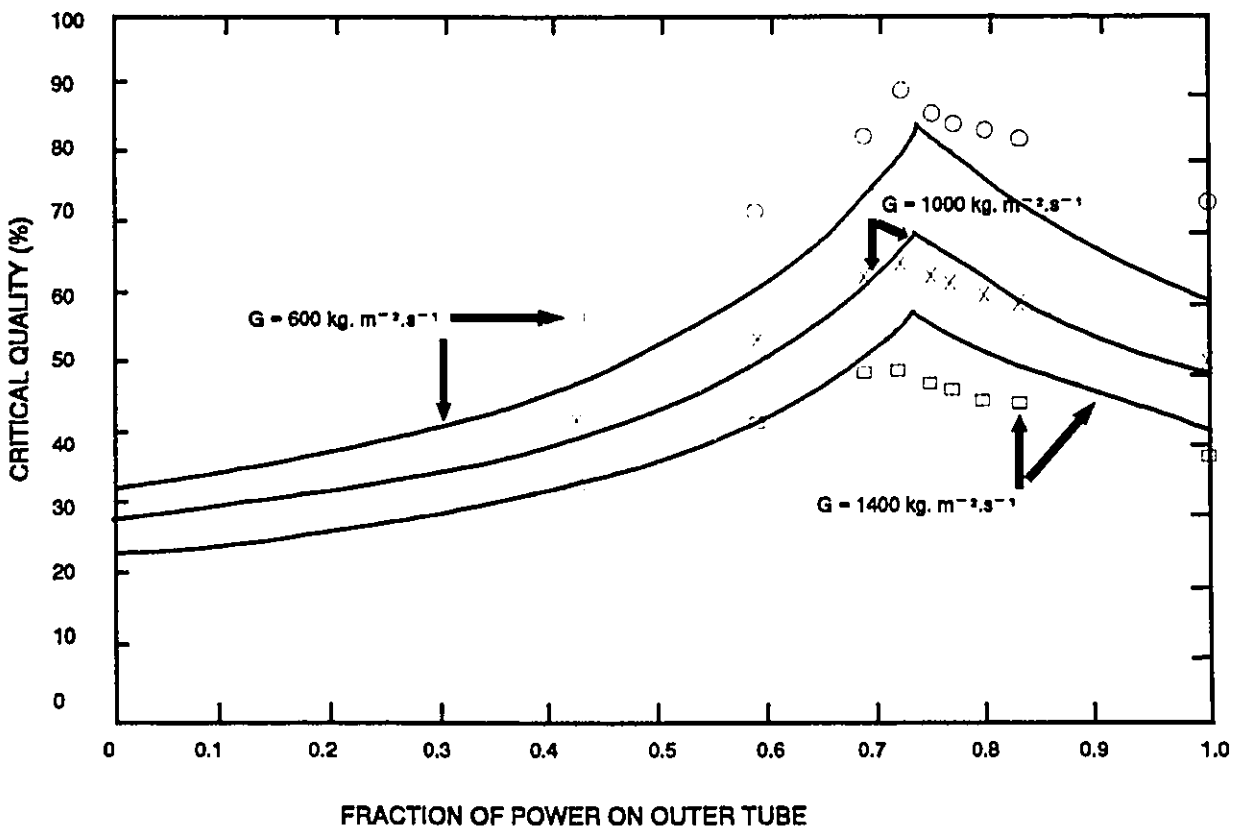

Figure 7.4: Variation of Critical Quality With Power Distribution Within Annular Channels. From Jensen and Mannov [1974].

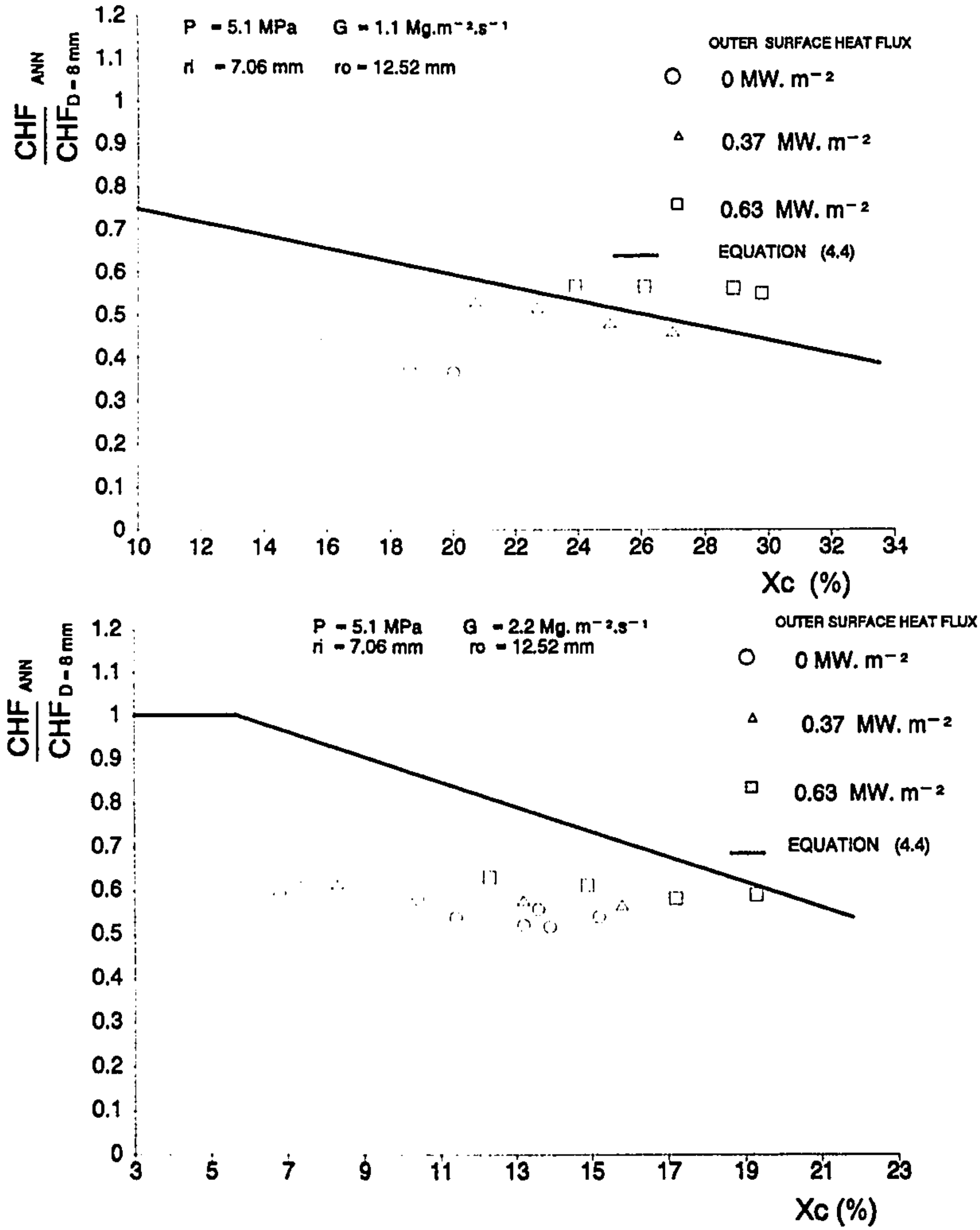

Figure 7.5: Effect of Outer Surface Heat flux on Inner Surface CHF. Data From Kirrilov and Smogalev [1974].

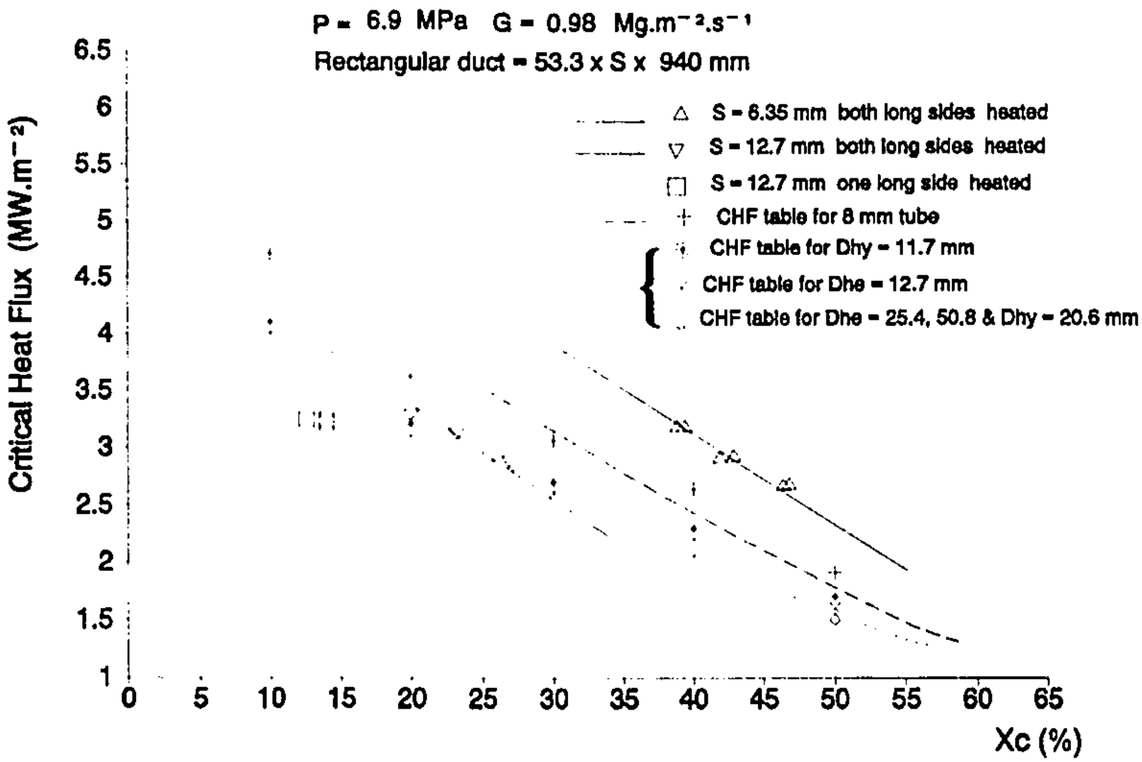

Figure 7.6: Effect of Bilateral Heating in Rectangular Channel. Data From Tippets [1962].

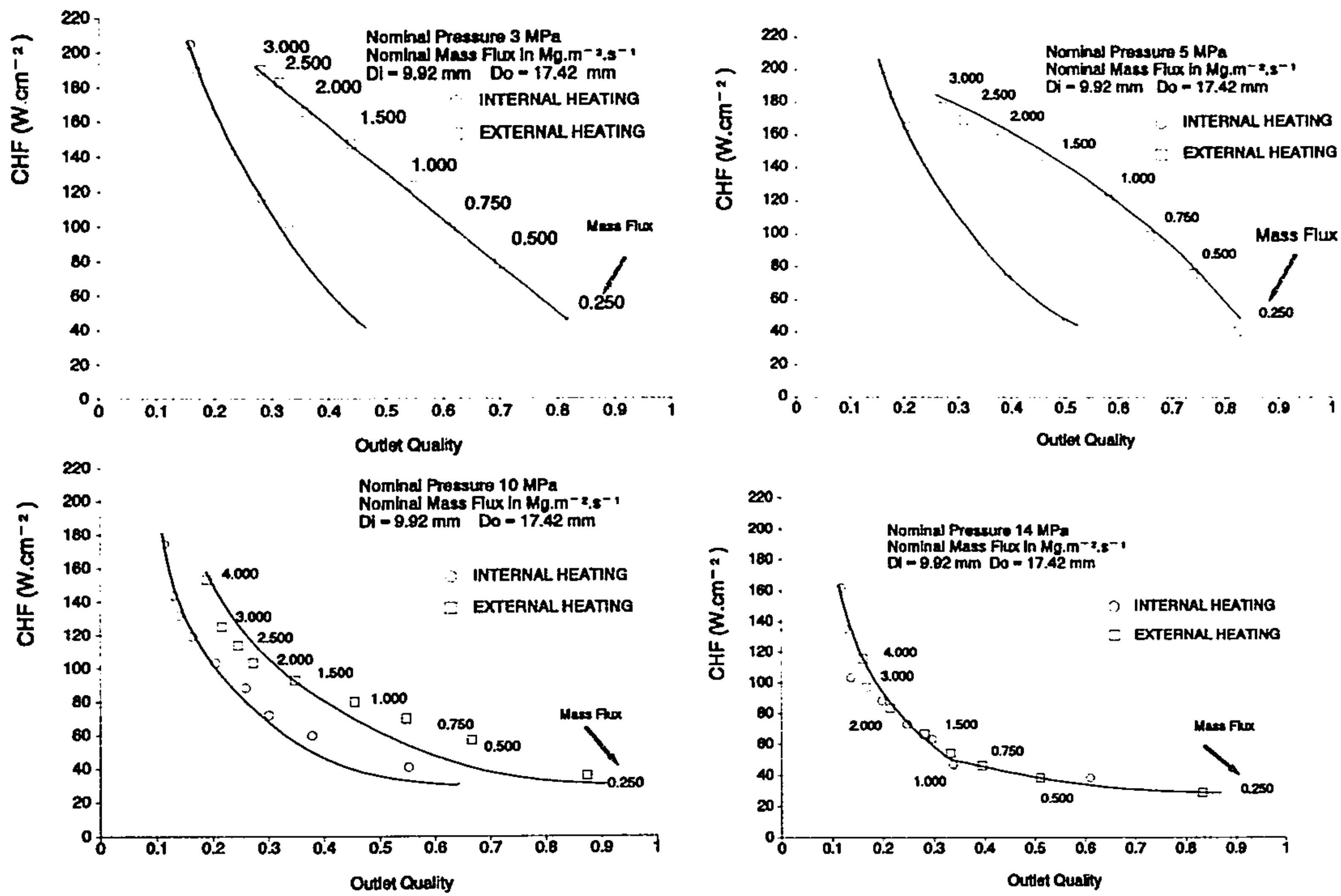

Figure 7.7: Curvature Effect on CHF in Annuli (Mass Flux as a Parameter). Data From Becker *et al.* [1965].

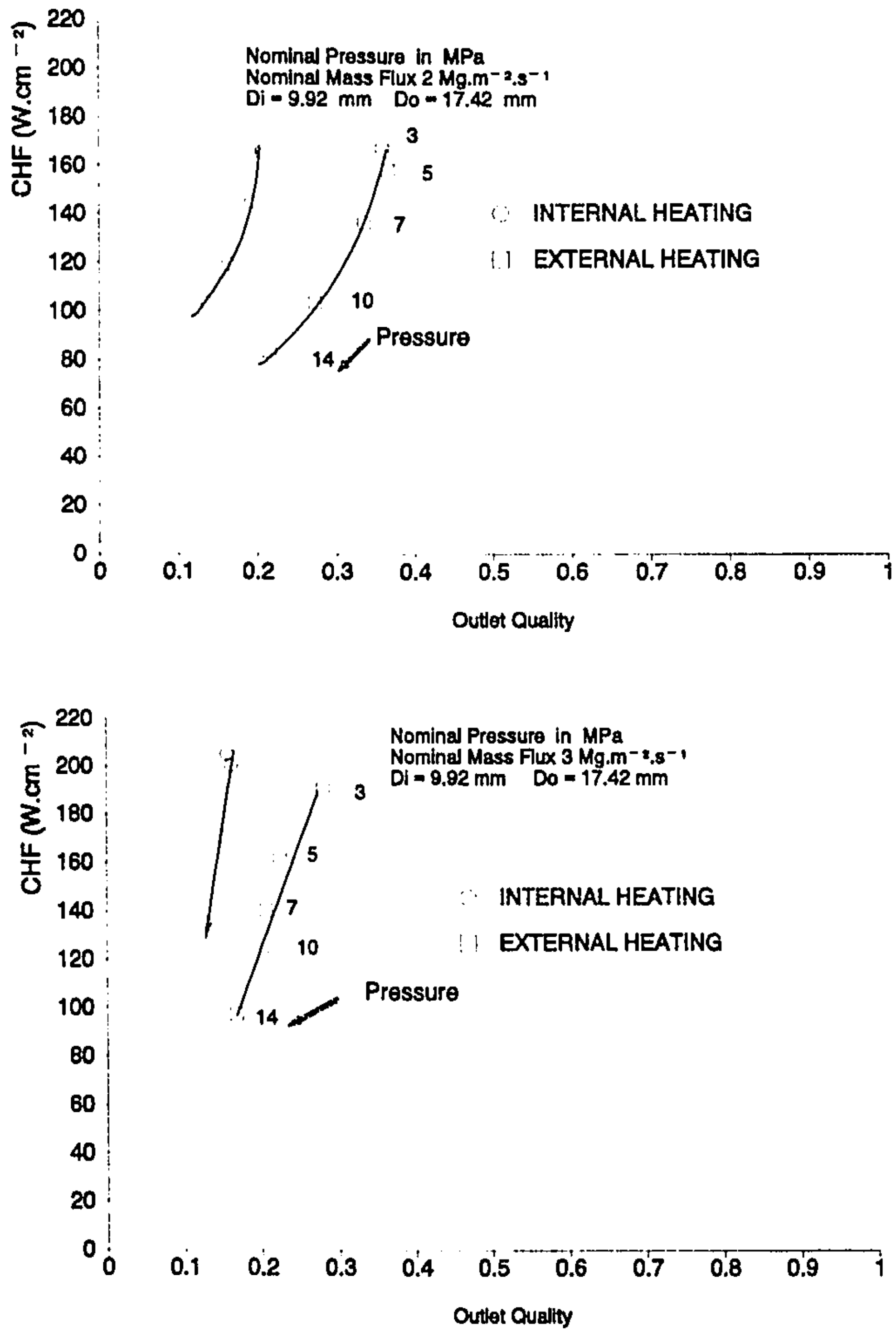

Figure 7.8: Curvature Effect on CHF in Annuli (Pressure as a Parameter). Data From Becker *et al.* [1965].

8. MECHANISTIC CONSIDERATIONS OF THE GAP SIZE EFFECT

8.1 General

In Chapters 4, 5 and 6 the gap size was seen to have an important effect when it is reduced below a certain value depending on the geometry and the flow conditions. Most researchers (e.g., Tolubinskiy *et al.* [1970b] and Ornatskiy *et al.* [1969a]) suggested a value of about 1 mm below which the gap size starts to have an effect on the CHF. In this chapter an assessment of the minimum gap size is performed for CANDU flow conditions of interest, based on analytical and experimental approximation of the size of droplets, bubbles and liquid film thickness.

8.2 Bubble and Droplet Sizes During Flow Boiling

Depending on the flow regime and the heat transfer mode either the droplet or the bubble size may play an important role in predicting the effect of gap size on the CHF. It has been noted by some investigators that the effect of gap size on the CHF becomes important when its size is comparable to the maximum bubble or droplet diameter. In the next two sections bubble and droplet sizes are evaluated and some conclusions about their expected effects on the CHF for minimum gaps are drawn.

8.2.1 Bubble Size Prediction

In case of subcooled boiling (CHF Type-I, II and III), if the gap size becomes relatively small, the bubble can block the complete gap, thus resulting in a premature CHF condition. This interpretation is more appropriate for annular geometries (eccentric and concentric annuli) and subchannels than for round tubes. As mentioned by Tolubinskiy [1969], when a bubble blocks the small tube diameter, it leads to an increase in flow velocity in the blocked cross section. The upstream liquid pushes out the accumulated vapour and scatters it in small bubbles. However, in annular channels or subchannels, a bubble blocks only a portion of the cross section and the liquid can move to the vapour-free cross section. This relatively stagnant bubble could lead to a premature CHF occurrence.

Four prediction methods are used to assess the bubble size. The first method is based on Levy's [1966] model. This model uses a force balance between the drag force and the surface tension force to determine the bubble diameter which is given by

$$D_b = 0.015 \left(\frac{2\ \sigma\ D_{hy}\ \rho}{f\ G^2} \right)^{0.5} \tag{8.1}$$

where f is the Fanning friction factor, $f = 0.046\ Re^{-0.2}$. Levy's equation is for the bubble size at the Onset of Significant Void (OSV) point, bubble departure point in subcooled boiling. Hence, it will not describe the bubble diameter at CHF in any case. Since, only an approximation of the bubble diameter is needed then this model will be still used for other cases. Weisman and Pei [1983] used Levy's model for the quality region, substituting for the liquid properties an average two-phase properties as follows:

$$\rho = \frac{\rho_g}{x + (1-x)\,\dfrac{\rho_g}{\rho_f}}$$

$$\alpha = \frac{x\,\rho}{\rho_g} \tag{8.2}$$

$$\mu = \mu_f \exp\left(\frac{2.55\alpha}{1-\dfrac{39\alpha}{64}}\right)$$

The same procedure for calculating the average properties is used here to evaluate the bubble diameter for positive qualities.

The second model tested is proposed for pool boiling by Cole and Rohsenow [1968], but has also been used by Lee and Mudawwar [1988] for forced convection boiling provided the shear force is much smaller than the buoyancy force. This model also predicts the bubble departure diameter and have the same weakness as Levy's model

$$D_b = 0.00015\left(\frac{\sigma}{g\,(\rho_f-\rho_g)}\right)^{0.5}\left(\frac{\rho_f\,C_{pf}\,T_{sat}}{\rho_g\,h_{fg}}\right)^{1.25} \tag{8.3}$$

Note that Equation (8.3) is based on a force balance between buoyancy and surface tension forces, thus its application to high mass flux values may be questionable.

The third model is given by Smogalev [1981] which predicts the bubble departure diameter as follows:

$$D_b = 0.0208\left(\frac{\sigma}{g\,(\rho_f-\rho_g)}\right)^{0.5}\left[1-0.65\,(P_{cr}-P)^3\,\frac{\rho_g\,\nu_f\,G}{\rho_f\,\sigma\,g}\right]^2 \tag{8.4}$$

This model also presents the same weakness as Levy's model and also the same reasons are used to justify its use.

The fourth model tested is developed by Hinze [1955], which predicts the maximum stable dispersed-phase diameter (in this case the dispersed-phase is the vapour). The same expression is used to predict the droplet diameter in the next section, where in that case liquid instead of vapour becomes the dispersed phase.

$$D_b = 0.725 \left(\frac{\sigma}{\rho_f}\right)^{0.6} \left(\frac{dP}{dz}\ \frac{G}{\rho^2}\right)^{-0.4} \tag{8.5}$$

where the pressure gradient is given by

$$\frac{dP}{dz} = \frac{2 f\, G^2}{\rho\ D_{hy}} \tag{8.6}$$

Figure 8.1 shows the bubble diameter predictions based on the above four models. The largest bubble diameter is the one predicted using Hinze's model (predicts bubbles up to 1 mm in diameter). The other three models predicted much smaller bubble diameters (sometimes one order of magnitude smaller). This difference is expected, since Hinze's expression estimates the maximum stable bubble diameter and the other models give the departure bubble diameter. Except for Smogalev's expression which shows a minimum when plotted as a function of the mass flux, all other methods showed similar trends when plotted against pressure, mass flux and quality. According to these results, gaps of the order of 1 mm or less may result in a decrease in the CHF by vapour blocking. This 1 mm gap size dimension has been mentioned by several studies as the gap size below which the gap effect start to become important. However, from Figure 8.1 it is seen that for CANDU dryout conditions of interest ($P \approx 10$ MPa, $G \approx 5$ Mg.m^{-2}.s^{-1} and $X = 5$-25 %) the maximum bubble diameter predicted is ≤ 0.3 mm. Hence for such conditions, the effect of gap size on CHF due to vapour blocking starts at minimum gap size less than the 1 mm predicted before. It is also important to note that all the prediction methods for the bubble diameter are developed for a tubular geometry. In most of these expressions the hydraulic diameter is used, which does not reflect the effect of non-symmetry of the cross-section on the bubble size. In fact, for non-symmetric cross sections (e.g, eccentric annulus) the local properties of the fluid at the minimum gap size can be very different from the overall properties for the cross sections (e.g., slower liquid in the gap, higher liquid temperature in the gap region). Hence, for non-symmetric cross sections the minimum gap size at which the effect of gap size is noticed may be higher than the one predicted. This may be the case for eccentric annuli and subchannels: hence the minimum gap size could be higher than 0.3 mm for CANDU fuel-subchannels at conditions of interest.

In the previous analysis the effect of enthalpy imbalance in rod bundle was not considered. In some cases where there is a significant enthalpy imbalance as in a rod bundle with different subchannel sizes and shapes, the CHF could be affected by gaps much less than predicted above. Although this effect is very important it was not considered in this work because its extensive scope. This effect of enthalpy imbalance on the minimum gap size could be the subject of a very interesting future research subject.

8.2.2 Droplet Size Prediction

In case of annular flow, entrained droplets play an important role in the CHF occurrence. Droplets comparable to the gap size can bridge the cross section and provide extra cooling to the heating surface. This may result in delaying CHF occurrence. Four methods are also used to evaluate the droplet diameter.

The first method used is the one proposed by Kataoka *et al.* [1983] which determines the volume mean diameter as

$$D_d = 0.01 \frac{\sigma}{\rho_g\, j_g^2}\, Re_g^{2/3} \left(\frac{\rho_g}{\rho_f}\right)^{-1/3} \left(\frac{\mu_g}{\mu_f}\right)^{2/3} \tag{8.7}$$

where $j_g = \frac{G\,X}{\rho_g}$ is the gas superficial velocity and $Re_g = \frac{\rho_g\, j_g\, D_{hy}}{\mu_g}$ is the gas Reynolds number. This expression correlates the experimental data within $\pm$ 40 % error. Kataoka also correlated the maximum droplet diameter by $D_{d,max} = 3.13\ D_d$.

Tatterson *et al.* [1977] developed an expression for predicting the average droplet diameter and is given by

$$D_d = 0.106 \left(\frac{\sigma\, D_{hy}}{\rho_g\, j_g}\right)^{0.5} Re_g^{0.1} \tag{8.8}$$

where j_g and Re_g are defined as in the previous equation. After testing Tatterson's empirical correlation, Ueda [1979] proposed another correlation which fits his data better and can be represented by

$$\frac{D_d}{D_{hy}} = 5.8\ 10^{-3} \left[\frac{\sigma}{\mu_g} \left(\frac{\rho_g}{\rho_f}\right)^{1.25}\right]^{0.34} \tag{8.9}$$

The last correlation predicts the maximum stable droplet diameter (Hinze [1955]). This expression which is similar to the one proposed previously to determine the bubble diameter, except here the dispersed phase is liquid and the continuous phase is vapour. Thus Equation (8.6) becomes

$$D_d = 0.725 \left(\frac{\sigma}{\rho_g}\right)^{0.6} \left(\frac{dP}{dz}\ \frac{G}{\rho^2}\right)^{-0.4} \tag{8.10}$$

where ρ and the pressure gradient, $\frac{dP}{dz}$, are defined by Equations (8.2) and (8.7) respectively.

As for the bubble diameter, the discrepancy between the prediction of different correlations of the droplet diameter is sometimes quite high. Some of these correlations are derived for the average maximum droplet diameter and others for the volume mean diameter. As shown in Figure 8.2 the maximum droplet diameter is 0.3 mm which is predicted by Kataoka's maximum droplet diameter expression. Figure 8.2 also shows that some of the expressions are relatively close to each other. For example Hinze's expression and Kataoka's expression for the maximum diameter follow each other closely since both of them estimate the maximum diameter. Tatterson's expression and Kataoka's one for the volume median diameter also show close similarity. In general Figure 8.2 shows that droplet sizes are within this range: 0.01 to 0.3 mm in diameter. For CANDU dryout conditions of interest droplets are smaller than 0.1 mm in diameter. These empirical results are supported by the few experimental data shown in Figure 8.3. Although, most of the experimental work is based on air-water studies at atmospheric conditions, the droplet size did not exceed the 0.1 mm. From these results it seems that the vapour gap size (the part of the gap size which is occupied by vapour) for annular flow can be reduced to around 0.1 mm without noticing any effect in CHF. However, in this analysis the film thickness was not considered. The liquid film bridging together (e.g., wave tips joining) might be a more important cause of the CHF enhancement in annular flow regime than droplets bridging the gap. An assessment of liquid film thickness is needed to estimate the gap size for which liquid bridging of the gap might occur.

8.3 Liquid Film Thickness Assessment

Liquid film thickness measurements have been made by few investigators such as, Gill *et al.* [1965] and Pogson *et al.* [1970]. For detailed information on evaluation methods for the film thickness the reader is referred to Hewitt and Hall-Taylor [1970]. For the purpose of this study, only an estimate of the film thickness is needed and can be achieved by examining the experimental results.

Hewitt and Hall-Taylor [1970] stated that liquid films are rather thin and do not generally exceed 2.54 mm (<0.1 in.). Figure 8.4 shows the variation of water film thickness with either the water flow rate (a) or the steam flow rate (b). From this figure it can be seen that

(i) liquid film thickness decreases with an increase in vapour mass flux; and

(ii) as the quality increases the liquid film thickness decreases.

Figure 8.5a shows a comparison between experimental results of Gill *et al.* [1965] and predictions from Turner and Wallis' [1965] empirical equation, while Figure 8.5b shows a comparison between experimental results of Pogson *et al.* [1965] and calculated results from an empirical correlation developed by the same authors. The two figures show a maximum film thickness of less than 0.8 mm (0.03 in.).

As noted in the previous section, most of the experimental work was done at low pressures (atmospheric conditions), low mass flux and for air-water mixture. As the mass flux increases it was noted the film thickness decreases. Moreover, empirical correlations (e.g., Pogson *et al.* [1965]) showed that the film thickness is proportional to surface tension, σ. Since, the surface tension decreases with increasing pressure then so does the film thickness. Hence, for CANDU dryout conditions of interest ($P \approx 10$ MPa and $G \approx 5$ $Mg.m^{-2}.s^{-1}$), the liquid film thickness is expected to be much thinner than the maximum film thickness predicted by the previous experiments. The film thickness for these conditions would not exceed 0.4 mm. Hence the total thickness occupied by the liquid film is about 0.8 mm. If the maximum droplet diameter (predicted in the previous section) is considered with this analysis then the total liquid film thickness is 0.9 mm. In conclusion for gaps less or equal to 1 mm, and in the case of annular flow, the gap may be bridged by the liquid resulting in CHF enhancement. This interpretation might be used to explain the convergence of the eccentric and concentric annuli results for the annular flow regime as seen in Chapter 5.

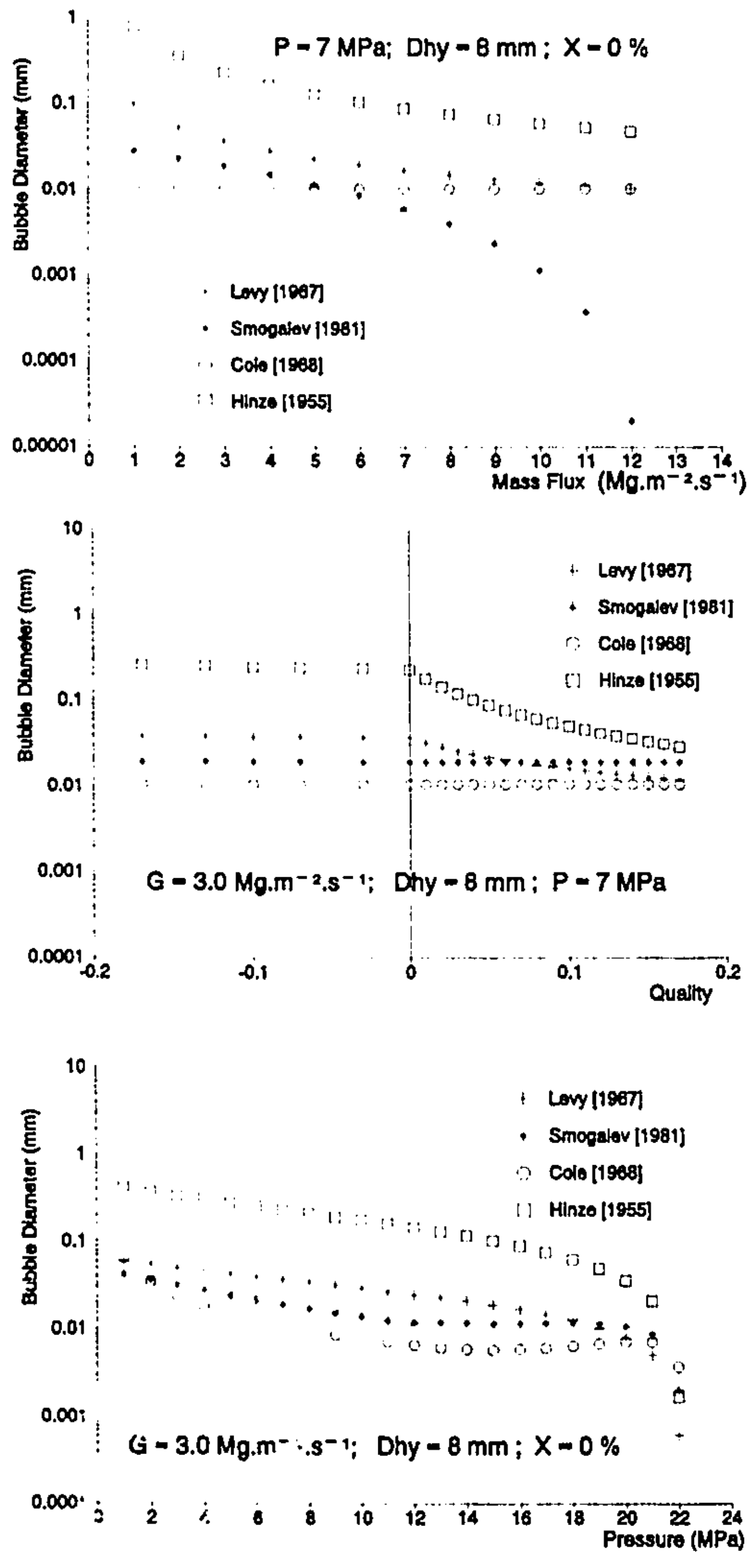

Figure 8.1: Bubble Diameter Predictions as a Function of Quality, Mass Flux and Pressure.

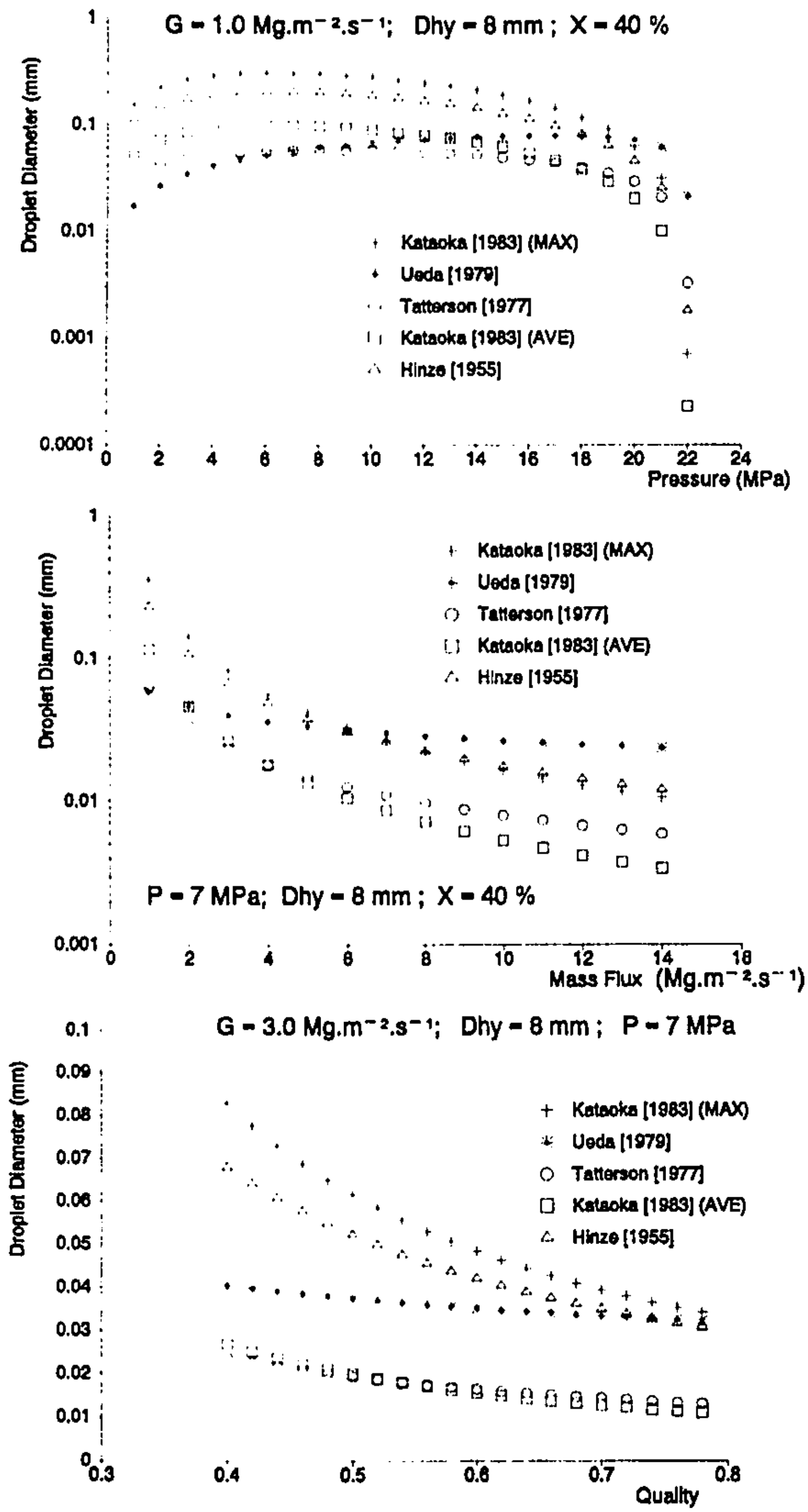

Figure 8.2: Droplet Diameter Predictions as a Function of Quality, Mass Flux and Pressure.

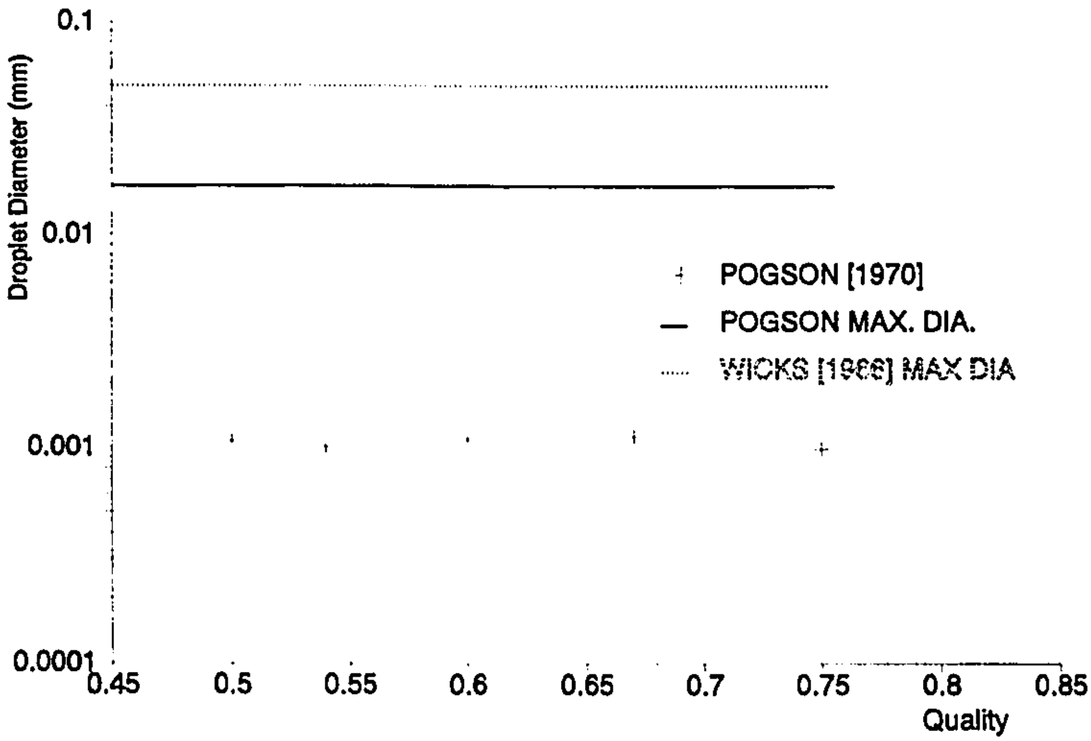

Figure 8.3: Some Experimental Measurements of the Droplet Diameter.

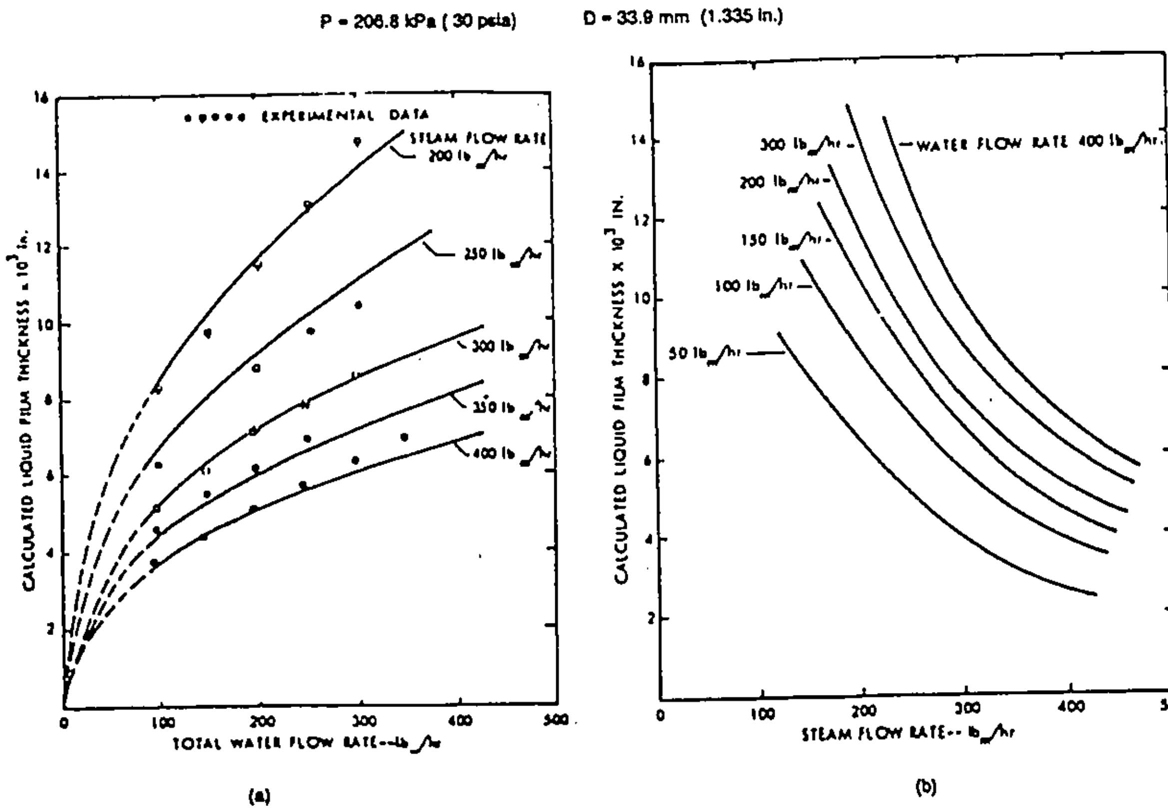

Figure 8.4: A Comparison of the Liquid Film Thickness: (a)- With the Water Flow Rate for Various Steam Flow Rates; (b)- With Steam Flow Rate for Various Water Flow Rates. From Pogson *et al.* [1970].

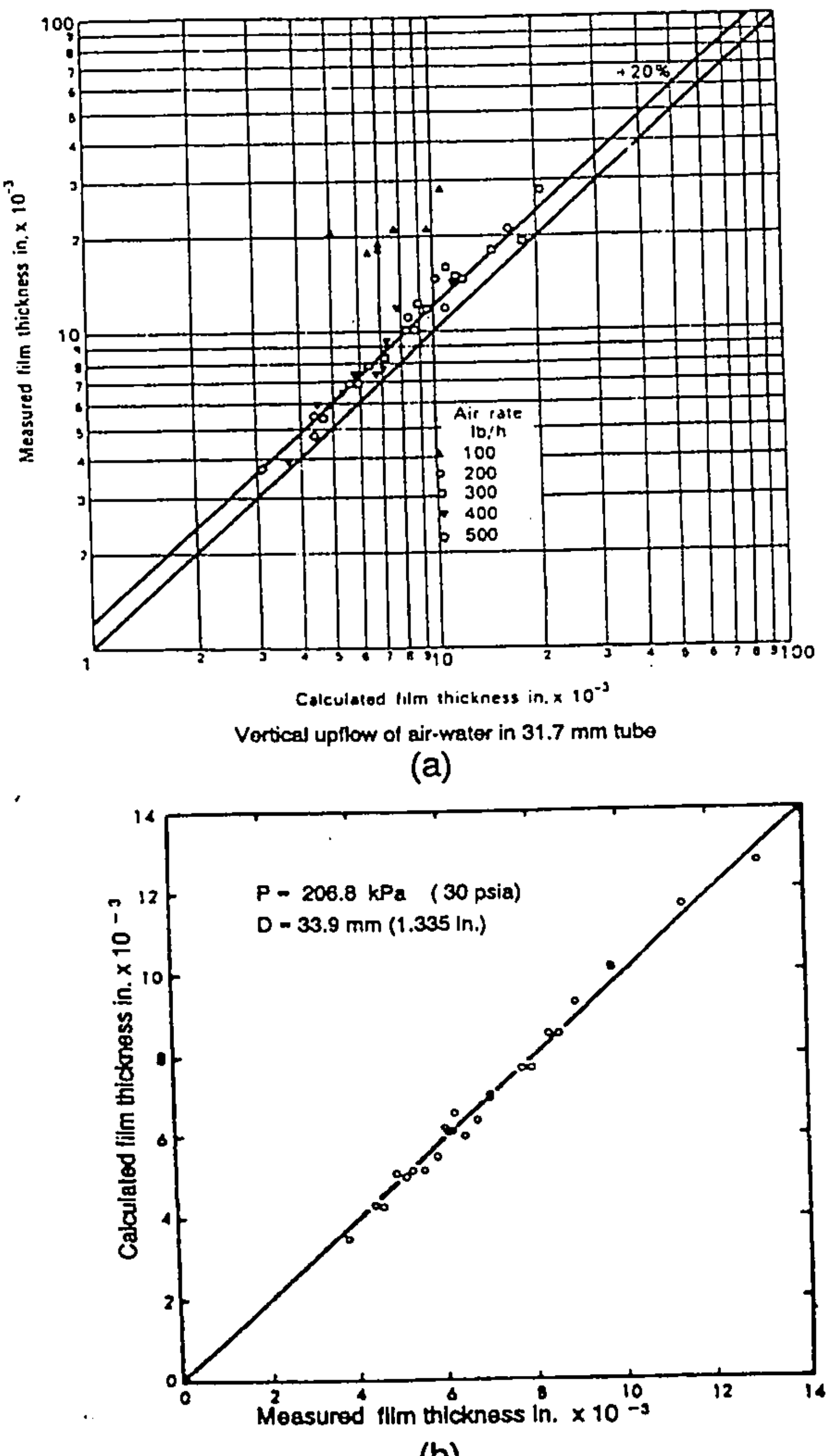

Figure 8.5: Comparison of Measured Film Thickness With Values Calculated From Correlations: (a) Gill *et al.* (1965); (b) Pogson *et al.* (1970).

9. SUBCHANNEL CHF PREDICTION METHOD

9.1 General

This chapter uses equations and observed trends discussed in the previous chapters to recommend an interim prediction method for subchannels at CANDU flow conditions of interest. As discussed in other chapters, in addition to the lack of reliable CHF data in geometries other than tubes and concentric annuli, there are some observed conflicting trends and results. These two reasons, with the complexity of the CHF phenomenon in general, render the task of deriving an accurate prediction method for a fuel bundle subchannel difficult.

Since the tube CHF has been measured extensively (especially the CHF in an 8 mm tube) these CHF values are generally used as a reference and CHF values in other geometries are related to the tube values by applying correction factors. A similar procedure has been used in CRL, where correction factors to the 8 mm tube CHF for effects such as flux distribution, orientation and transient have been derived (Groeneveld and Leung [1989]). The following general form for the subchannel CHF correlation is proposed:

$$CHF_{subchannel} = CHF_{D=8mm} \times F_i \times F_j \times F_k \ldots \qquad (9.1)$$

where F_i, F_j and F_k are correction factors to account for specific differences between the CHF occurrence in tubes and subchannels. Equation (9.1) will have the same parametric and asymptotic trends as the table look-up values. This is the advantage of using this procedure to another empirically derived correlations, which frequently give the wrong asymptotic trends due the their limited range of application. The correction factors are discussed in the sections below.

9.2 Turbulent-Mixing and Cross-Flow Correction Factors

Due to the presence of many different subchannel geometries and flow obstructing devices (e.g., grid spacers) in the CANDU fuel bundle, there is a higher turbulence level and cross flow effect in a bundle geometry compared to a tube. Correction factors are needed to account for these effects. Groeneveld *et al.* [1992] presented these effects as follows:

CHF Enhancement Factor: This factor accounts for the high turbulence generated by upstream bundle appendages and is given by

$$F_{enh} = 1+1.5\ K^{0.5}\ G^{0.2}\ \exp\left[-0.1\frac{L_{sp}}{D_{hy}}\right] \tag{9.2}$$

where K is the spacer-plane loss coefficient, L_{sp} is the distance to the nearest upstream flow obstruction ($L_{sp} \approx 240$ mm for CANDU fuel bundle), D_{hy} and G are the hydraulic-equivalent diameter of the subchannel and the mass flux in the subchannel, respectively. This effect was investigated in CRL and found to be large just downstream of a bundle appendage. It reaches a minimum value just upstream of a bundle appendage.

Turbulent Mixing: Doerffer *et al.* [1992] evaluated the mixing coefficient, β, for several proposed correlations (e.g., Rogers and Tahir [1975], Rogers and Rosehart [1972], and Rowe and Angle [1969]). Doerffer *et al.* [1992] found that β values in gaps are in general small ($\beta < 0.01$ for single-phase flow). Hence turbulent mixing will not have a strong effect on CHF in the gap region and the correction factor for turbulent mixing effect is set equal to 1.0. Further analysis is needed to give a more accurate estimation for this factor.

Cross-Flow Factor: Cross flow is important specially in the quality region and is caused by differences in vapour-generation rates between dissimilar subchannels. For very dissimilar adjacent subchannels the presence of cross flow suppresses the occurrence of CHF in the gap region. To account for the beneficial cross-flow effect, the quality correction factor in Section 9.3 will be modified accordingly.

9.3 Flow Conditions Effect

Quality: It was shown in Chapter 4 that, as the quality increases, the quality correction factor, K_X, defined in Equation (4.3) decreases. The interpretation given was that in the quality region, the unheated outer surface liquid film is considered wasted or bypassed, as it is not used for the inner surface cooling. However, when comparing CHF data obtained in annuli with those for "outer" subchannels of rod bundles, it appears that the detrimental effect of a liquid sink on the unheated wall is more significant in annuli than in bundles. It may be that the liquid on the pressure-tube wall originates from across the bundle and thus does not just rob the adjacent surface from much needed deposition. Also, as discussed in Chapter 8 for small gaps, liquid film bridging might also reduce the effect of liquid film presence on the unheated surface and cause a CHF enhancement. Hence, the quality correction factor for CANDU fuel bundle subchannels should be less severe than for the annuli case and an interim expression of this correction factor is given by

$$F_{x,unheated} = 1-0.25\, K_1 \left(1-K_x\right) \tag{9.3}$$

where K_x is defined by Equation (4.3) and K_1 accounts for the cross-flow effect and is equal to 1.0 for the no cross-flow cases and 0.0 for cases where cross flow is important (i.e., very dissimilar subchannels).

Mass Flux and Pressure: Though some empirical correlations have indicated strong effects of mass flux and pressure, not enough data is available in the literature to assess these predictions. However, it appears that the mass-flux effect is stronger in tubes than in complex geometries (e.g., Tables 6.3 and 7.1), and as the pressure increases, the effect of minimum gap size becomes less severe as seen in Chapter 8.

9.4 Gap Effect

The CHF does not occur simultaneously around the subchannel perimeter, because the near-wall conditions around the heated perimeter can change significantly, depending on whether the surface sees an open subchannel area, an adjacent unheated surface or an adjacent heated surface. Ouma and Tavoularis [1991a] concluded that the wall shear stress reaches a minimum in the gap region (rod-rod gap and rod-wall gap) and a maximum in the open flow region. It is also found that the velocity is least in the narrow gap area, thus lowering the local turbulence. Consequently, the vapour-removal mechanism by vapour shear and mixing is reduced, which will affect Type-II and Type-III CHF. The worst effect on local CHF is expected for narrow gaps, where laminar flow may occur (for a flow of 1 $Mg.m^{-2}.s^{-1}$ and P = 10 MPa, turbulent-laminar flow transition can occur for gaps around 0.1-0.5 mm). The effect of gap size is seen to be less important as the quality increases (see Chapter 5) and for rapid lateral change in the local gap width as shown by the difference between Moeck's *et al.* [1966] and Levy's *et al.* [1962] results (parallel surfaces will present the worst case).

Heron *et al.* [1969] experiment showed that the gap effect is particularly strong when two adjacent heated surfaces approach each other, but little loss in dryout power was observed when the heated outer rods approached the unheated wall. Similar observations were made by other authors (see Sections 5.3 and 6.3.3).

The effect of distance from an adjacent surface (or minimum gap, mg) may be expressed by the correction factor F_{mg}, which is similar to the K_δ factor described by Equation (4.5). For the case of an adjacent unheated surface (as the case for rod-wall gaps) the following empirical expression is recommended (Groeneveld *et al.* [1992]):

$$F_{mg,unheated} = MIN\left[1, 0.5+6.0\ \frac{\delta_{min}}{d}\right] \tag{9.4}$$

For the gap between two adjacent heated elements, F_{mg} is given by

$$F_{mg,heated} = MIN\left[1, 0.2+9.0\ \frac{\delta_{min}}{d}\right] \tag{9.5}$$

In both cases the maximum value of F_{mg} would be reached for minimum gaps of around 1.0 mm, which is below the minimum gap values in CANDU fuel geometries ($d \approx 12.7$ mm for CANDU geometry).

From Chapter 8 it was found that only gaps less than about 1 mm would affect the CHF. This is consistent with Equations (9.4) and (9.5) where for gaps larger than 1 mm, the gap correction factor would be 1.

9.5 Size Effect

The effects of gaps, cross flow and turbulent mixing in the gaps become unimportant for the rod perimeter sections facing the open subchannels, and here the CHF dependence on geometry is more like that of the size dependence in a tube, as described in Chapter 3. This requires a dimension to characterize the subchannel size, which could be either D_{he} or D_{hy}. One could argue that D_{he} should be used, as it defines the enthalpy-rise rate (for a given G and P) in each subchannel. One could also argue that D_{hy} should be used, as the dryout mechanism is driven mostly by the flow phenomenon at high flow (e.g., CHF seems to be a function of the turbulent structure inside the channel). Tentatively, it seems that D_{hy} is the most appropriate dimension and it is the most widely used. Hence

$$F_{size} = \left(\frac{8}{D_{hy}}\right)^{1/3} \tag{9.6}$$

with an upper and lower limit of 1.2 and 0.8. The upper and lower limit set limits where this correction factor is no longer valid. Note that, in the gap region, this correction factor should not be used, but instead the value as predicted by $F_x \times F_{cf} \times F_{mg}$ should be used.

9.6 Recommendation

The following equation is tentatively recommended for the prediction of

CHF in subchannels as given by Groeneveld *et al.* [1992]

$$CHF_{subchannel} = CHF_{D=8mm} \times F_{enh} \times MIN\left(F_{size}, F_{gap}\right) \tag{9.7}$$

where:

$F_{gap} = F_x \quad MIN[F_{mg,heated}, F_{mg,unheated}]$

F_{enh} is given by Equation (9.2)

F_x is given by Equation (9.3) with an upper and lower limit of 1.00 and 0.825, respectively,

$F_{mg,unheated}$ is given by Equation (9.4),

$F_{mg,heated}$ is given ny Equation (9.5) and

F_{size} is given by Equation (9.6) with an upper and lower limit of 1.2 and 0.8, respectively.

The above empirical equation has been tested for several flow conditions and found to have the correct parametric and asymptotic trends. This interim recommendation is a considerable improvement over the currently used tube CHF value, and it could be used for making a preliminary assessment of subchannel geometry or flow geometry changes on subchannel CHF. More factors could be introduced to Equation (9.7) to account for other effects which are neglected in this work but could be important in some cases (eg., the effect of the enthalpy imbalance). Further improvements will be made in the future, when additional experimental data on the effect of geometry on CHF become available.

10. CONCLUSIONS AND RECOMMENDATIONS

After finishing this exhaustive investigation on the effect of flow geometry on the CHF several trends have been discovered. A prediction method for concentric annuli in Chapter 4 has been recommended. Another prediction method for a subchannel geometry has been recommended in Chapter 9 based on the most important and consistent observed trends. However, some of the opposing trends cannot be explained by means and information gathered in this study. This could be due to experimental results obtained using different techniques and in different laboratories, in addition to the usual experimental errors. Some of the most consistent and common conclusions arrived at by most investigators are given below :

- Compared to the reference CHF look-up table for 3-mm internal diameter tubes, the CHF in internally heated annuli is considerably lower. The discrepancy is primarily a function of quality, with gap-size effect becoming important especially for gaps less than about 1 mm.

- In general, the ratio $CHF_{ann}/CHF_{D=8mm}$ is close to unity for subcooled conditions (where the bulk temperature is the most important parameter and is relatively unaffected by the presence of an unheated wall). This ratio decreases gradually in the quality region (entrainment-controlled CHF, because of the effect of the thicker liquid film on the unheated wall becoming more important), and the ratio is least for the higher quality region where deposition-controlled CHF becomes dominant (here, the presence of the liquid located on the unheated surface is felt most severely and has the greatest detrimental effect on CHF).

- Most experiments in annuli (Becker and Letzter [1975], Kirillov and Smogalev [1974], Alekseev *et al.* [1965]) and rectangular channels (Tippets [1962]) have shown that the CHF increases if both surfaces are heated instead of only a single surface. For bilateral heating, the ratio $CHF_{ann}/CHF_{D=8mm}$ becomes closer to 1.0 as the detrimental effect of parasitic liquid film on the unheated wall is not as important. In bundles, however, the pressure tube does not appear to have the same negative effect on CHF as for annuli.

- The effect of gap size on CHF is most severe at low flows and subcooled conditions, where noticeable reductions in CHF are observed when the gap size is reduced below a critical value. This critical gap size is assessed and found to be around 1 mm for CANDU flow conditions. Tolubinskiy *et al.* [1970a] report that this effect diminishes at higher flows because the higher turbulence level of the flow suppresses the formation of stagnant or near-stagnant spots in the narrow-gap region. It is noted also that, in the case of annular flow (CHF Type-V and -IV), reducing the gap size might cause enhancement of CHF due to the liquid film bridging together for small gaps.

- The effect of curvature can be isolated from experiments in annuli where the CHF for a concave surface (the outer tube) is significantly higher than the CHF for a convex surface. This is interpreted by the fact that the entrainment is greater for a convex surface than a concave one. Also by the fact that droplets entrained from a convex surface cannot be deposited on the same surface, however droplets entrained from a concave surface can be deposited on the same surface (due to the linear trajectory of the droplets in the radial direction). This suggests that (i) tube-based CHF correlations may not apply to bundles or subchannel whose heated surfaces are convex, and (ii) different CHF values apply to a given flow area, depending on the curvature of the heated surfaces surrounding the flow area.

- In many cases the observed trends were masked by data scatter. In other cases the isolation of specific geometric effects on CHF was not possible, because of unequal flow conditions.

This study represents a first attempt to determine the effect of flow geometry on CHF. The scope of this subject is very wide and more work in this area is needed to provide a general and more accurate prediction method for CHF. At present it can be said that the CHF phenomenon (even in the most simple geometry such as tube) is not well understood. I would recommend more experimental work to be done, especially oriented towards the study of specific geometric effects, for example eccentricity. After more data become available in this area, a better assessment of this prediction is recommended, especially to determine whether multiplying correction factors together would not alter the results. Though this has been tested but it was not done for large enough data base. I also recommend that more researchers provide in tabulated format their full experimental results in case others would like to use their data for further analysis; finding experimental results was very tedious in this work because most of the results are presented in graphical form.

REFERENCES

Ahmad, S. Y., "*Fluid to Fluid Modelling of Critical Heat Flux, a Compensated Distortion Model*", Int. J. Heat Mass Transfer, Vol. 16, pp. 641-661, 1973.

Alekseev, G.V., Peskov, O.L., Remizov, O.V., Zenkevich, B.A. and Subbotin, V.I., "*Critical Heat Flux Densities With Forced Flow of Water*", Teploenergetika, Vol. 12, No. 3, pp. 47-51, 1965.

Alvensleben, B., Casper, C. and Lochman, K.H., "*Some Experiments Concerning Steady-State Burnout in Vertical Annular Channels*", AEG-Kernenergieanlagen, Frankfurt, Germany. Paper Presented at EAES Symposium, in Studvisk, 1963 October.

Anderson, P.S., Jensen, A., Mannov, G. and Olsen, A., "*Burn-out, Circumferential Film Flow Distribution and Pressure Drop for Eccentric Annulus With Heated Rod*", Int. J. Multiphase Flow, Vol. 1, pp. 585-600, 1974.

Barnett, P.G., "*A Comparison of the Accuracy of Some Correlations for Burnout in Annuli and Rod Bundles*", AEEW-R 558, 1968.

Barnett, P.G., "*A Correlation of Burnout Data for Uniformly Heated Annuli and Its Use For Predicting Burnout in Uniformly Heated Rod Bundles*", AEEW-R 463, 1966.

Barnett, P.G., "*An Investigation into the Validity of Certain Hypothesis Implied by Various Burnout Correlations*", AEEW-R214, 1963.

Becker, K.M. and Letzter, A., "*Burnout Measurements for Flow of Water in Annulus With Two Side Heating*", Paper Presented at the European Two-Phase Flow Group Meeting in Haifa, Israel, 1975 June.

Becker, K.M., "*An Analytical and Experimental Study of Burnout Conditions in Vertical Round Ducts*", Nukleonik, Vol. 9, No. 6, pp. 257-270, 1967.

Becker, K.M., Hernborg, G., Bode, M. and Erikson, O. "*Burnout Data for Flow*

Boiling Water in Vertical Round Ducts, Annuli and Rod Clusters", AE-177, 1965 March.

Becker, K.M. and Hernborg, G., "*Measurements of Burnout Conditions for Flow of Boiling Water in a Vertical Annulus*", Journal of Heat Transfer, Vol. 86, pp. 393-407, 1964 August.

Bennett, A.W., Collier, J.G. and Kearsy, H.A., "*Heat Transfer to Mixtures of High Pressure Steam and Water in an Annulus Part IV The Effect of Test Section Geometry*", AERE-R 3961, 1964.

Bergles, A.E., Lopina, R.F. and Fiori, M.P., "*Critical-Heat-Flux and Flow Pattern Observations for Low Pressure Water Flowing in Tubes*", Journal of Heat Transfer, Vol. 89, pp. 69-74, 1967.

Bergles, A.E., "*Subcooled Burnout in Tubes of Small Diameter*", ASME 63-WA-182, 1963.

Biasi, L., Clerici, G.C., Garribba, S., Sala, R. and Tozzi, A., "*Studies on Burnout. Part 3: A New Correlation for Round Ducts and Uniform Heating and Its Comparison With World Data*", Energia Nucleare, Vol. 14, pp. 530-536, 1967.

Boltienko, E.A., Pomietko, R.S., Katan, I.B. and Ziatnina, O.A., "*Effect of Diameter on CHF*", (Translated by Doerffer, S., Chalk River, 1991 April), 1989.

Boltienko, E.A., Winogradov, W.N., Katan, I.B. and Pomietko, R.S., "*Effect of Tube Diameter on CHF at Various Two-phase Flow Regimes*", Report IPE-1889, Obninsk, (Translated by Doerffer, S., 1991), 1988.

Bowditch, F.H. and Lee, D.H., "*An Experimental Investigation into Dryout SHOULD an SGHWR Rod Bow into Contact With a Pressure Tube*", AEEW-R 903, 1973.

Bowring, R.W., "*A Simple But Accurate Round Tube Uniform Heat Flux Dryout Correlation Over the Pressure Angle 0.7-17 MN.m^{-2}*" AEEW-R789, 1972.

Chernobay, V.A., *"Critical Heat Loads in a Rectangular Duct With Non-uniformly Heated Perimeter"*, Heat Transfer- Soviet Research, Vol. 2, No. 1, pp. 167-169, 1970 January.

Cole, R. and Rohsenow, W.R., *"Correlation of Bubble Departure Diameters for Boiling of Saturated liquid"*, Chem. Engng. Prog. Symp., Vol. 92, pp. 211-213, 1968.

Collier, J.G., *"Convective Boiling and Condensation"*, McGraw-Hill, 2nd edn., 1981.

Collier, J.G., Lacey, P.M.C. and Pulling, D.J., *"Heat Transfer to Two-Phase Gas-Liquid Systems Part 3. The effects of Proximity of Other Heated Surfaces"*, AERE-R 3960, 1964.

De Bortoli, R.A., Green, S.J., Letourneau, B.W., Troy, M. and Weiss, A., *"Forced Convection Heat Transfer Burnout Studies for Water in Rectangular Channels and Round Tubes at Pressures Above 500 p.s.i.a."*, WAPD-188, 1958.

Doerffer, S., Groeneveld, D.C. and Cheng, S.C., *"A comparison of Mixing in Tightly Spaced Bundle Geometries With Different Coolants"*, AECL Report, ARD-TD-363, 1992 April.

Doroshchuk, V.E., Levitan, L.L. and Lantzman, F.P., *"Investigations into Burnout in Uniformly Heated Tubes"*, ASME Paper 75-WT/HT-22, 1975.

Doroshchuk, V.E. and Lantzman, F.P., *"Selecting Magnitudes of Critical Heat Fluxes With Water Boiling in Vertical Uniformly Heated Tubes "*, Thermal Engineering, Vol. 17, No. 12, pp. 18-21, 1970.

Gambill, W.R. and Bundy, R.D., *"HFIR Heat-Transfer Studies of Turbulent Water Flow in Thin Rectangular Channels"*, ORNL-3079, 1961 June.

Gill, L.E., Hewitt, G.F. and Lacey, P.M.C., *"Data on the Upwards Annular Flow of Air-Water Mixtures"*, Chem. Eng. Sci., Vol. 20, No. 71, 1965.

Green, S.J., Sladna, E.F., LeTourneau, B.W. and Sherba, P.S., "*Critical Heat Flux Tests on a Coolant Channel, Simulating a Closely Spaced Lattice of Rods*", Proceedings of ASME Winter Meeting, pp. 72-80, 1969.

Groeneveld, D.C., Joober, K., Doerffer, S., Wong, W., Leung, L.K.H. and Cheng, S.C., "*The Effect of Fuel Subchannel Geometry on CHF*", Paper Presented at the NURETH-5 Meeting, Salt Lake City, 1992 September.

Groeneveld, D.C. and Leung, L.K.H., "*Tabular Approach for Predicting Critical Heat Flux and Post-Dryout Heat Transfer*", Paper Presented at the NURETH-4 Meeting, Karlsruhe, F.R.G., 1989 October.

Groeneveld, D.C., Cheng, S.C. and Doan, T., "*1986 AECL-UO Critical Heat Flux Lookup Table*", Heat Transfer Engineering, Vol. 7, No. 1-2, pp. 46-62, 1986a.

Groeneveld, Kiameh, B.P. and Cheng, "*Prediction of Critical Heat Flux (CHF) for Non-Aqueous Fluids in Forced Convective Boiling*", Proceedings of 8th Int. Heat Transfer Conf., San Francisco, California, Vol. 5, pp. 2209-2214, 1986b.

Groeneveld, D.C., "*Heat Transfer Phenomenon Related to the Boiling Crisis*", AECL Report, AECL-7239, Chalk River Nuclear Laboratories, 1981.

Groeneveld, D.C. and Merilo, M., AECL Unpublished Report, 1974.

Heron, R.A., Kinneir, J.H., Stevens, G.F. and Wood, R.W., "*Burn-Out Power and Pressure Drop Measurements on 12 ft. 7-Rod Clusters Cooled by Freon-12 at 155 PSIA*", AEEW-R 655, 1969.

Hewitt, G.F. and Hall-Taylor, N.S., "*Annular Two Phase Flow*", Pergamon Press, 1970.

Hewitt, G.F., Kearsey, H.A., Lacey, P.M.C. and Pulling, D.G., "*Burn-out and Nucleation in Climbing Film Flow*", AERE-R 4374, 1963.

Hill, K.W., Motley, F.E. and Casterline, J.E., "*Effect of a Rod Bowed to Contact* *on Critical Heat Flux in Pressurized Water Reactor Rod Bundles*", ASME Paper No. 75-WA/HT-77, 1975.

Hinze, J.O., "*Fundamentals of Hydrodynamic Mechanism of Splitting in Dispersion Processes*", A.I.Ch.E. Journal, Vol. 1, No. 3, pp. 289-295, 1955.

Howard, C.L., "*Fuel Cycle Program. A Boiling Water Reactor Research and Development Program*", GEAP-4215, 1963.

Hung, Y.H. and Yao, S.C., "*Critical Heat Flux of Convective Freon-113 in Very Narrow Annuli*", ASME Paper No. 83-HT-10, 1983.

Israel, S., Casterline, J. and Matzner, B., "*Critical Heat Flux Measurements in a 16-Rod Simulation of a BWR Fuel Assembly*", Journal of Heat Transfer, Vol. 91, pp. 355-363, 1969 August.

Ivey, H.J. and Morris, D.J., "*On the Relevance of The Vapour-Liquid Exchange Mechanism for Subcooled Boiling Heat Transfer at High Pressure*", UKAEA Report AEEW-R-137, 1962.

Jacket, H.S., Roarty, D.J. and Zerbe, "*Investigation of Burnout Heat Flux in Rectangular Channels at 2000 Psia*", Transactions of the ASME, pp. 391-401, 1958 February.

Janssen, E. and Kervinen, J.A., "*The Critical Boiling Heat Flux at High Flows and High Qualities*", APED-4554, 1964 January.

Janssen, E. and Kervinen, J.A., "*Burnout Conditions for Single Rod in Annular Geometry, Water at 600 to 1400 PSIA*", GEAP-3899, 1963 February.

Janssen, E., Levy, S. and Kervinen, J.A., "*Investigations of Burnout in Internally Heated Annulus Cooled by Water at 600 to 1450 PSIA*", ASME Paper No. 63-WA-149, 1963 November.

Jensen, A. and Mannov, G., "*Burnout, Film Flow, Film Thickness and Pressure Drop* *in a Concentric Annulus 3500x26x17 With Heated Rod and Tube"*, Danish Atomic Energy Commission, SDS-77, 1974.

Judd, R.A., Tahir, A., Carver, M.B., Kiteley, J.C., Rowe, D.S., Stewart, D.G. and Thibeault, P.R., "*ASSERT-4 User's Manual*", AECL-8573, 1984 September.

Kataoka, I., Ishii, M. and Mishima, K., "*Generation and Size Distribution of Droplet in Annular Two-Phase Flow*", Journal of Fluid Engineering, Vol. 105, pp. 230-238, 1983.

Katto, Y., "*Generalized Correlations of Critical Heat Flux for the Forced Convection Boiling in Vertical Uniformly Heated Annuli*", Int. J. Heat Mass Transfer, Vol. 22, pp 575-584, 1979.

Katto, Y., "*Generalized Correlations of Critical Heat Flux for the Forced Convection Boiling in Vertical Uniformly Heated Round Tubes*", Int. J. Heat Mass Transfer, Vol. 22, pp 1527-1542, 1978.

Kirillov, P.L. *et al.*, "*On Standard Critical Heat Flux Data for Round Tubes*", Proc. of the 4th Int'l Topical Meeting on Nuclear Reactor Thermal-hydraulics, Karlsruhe, F.R.G., Vol. 1, pp. 103-108, 1989.

Kirillov, P.L. and Smogalev, I.P., "*Calculation of Heat-Transfer Crisis for Annular Two-Phase Flow of a Steam-Liquid Mixture Through an Annular Channel*", Translated From report FEI-297 of the Physics and Power-Engineering Institute, Obninsk, USSR, 1972. AECL Report, AECL-4752, 1974 February.

Kobori, T., "*Critical Heat Flux Measurements in a Full Scale Rod Cluster*", Bulletin of the JSME, Vol. 19, No. 131, pp. 540-546, 1976.

Lee, C.H. and Mudawwar I., "*A Mechanistic Critical Heat Flux Model for Subcooled Flow Boiling Based on Local Bulk Flow Conditions*", Int. J. Multiphase Flow, Vol. 14, No. 6, pp. 711-728, 1988.

Lee, D.H., "*An Experimental Investigation of Forced Convection Burnout in High*

Pressure Water - Part IV, Large Diameter Tubes at about 1600 p.s.i.", AEEW-R 479, 1966.

Levy, S., "*Forced Convection Subcooled Boiling Prediction of Vapour Volumetric Fraction*", General Electric Company, GEAP-5157, 1966.

Levy, S., Polomik, E.E., Swan, C.L. and McKinney, W., "*Eccentric Rod Burnout at 1000 lbf/in^2 With Net Steam Generation*", Int. J. Heat Mass Transfer, Vol.5, pp. 595-614, 1962.

Levy, S., Fuller, R.A. and Niemi, R.O., "*Heat Transfer to Water in Thin Rectangular Channels*", Journal of Heat Transfer, Vol. 81, No. 2, pp. 129-143, 1959 May.

Lienhard, J.H. and Dhir, V.K., "*Extended Hydrodynamic Theory of the Peak and Minimum Pool Boiling Heat Fluxes*", NASA CR-2270, 1973.

Lund, K.O., "*Critical Heat Flux in Subcooled, Low-Pressure Rod Bundle With Various Rod Spacings*", ASME Paper No. 75-HT-49, 1975.

Macbeth, R.V., " *The Burnout Phenomena in Forced-Convective Boiling*", Advances in Chemical Engineering, Vol. 7, 1968.

Macduff, R.B. and Fighetti, C.F., "*Effect of Rod Bow to Partial Closure on Critical Heat Flux in PWR Fuel Assembly*", ASME Paper No. 83-HT-105, 1983.

Markowski, E.S., Lee, L., Biderman, R. and Casterline, J.E., "*Effect of Rod Bowing on CHF in PWR Fuel Assemblies*", ASME Paper No. 77-HT-91, 1977.

Midvidy, W.I., "*CHF in Element Assemblies Relevant to CANDU Fuel: A Critical Review*", CWAPD-288, 1976.

Moeck, E.O., Matzner, B., Casterline, J.E. and Yuill, G.K., "*Critical Heat Fluxes in Internally Heated Annuli of Large Diameter Cooled by Boiling Water at 1000 psia*", Proceedings of the 3rd International Heat Transfer Conference, Vol. III, pp. 86-97, A.I.Ch.E., New York, 1966.

Nagino, Y., Shodai, N., Matsumoto, C. and Ueji, M., "*Rod Bowed to Contact Departure From Nucleate Boiling Tests in Cold Wall Thimble Cell Geometry*", Journal of Nuclear Science and Technology, Vol. 15, pp. 568-573, 1978.

Nakajima, I., Kikuchi, A. and Kobori, T., "*A Study of the Effect of Rod-Bowing on Critical Heat Flux*", Nuc. Eng. and Des., Vol. 42, pp. 237-245, 1977.

Nixon, R.B., Matzner, B. and Lahey, R.T. Jr., "*The Effect of Reduced Clearance and Rod Bow on Critical Power in Full-Scale Simulations of 8x8 BWR Fuel*", ASME Paper No. 75-HT-69, 1975.

Ornatskiy, A.P., "*The Effect of Basic Regime Parameters and Channel Geometry on Critical Heat Fluxes in Forced Convection of Subcooled Water*", Heat Transfer-Soviet Research, Vol. 1, No. 3, pp. 17-22, 1969a.

Ornatskiy, A.P., Glushchenko, L.F. and Kichigin, A.M., "*Burnout in Annular Channel With Two-Sided Heating*", Heat Transfer-Soviet Research, Vol. 1, No. 6, pp. 12-16, 1969b.

Ornatskiy, A.P., Chernobay, V.A., Lazarev, N.A. and Furaev, V.S., "*Investigation of the Influence of Eccentricity on Burnout Heat Transfer in Annular Channels*", Teploenergetika, 16(7), 74-76, 1969c.

Ornatskiy, A.P., Kichigin, A.M. and Glushchenko, L.F., "*A Study of Critical Heat Flux in Externally Heated Annular Channels*", Therm. Eng. (Eng. Transl.), 13(10): 100-104, 1966 October.

Ouma, B.H. and Tavoularis S., "*Flow Measurements in Rod Bundle Subchannels With Varying Rod-Wall Proximity*", Nuclear Engineering and Design, 131: 193-208, 1991a.

Ouma, B.H. and Tavoularis S., "*Turbulence Structure in Triangular Subchannels of a Reactor Bundle Model*", Nuclear Engineering and Design, 128: 271-287, 1991b.

Pexton, A.F., "*A Review of Data on Burnout Heat Flux for Steam-Water Mixtures in Uniformly Heated Channels*", DEG Report 203 (R), 1961.

Pogson, J.T., Roberts, J.H. and Waibler, P.J., "*An Investigation of the Liquid Distribution in Annular Mist Flow*", Journal of Heat Mass Transfer, Vol. 92, No. 65, 1970.

Rogers, J.T. and Tahir, A.E.E., "*Turbulent Interchange Mixing in Rod Bundles and the Role of Secondary Flows*", New York, ASME Publication 75-HT-31, 1975.

Rogers, J.T. and Rosehart, R.G., "*Mixing by Turbulent Interchange Bundles, Correlation and Inference*", Paper 72-H7-53, ASME-AICHE Heat Transfer Conf., New York, 1972.

Rogers, J.T., "*Heat Transfer Limitations on Nuclear Reactor Fuel Elements*", The Canadian Journal of Chemical Engineering, pp. 289-298, 1966 October.

Rowe, D.S. and Angle, C.W., "*Cross-Flow Mixing Between Parallel Flow Channels During Boiling, Part III: Effect of Spacers on Mixing Between Channels*", BNWL-371, Pacific North-West Laboratory, 1969.

Rudzinski, K.F., AECL (CRL) Unpublished Data, 1992.

Rudzinski, K.F., AECL (CRL) Unpublished Report, 1991.

Snoek, C.W., "*An Analysis of Critical Heat Flux in Interconnected Subchannels*", Paper Presented at the 5th Miami International Symposium on Multi-Phase Transport & Particulate Phenomena, , Miami Beach, Florida, December 12-14, 1988. Also AECL Report, AECL-9882.

Smogalev, I.P., "*Calculation of the Critical Heat Fluxes With Flow of Subcooled Water at Low Velocity*", Thermal Engineering, Vol. 28, pp. 208-211, 1981.

Stevens, G.F., Elliott, D.F. and Wood, R.W., "*An Experimental Investigation into Forced Convection Burn-out in Freon, With Reference to Burn-out in Water -*

Uniformly Heated Round Tubes With Vertical Up-Flow", AEEW-R 321, 1964.

Tatterson, D.F., Dallman, J.C. and Hanratty, T.J., "*Drop Sizes in Annular Gas-Liquid Flows*", AIChe Journal, Vol. 23, No. 1, pp. 68-76, 1977.

Tippets, F.E., "*Critical Heat Fluxes and Flow Patterns in High Pressure Boiling Water Flows*", Paper 62-WA-162 Presented at ASME Winter Annual Meeting, New York, 1962.

Tolubinskiy, V.I., Domashev, Ye.D., Litoshenko, A.K. and Matorin, A.S., "*Boiling Crisis in Concentric and Eccentric Annuli*", Heat Transfer-Soviet Research, Vol. 9, No. 1, 1977 January-February.

Tolubinskiy, V.I, Litoshenko, A.K. and Shevtsov, V.L., "*Effect of Curvature on the Critical Heat Flux Density in Forced-Convection Flow*", Heat Transfer-Soviet Research, Vol. 5, No. 1, pp. 21-25, 1973a.

Tolubinskiy, V.I, Litoshenko, A.K., Shevtsov, V.L., Domashev, YE.D. and Struchenko, G.YE., "*Heat Transfer Crisis at the Inward Surface of Annuli Heated From Both Sides*", Heat Transfer-Soviet Research, Vol. 5, No. 3, pp.93-96, 1973b.

Tolubinskiy, V.I, Litoshenko, A.K., Domashev, YE.D., Kravchenko, A.S. and Chirov, D.A., "*Critical Heat Transfer in Eccentric Annuli*", Teploenergetika, Vol. 18, No. 6, pp. 64-66, 1971.

Tolubinskiy, V.I, Litoshenko, A.K. and Shevtsov, V.L., "*Critical Heat Flux Densities in Internally-Heated Annuli*", Heat Transfer-Soviet Research, Vol. 2, No. 6, pp. 183-186, 1970a.

Tolubinskiy, V.I, Litoshenko, A.K. and Shevtsov, V.L., "*Heat Transfer Crisis at Water Boiling in Annular Channels With External and Internal Heating*", Paper No. B 6.11, Fourth Int. Conf. on Heat Transfer, Paris 1970b.

Tolubinskiy, V.I, Litoshenko, A.K. and Shevtsov, V.L., "*Correlation of Experimental Data on Critical Heat Fluxes in Annular Channels*", Heat Transfer-

Soviet Research, Vol. 1, No. 1, pp.80-87, 1969 January.

Tong, L.S., "*Boiling Crisis and Critical Heat Flux*", USAEC Report TID-25887, Westinghouse Electric Corp., 1972.

Tong, L.S., Steer, R.W., Wenzel, A.H., Bogaardt, M. and Spigt, C.L., "*Critical Heat Flux on a Heater Rod in The Center of Smooth and Rough Sleeves, and in Line Contact With an Unheated Wall*", ASME Paper 67-WA/HT-29, 1967.

Tong, L.S., "*Boiling Heat Transfer and Two-Phase Flow*", John Wiley & Sons, 1965.

Turner, J.M. and Wallis, G.B., "*An Analysis of the Liquid Film in Annular Flow*", NYO-3114-13, 1965.

Ueda, T., "*On the Droplets Entrained in Two-Phase Annular and Mist Flow*", From the Two-Phase Flow Dynamics, Japan-U.S. Seminar, Edited by Bergles, A.E. and Ishigai, S., pp. 75-94, 1979.

Weisman, J. and Pei, S., "*Prediction of Critical Heat Flux in Flow Boiling* at *Low Qualities*", Int. J. Heat Mass Transfer, Vol. 26, No. 10, pp. 1463-1477, 1983.

Whalley, P.B., Hutchinson, P. and Hewitt, G.F., "*The Calculation of Critical Heat Flux in Forced Convective Boiling*", Heat Transfer, Vol. 4, pp. 209-294, 1974.

Whalley, P.B., "*Boiling Condensation and Gas-Liquid Flow*", Oxford University Press, 1987.

Wicks, M. and Dukler, A.E., "*In Situ Measurements of Drop Size Distribution in Two-Phase Flow: A New Method for Electrically Conducting Liquids*", Paper Presented at the International Heat Transfer Conference, Chicago, Vol. III, pp. 39-49, 1966.

Youk, G.U., Lee, B.R., Smith, A.H. and Dimmick, G.R., "*Effect of Cross-sectional Shape on Critical Heat Flux and Pressure Drop in a Vertical Tube Cooled by Freon-12*", 2nd. International Topical Meeting on Nuclear Power Plant Thermal Hydraulics and Operations, Tokyo, pp. 22-26, 1986 April.

Zeigarnik, Yu.A., Privalov, N.P. and Klimov, A.I., "*Critical Heat Flux With Boiling of Subcooled Water in Rectangular Channels With One-Sided Supply of Heat*", Thermal Engineering, Vol. 28, No. 1, 1981.

Zuber, N., "*Hydrodynamic Aspects of Boiling Heat Transfer*", AECU-4439, 1959.

APPENDIX A

CHF DATA FOR CONCENTRIC ANNULI

Table A.1: Sample of Barnett [1966,1968] Results for Internally Heated Concentric Annuli.

D_i m	D_o m	L m	P kPa	G $kg.m^{-2}.s^{-1}$	X_c	X_i	CHF $kW.m^{-2}$
.00953	.01410	1.778	6894.6	2278.4	.039	-.516	3047.7
.00953	.01410	1.778	6894.6	2292.0	.053	-.422	2628.1
.00953	.01410	1.778	6894.6	2305.5	.177	-.081	1435.5
.00953	.01410	1.778	6894.6	2305.5	.107	-.242	1940.3
.00953	.01410	1.778	6894.6	2305.5	.066	-.366	2401.0
.00953	.01410	1.778	6894.6	2305.5	.044	-.456	2776.4
.00953	.01410	1.778	6894.6	2319.1	.085	-.312	2224.3
.00953	.01410	1.778	6894.6	3024.3	.132	-.142	1997.1
.00953	.01410	1.778	6894.6	3037.9	.086	-.212	2186.4
.00953	.01410	1.778	6894.6	3051.4	.056	-.280	2470.4
.00953	.01410	1.778	6894.6	3051.4	.034	-.336	2725.9
.00953	.01410	1.778	6894.6	3065.0	.116	-.160	2035.0
.00953	.01410	1.778	6894.6	3078.6	.005	-.437	3284.4
.00953	.01803	1.778	6894.6	754.0	.224	-.523	2949.9
.00953	.01803	1.778	6894.6	758.1	.296	-.223	2060.2
.00953	.01803	1.778	6894.6	766.3	.300	-.167	1874.1
.00953	.01803	1.778	6894.6	766.3	.295	-.168	1858.3
.00953	.01803	1.778	6894.6	766.3	.293	-.264	2233.7
.00953	.01803	1.778	6894.6	766.3	.212	-.614	3315.9
.00953	.01803	1.778	6894.6	771.7	.314	-.093	1640.6
.00953	.01803	1.778	6894.6	777.1	.258	-.349	2467.2
.00953	.01803	1.778	6894.6	777.1	.236	-.429	2707.0
.00953	.01803	1.778	6894.6	783.9	.217	-.441	2700.7
.00953	.01803	1.778	6894.6	1518.9	.204	-.053	2047.6
.00953	.01803	1.778	6894.6	1518.9	.146	-.178	2574.5
.00953	.01803	1.778	6894.6	1518.9	.096	-.288	3054.0
.00953	.01803	1.778	6894.6	1518.9	.085	-.341	3391.6
.00953	.01803	1.778	6894.6	1532.5	.203	-.067	2167.5
.00953	.01803	1.778	6894.6	1532.5	.177	-.109	2293.7
.00953	.01803	1.778	6894.6	1532.5	.120	-.208	2634.4
.00953	.01803	1.778	6894.6	1532.5	.115	-.246	2896.3
.00953	.01803	1.778	6894.6	1532.5	.101	-.289	3129.8
.00953	.01803	1.778	6894.6	1532.5	.067	-.385	3625.1
.00953	.01803	1.778	6894.6	1546.1	.194	-.068	2120.2
.00953	.01803	1.778	6894.6	2278.4	.124	-.123	2940.5
.00953	.01803	1.778	6894.6	2278.4	.114	-.129	2896.3
.00953	.01803	1.778	6894.6	2278.4	.090	-.188	3319.1
.00953	.01803	1.778	6894.6	2278.4	.055	-.261	3770.2

continued...

Table A.1 (continued)

.00953	.01803	1.778	6894.6	2278.4	.044	-.264	3672.4
.00953	.01803	1.778	6894.6	2278.4	.055	-.264	3808.1
.00953	.01803	1.778	6894.6	2292.0	.155	-.040	2341.0
.00953	.01803	1.778	6894.6	2292.0	.030	-.301	3965.8
.00953	.01803	1.778	6894.6	2292.0	.004	-.373	4521.1
.00953	.01803	1.778	6894.6	2305.5	.159	-.036	2347.3
.00953	.01803	1.778	6894.6	2305.5	.152	-.057	2520.8
.00953	.01803	1.778	6894.6	2305.5	.021	-.322	4139.4
.00953	.01803	1.778	6894.6	3037.9	.026	-.220	3918.5
.00953	.01803	1.778	6894.6	3037.9	.018	-.240	4092.0
.00953	.01803	1.778	6894.6	3037.9	.016	-.253	4281.3
.00953	.01803	1.778	6894.6	3037.9	.006	-.254	4139.4
.00953	.01803	1.778	6894.6	3051.4	.135	-.025	2549.2
.00953	.01803	1.778	6894.6	3051.4	.061	-.152	3401.1
.00953	.01803	1.778	6894.6	3051.4	.017	-.245	4189.8
.00953	.01803	1.778	6894.6	3051.4	-.010	-.298	4590.5
.00953	.01803	1.778	6894.6	3065.0	.118	-.036	2460.9
.00953	.01803	1.778	6894.6	3065.0	.090	-.098	3009.9
.00953	.01803	1.778	6894.6	3065.0	.026	-.208	3760.8
.00953	.01803	1.778	6894.6	3078.6	.113	-.067	2896.3
.00953	.01803	1.778	6894.6	3092.1	.056	-.153	3391.6
.00953	.01803	1.778	6894.6	3200.6	-.039	-.315	4628.4
.00953	.02222	1.778	6894.6	718.8	.232	-.111	2218.0
.00953	.02222	1.778	6894.6	722.9	.255	-.069	2107.5
.00953	.02222	1.778	6894.6	1505.4	.063	-.216	3782.8
.00953	.02222	1.778	6894.6	1518.9	.158	-.038	2684.9
.00953	.02222	1.778	6894.6	1518.9	.134	-.081	2934.1
.00953	.02222	1.778	6894.6	1518.9	.110	-.133	3319.1
.00953	.02222	1.778	6894.6	1518.9	.075	-.188	3596.7
.00953	.02222	1.778	6894.6	1518.9	.056	-.230	3912.2
.00953	.02222	1.778	6894.6	1518.9	.044	-.252	4054.2
.00953	.02222	1.778	6894.6	1518.9	.023	-.291	4297.1
.00953	.02222	1.778	6894.6	1518.9	.002	-.333	4574.8
.00953	.02222	1.778	6894.6	1518.9	-.017	-.377	4921.8
.00953	.02222	1.778	6894.6	1518.9	-.033	-.409	5145.8
.00953	.02222	1.778	6894.6	2264.9	.040	-.148	3836.5
.00953	.02222	1.778	6894.6	2292.0	.011	-.194	4211.9
.00953	.02222	1.778	6894.6	2292.0	.112	-.030	2934.1
.00953	.02222	1.778	6894.6	2292.0	.106	-.032	2852.1
.00953	.02222	1.778	6894.6	2292.0	.079	-.085	3385.3
.00953	.02222	1.778	6894.6	2292.0	.042	-.144	3852.3
.00953	.02222	1.778	6894.6	2292.0	.019	-.174	3994.2
.00953	.02222	1.778	6894.6	2292.0	-.025	-.254	4738.8
.00953	.02222	1.778	6894.6	2292.0	-.036	-.271	4858.7
.00953	.02222	2.713	6894.6	1518.9	.167	-.048	1924.6
.00953	.02222	2.713	6894.6	1518.9	.101	-.251	3155.0
.00953	.02222	2.713	6894.6	1532.5	.136	-.109	2218.0
.00953	.02222	2.713	6894.6	1546.1	.120	-.152	2476.7
.00953	.02222	2.743	6894.6	720.1	.287	-.073	1511.2

continued...

Table A.1 (continued)

.00953	.02222	2.743	6894.6	721.5	.293	-.076	1552.3
.00953	.02222	2.743	6894.6	731.0	.244	-.229	2019.2
.00953	.02222	2.743	6894.6	732.3	.256	-.160	1776.3
.00953	.02222	2.743	6894.6	735.1	.249	-.245	2117.0
.00953	.02222	2.743	6894.6	739.1	.220	-.368	2536.6
.00953	.02222	2.743	6894.6	741.8	.225	-.294	2243.2
.00953	.02222	2.743	6894.6	743.2	.222	-.374	2583.9
.00953	.02222	2.743	6894.6	743.2	.228	-.461	2984.6
.00953	.02222	2.743	6894.6	1160.9	.143	-.363	3423.2
.00953	.02222	2.743	6894.6	1162.3	.155	-.219	2536.6
.00953	.02222	2.743	6894.6	1165.0	.202	-.057	1757.3
.00953	.02222	2.743	6894.6	1165.0	.140	-.287	2905.8
.00953	.02222	2.743	6894.6	1166.3	.180	-.134	2135.9
.00953	.02222	2.743	6894.6	1518.9	.165	-.046	1867.8
.00953	.02222	2.743	6894.6	1518.9	.163	-.048	1864.6
.00953	.02222	2.743	6894.6	1518.9	.147	-.100	2189.6
.00953	.02222	2.743	6894.6	1518.9	.131	-.166	2634.4
.00953	.02222	2.743	6894.6	1518.9	.124	-.184	2732.2
.00953	.02222	2.743	6894.6	1518.9	.121	-.204	2886.8
.00953	.02222	2.743	6894.6	1518.9	.110	-.274	3404.2
.00953	.02222	2.743	6894.6	1518.9	.084	-.337	3726.1
.00953	.02222	2.743	6894.6	1532.5	.092	-.302	3521.0
.00953	.02222	2.743	6894.6	1546.1	.095	-.273	3315.9
.00953	.02222	2.743	6894.6	1546.1	.098	-.281	3413.7
.00953	.02222	2.743	6894.6	2264.9	.065	-.202	3530.4
.00953	.02222	2.743	6894.6	2278.4	.060	-.170	3063.5
.00953	.02222	2.743	6894.6	2292.0	.124	-.036	2142.2
.00953	.02222	2.743	6894.6	2292.0	.124	-.038	2164.3
.00953	.02222	2.743	6894.6	2292.0	.105	-.085	2536.6
.00953	.02222	2.743	6894.6	2292.0	.090	-.123	2849.0
.00953	.02222	2.743	6894.6	2292.0	.087	-.125	2830.0
.00953	.02222	2.743	6894.6	2292.0	.058	-.201	3454.7
.00953	.02222	2.743	6894.6	2292.0	.043	-.235	3707.1
.00953	.02222	2.743	6894.6	2292.0	.048	-.244	3902.7
.00953	.03175	1.778	6894.6	189.9	.343	-.127	1826.7
.00953	.03175	1.778	6894.6	191.2	.353	-.083	1706.9
.00953	.03175	1.778	6894.6	192.6	.319	-.272	2331.5
.00953	.03175	1.778	6894.6	192.6	.300	-.387	2707.0
.00953	.03175	1.778	6894.6	195.3	.319	-.224	2167.5
.00953	.03175	1.778	6894.6	381.1	.156	-.208	2842.7
.00953	.03175	1.778	6894.6	381.1	.154	-.212	2858.4
.00953	.03175	1.778	6894.6	381.1	.138	-.287	3319.1
.00953	.03175	1.778	6894.6	382.4	.169	-.157	2558.7
.00953	.03175	1.778	6894.6	382.4	.079	-.460	4221.4
.00953	.03175	1.778	6894.6	385.2	.214	-.053	2107.5
.00953	.03175	1.778	6894.6	385.2	.205	-.055	2047.6
.00953	.03175	1.778	6894.6	385.2	.197	-.062	2047.6
.00953	.03175	1.778	6894.6	385.2	.117	-.332	3543.1
.00953	.03175	1.778	6894.6	387.9	.199	-.085	2255.8

continued...

Table A.1 (continued)

.00953	.03175	1.778	6894.6	387.9	.104	-.408	4069.9
.00953	.03175	1.778	6894.6	762.2	.013	-.272	4454.9
.00953	.03175	1.778	6894.6	764.9	.030	-.229	4063.6
.00953	.03175	1.778	6894.6	770.3	.123	-.037	2520.8
.00953	.03175	1.778	6894.6	1518.9	.032	-.088	3710.3
.00960	.01400	.737	6894.6	2861.6	.152	-.052	3240.2
.00960	.01400	.737	6894.6	2861.6	.152	-.050	3205.5
.00960	.01400	.737	6894.6	2861.6	.148	-.060	3290.7
.00960	.01400	.737	6894.6	2875.1	.149	-.061	3341.1
.00960	.01400	.737	6894.6	2888.7	.137	-.079	3461.0
.00960	.01400	.737	6894.6	2888.7	.135	-.085	3511.5
.00960	.01400	.737	6894.6	2915.8	.128	-.094	3552.5
.00960	.01400	.737	6894.6	2915.8	.115	-.116	3732.4
.00960	.01400	.737	6894.6	2929.4	.103	-.138	3902.7
.00960	.01400	.737	6894.6	2956.5	.097	-.143	3934.3
.00960	.01400	.737	6894.6	2956.5	.083	-.165	4054.2
.00960	.01400	.737	6894.6	2943.0	.091	-.162	4101.5
.00960	.01400	.737	6894.6	2997.2	.057	-.199	4240.3
.00960	.01400	.737	6894.6	2997.2	.074	-.188	4341.3
.01270	.01905	.914	6894.6	2793.8	.002	-.218	4038.4
.01270	.01905	.914	6894.6	2793.8	-.012	-.240	4180.4
.01270	.01905	.914	6894.6	2793.8	-.065	-.315	4587.4
.01270	.01905	.914	6894.6	2807.3	.115	-.038	2807.9
.01270	.01905	.914	6894.6	2807.3	.065	-.111	3237.0
.01270	.01905	.914	6894.6	2807.3	.049	-.136	3423.2
.01270	.01905	.914	6894.6	2807.3	.031	-.166	3631.4
.01270	.01905	.914	6894.6	2807.3	.013	-.198	3883.8
.01270	.01905	.914	6894.6	2807.3	-.031	-.266	4335.0
.01270	.01905	.914	6894.6	2807.3	-.046	-.284	4388.6
.01270	.01905	.914	6894.6	2820.9	.088	-.078	3073.0
.01270	.01905	.914	6894.6	5587.5	.065	-.018	3019.3
.01270	.01905	.914	6894.6	5587.5	.039	-.057	3511.5
.01270	.01905	.914	6894.6	5587.5	-.041	-.158	4300.3
.01270	.01905	.914	6894.6	5614.7	.003	-.105	3972.1
.01270	.01905	.914	6894.6	5641.8	-.073	-.201	4719.9
.01270	.01905	.914	6894.6	8150.8	.048	-.013	3252.8
.01270	.01905	.914	6894.6	8367.8	.028	-.035	3445.3
.01270	.01905	.914	6894.6	8381.3	.004	-.064	3710.3
.01270	.01905	.914	6894.6	8381.3	-.011	-.082	3861.7
.01270	.01905	.914	6894.6	8394.9	-.026	-.101	4126.7
.01270	.01905	.914	6894.6	8408.4	-.041	-.121	4410.7
.01270	.01905	.914	6894.6	8408.4	-.057	-.142	4719.9
.01270	.02540	.610	6894.6	393.3	.172	-.081	2350.5
.01270	.02540	.610	6894.6	406.9	.142	-.136	2669.1
.01270	.02540	.610	6894.6	664.5	.136	-.058	3038.3
.01270	.02540	.610	6894.6	786.6	.082	-.098	3350.6
.01270	.02540	.610	6894.6	1112.1	.060	-.087	3861.7
.01270	.02540	.610	6894.6	1125.6	.088	-.055	3804.9
.01270	.02540	.610	6894.6	1220.6	.000	-.159	4600.0

continued...

Table A.1 (continued)

.01270	.02540	.610	6894.6	1396.9	.001	-.122	4060.5
.01270	.02540	.737	6894.6	275.3	.168	-.432	3227.6
.01270	.02540	.737	6894.6	275.3	.137	-.545	3675.6
.01270	.02540	.737	6894.6	276.7	.222	-.285	2738.5
.01270	.02540	.737	6894.6	276.7	.189	-.365	2997.3
.01270	.02540	.737	6894.6	278.0	.258	-.143	2176.9
.01270	.02540	.737	6894.6	279.4	.240	-.228	2558.7
.01270	.02540	.737	6894.6	549.3	.169	-.073	2596.6
.01270	.02540	.737	6894.6	549.3	.165	-.073	2552.4
.01270	.02540	.737	6894.6	549.3	.168	-.079	2653.4
.01270	.02540	.737	6894.6	549.3	.173	-.080	2716.5
.01270	.02540	.737	6894.6	550.6	.171	-.084	2738.5
.01270	.02540	.737	6894.6	553.3	.137	-.146	3060.4
.01270	.02540	.737	6894.6	553.3	.123	-.161	3076.1
.01270	.02540	.737	6894.6	553.3	.104	-.205	3347.5
.01270	.02540	.737	6894.6	553.3	.114	-.225	3675.6
.01270	.02540	.737	6894.6	553.3	.103	-.274	4076.3
.01270	.02540	.737	6894.6	554.7	.088	-.308	4290.8
.01270	.02540	.737	6894.6	815.1	-.093	-.458	5830.4
.01270	.02540	.737	6894.6	824.6	.126	-.056	2940.5
.01270	.02540	.737	6894.6	825.9	-.084	-.422	5467.6
.01270	.02540	.737	6894.6	827.3	.066	-.174	3896.4
.01270	.02540	.737	6894.6	828.6	-.007	-.285	4508.5
.01270	.02540	.737	6894.6	830.0	.105	-.093	3205.5
.01270	.02540	.737	6894.6	832.7	.038	-.236	4473.8
.01270	.02540	.737	6894.6	832.7	-.074	-.371	4833.5
.01270	.02540	.737	6894.6	832.7	-.064	-.391	5332.0
.01270	.02540	.737	6894.6	834.1	-.134	-.501	5991.3
.01270	.02540	.737	6894.6	2319.1	.024	-.052	3429.5
.01270	.02540	.737	6894.6	2319.1	-.011	-.098	3950.1
.01270	.02540	.737	6894.6	2319.1	-.033	-.123	4193.0
.01270	.02540	.737	6894.6	2319.1	-.044	-.140	4388.6
.01270	.02540	.737	6894.6	2319.1	-.072	-.177	4773.5
.01270	.02540	.737	6894.6	2332.7	.051	-.014	2962.5
.01270	.02540	.737	6894.6	2739.5	.042	-.020	3344.3
.01270	.02540	.737	6894.6	2766.6	.039	-.017	3022.5
.01270	.02540	.737	6894.6	2766.6	.021	-.046	3596.7
.01270	.02540	.737	6894.6	2766.6	-.005	-.072	3631.4
.01270	.02540	.737	6894.6	2766.6	-.015	-.085	3763.9
.01270	.02540	.737	6894.6	2766.6	-.031	-.105	4038.4
.01270	.02540	.737	6894.6	2766.6	-.053	-.133	4300.3
.01270	.02540	.737	6894.6	2766.6	-.071	-.154	4499.0
.01270	.02540	.737	6894.6	2766.6	-.087	-.173	4618.9
.01270	.02540	.737	6894.6	2766.6	-.115	-.204	4871.3
.01270	.02540	.737	6894.6	2780.2	.022	-.039	3312.7
.01270	.02540	.737	6894.6	2780.2	-.002	-.066	3502.1
.01270	.02540	.737	6894.6	5913.0	.021	-.009	3502.1
.01270	.02540	.914	6894.6	5519.7	-.025	-.074	4281.3
.01270	.02540	.914	6894.6	5519.7	-.038	-.091	4587.4

continued...

Table A.1 (concluded)

.01270	.02540	.914	6894.6	5533.3	.035	-.005	3413.7
.01270	.02540	.914	6894.6	5533.3	.006	-.037	3786.0
.01270	.02540	.914	6894.6	5546.9	-.004	-.049	3896.4
.01270	.02540	.914	6894.6	8313.5	-.001	-.032	4082.6
.01270	.02540	.914	6894.6	8313.5	-.022	-.057	4574.8
.01270	.02540	.914	6894.6	8313.5	-.032	-.068	4751.4
.01270	.02540	.914	6894.6	8327.1	.025	-.001	3413.7
.01372	.02222	1.829	6894.6	474.7	.455	-.136	1107.4
.01372	.02222	1.829	6894.6	758.1	.278	-.469	2609.2
.01372	.02222	1.829	6894.6	760.8	.302	-.242	1908.8
.01372	.02222	1.829	6894.6	760.8	.305	-.403	2479.8
.01372	.02222	1.829	6894.6	766.3	.341	-.090	1523.9
.01372	.02222	1.829	6894.6	773.0	.353	-.079	1539.6
.01372	.02222	1.829	6894.6	1518.9	.192	-.121	2189.6
.01372	.02222	1.829	6894.6	1518.9	.177	-.175	2464.1
.01372	.02222	1.829	6894.6	1518.9	.142	-.293	3047.7
.01372	.02222	1.829	6894.6	1532.5	.201	-.058	1829.9
.01372	.02222	1.829	6894.6	1532.5	.204	-.063	1883.5
.01372	.02222	1.829	6894.6	1532.5	.202	-.063	1867.8
.01372	.02222	1.829	6894.6	1532.5	.202	-.065	1883.5
.01372	.02222	1.829	6894.6	1532.5	.186	-.109	2082.3
.01372	.02222	1.829	6894.6	1532.5	.185	-.111	2091.8
.01372	.02222	1.829	6894.6	1532.5	.180	-.149	2322.1
.01372	.02222	1.829	6894.6	1532.5	.155	-.263	2946.8
.01372	.02222	1.829	6894.6	1532.5	.121	-.376	3508.4
.01372	.02222	1.829	6894.6	1546.1	.210	-.058	1908.8
.01372	.02222	1.829	6894.6	1925.8	.202	-.047	2205.3
.01372	.02222	1.829	6894.6	2292.0	.093	-.274	3880.7
.01372	.02222	1.829	6894.6	2319.1	.103	-.192	3155.0
.01372	.02222	1.829	6894.6	2346.2	.158	-.030	2038.1
.01372	.02222	1.829	6894.6	2346.2	.120	-.115	2539.8
.01372	.02222	1.829	6894.6	2359.8	.138	-.048	2031.8
.01372	.02222	2.591	6894.6	354.0	.612	-.109	829.8
.01372	.02222	2.591	6894.6	457.0	.536	-.092	933.9
.01372	.02222	2.591	6894.6	564.2	.458	-.137	1091.6
.01372	.02222	2.591	6894.6	572.3	.480	-.129	1132.6
.01372	.02222	2.591	6894.6	573.7	.461	-.125	1091.6
.01372	.02222	2.591	6894.6	599.4	.458	-.080	1047.5
.01372	.02222	2.591	6894.6	724.2	.403	-.115	1217.8
.01372	.02222	2.591	6894.6	724.2	.394	-.123	1217.8
.01372	.02222	2.591	6894.6	724.2	.348	-.421	1811.0
.01372	.02222	2.591	6894.6	725.6	.405	-.060	1097.9

APPENDIX B

CHF DATA FOR ECCENTRIC ANNULI

Table B.1: Anderson *et al.*[1974] eccentric annulus data*

P (MPa)	Gap (mm)	G ($Mg.m^{-2}.s^{-1}$)	X_c (%)	CHF ($MW.m^{-2}$)	CHF_{ecc}/CHF_{conc}
7	2.1	1.4	7.84	1.73	0.83
7	2.6	1.4	10.02	1.82	0.88
7	3.6	1.4	10.64	1.84	0.89
7	4.35	1.4	13.29	1.95	0.94
7	5.1	1.4	16.41	2.07	1.00
7	2.1	1.5	6.84	1.81	0.82
7	2.6	1.5	8.73	1.89	0.86
7	3.6	1.5	9.17	1.91	0.87
7	4.35	1.5	11.79	2.02	0.92
7	5.1	1.5	16.00	2.20	1.00
7	2.1	0.6	27.05	1.07	0.93
7	2.6	0.6	28.61	1.10	0.95
7	3.6	0.6	29.24	1.11	0.96
7	4.35	0.6	31.11	1.14	0.99
7	5.1	0.6	31.74	1.15	1.00

* For annulus dimension refer to Table 5.1.

APPENDIX C

CHF DATA FOR OTHER CROSS SECTIONS

Table C.1: Rectangular Channel CHF Data*. From De Bortoli *et al.* [1958].

P (psia)	ΔT_i (F^o)	$G \times 10^{-6}$ ($lb.ft^{-2}.hr^{-1}$)	$CHF \times 10^{-6}$ ($Btu.ft^{-2}.hr^{-1}$)	h_c ($Btu.lb^{-1}$)	X_c (%)
1200	216	0.212	1.202	1001	70.1
1200	215	0.298	1.513	932	58.8
1200	213	0.415	1.802	848	45.1
1200	213	0.606	2.080	739	27.3
1200	213	0.780	2.132	655	13.6
1200	25	0.181	1.005	1123	90.0
1200	21	0.280	1.360	1054	78.8
1200	19	0.372	1.510	973	65.5
1200	16	0.554	1.618	857	46.6
1200	17	0.704	1.629	794	36.3
2000	534	0.050	0.454	1087	89.7
2000	533	0.076	0.645	1021	75.4
2000	537	0.096	0.770	955	61.2
2000	534	0.146	0.887	749	16.8
2000	525	0.163	1.007	750	17.0
2000	532	0.184	1.171	762	19.6
2000	531	0.207	1.290	748	16.5
2000	534	0.256	1.300	697	5.6
2000	532	0.269	1.579	707	7.7
2000	532	0.316	1.561	608	-13.7
2000	530	0.346	1.736	618	-11.6
2000	531	0.453	1.985	548	-26.6
2000	521	0.554	2.407	555	-25.1
2000	433	0.192	1.102	790	25.6
2000	432	0.228	1.245	763	19.7
2000	437	0.289	1.452	712	8.8
2000	432	0.334	1.389	618	-11.6
2000	431	0.534	1.881	548	-26.6
2000	430	0.724	2.464	538	-28.8
2000	234	0.071	0.477	1124	97.6
2000	230	0.095	0.592	1071	86.3
2000	234	0.146	0.746	946	59.2
2000	235	0.188	0.841	922	54.0
2000	235	0.383	1.243	772	21.7
2000	236	0.611	1.550	685	3.0
2000	229	0.812	1.632	629	-9.2
2000	181	0.190	0.828	937	57.3

continued...

* s = 1.27 mm, w =25.4 mm and L = 152 mm

Table C.1 (concluded)

2000	185	0.397	1.154	756	18.3
2000	178	0.570	1.377	691	4.2
2000	181	0.766	1.700	684	2.8
2000	129	0.182	0.768	969	64.2
2000	132	0.377	1.052	803	8.3
2000	131	0.555	1.192	712	18.8
2000	130	0.713	1.287	684	2.8
2000	42	0.201	0.639	941	55.6
2000	39	0.287	0.736	881	45.2
2000	41	0.371	0.838	845	37.5
2000	36	0.553	0.911	788	25.2
2000	35	0.715	1.000	756	18.3

Table C.2: Rectangular Channel CHF Data*. From De Bortoli *et al.* [1958].

P (psia)	ΔTi (F^o)	$Gx10^{-6}$ ($lb.ft^{-2}.hr^{-1}$)	$CHFx10^{-6}$ ($Btu.ft^{-2}.hr^{-1}$)	h_c ($Btu.lb^{-1}$)	X_c (%)
2000	552	0.026	0.120	1127	98.7
2000	555	0.030	0.142	1119	96.7
2000	554	0.040	0.165	993	69.4
2000	553	0.040	0.171	1019	75.1
2000	537	0.101	0.422	1040	79.5
2000	538	0.126	0.498	987	68.1
2000	535	0.151	0.564	935	57.0
2000	535	0.176	0.622	845	37.5
2000	531	0.201	0.675	809	29.7
2000	539	0.261	0.834	751	17.2
2000	542	0.267	0.843	760	19.0
2000	541	0.267	0.825	745	15.8
2000	540	0.270	0.835	745	15.8
2000	535	0.339	0.945	679	1.8
2000	544	0.405	1.062	643	-6.2
2000	438	0.100	0.388	1067	85.3
2000	437	0.127	0.477	1039	79.2
2000	434	0.150	0.531	945	59.0
2000	431	0.176	0.570	887	46.4
2000	428	0.198	0.619	863	41.3
2000	342	0.075	0.252	1057	83.3
2000	342	0.100	0.357	1091	90.6
2000	348	0.123	0.423	1062	84.2
2000	339	0.149	0.483	1019	74.9
2000	335	0.174	0.534	975	65.5
2000	327	0.198	0.575	952	60.5
2000	332	0.208	0.613	958	61.8
2000	330	0.406	0.903	792	26.0
2000	316	0.529	0.851	666	-1.2
2000	327	0.607	1.040	678	1.5
2000	333	0.836	1.374	656	-3.4
2000	332	1.025	1.570	630	-9.0
2000	247	0.074	0.239	1112	95.2
2000	242	0.148	0.441	1060	83.8
2000	236	0.172	0.478	1022	75.6
2000	231	0.198	0.514	982	67.0
2000	233	0.206	0.537	980	66.6
2000	233	0.439	0.853	839	36.1
2000	234	0.632	0.893	711	8.6
2000	233	0.850	0.901	725	11.6
2000	209	0.888	0.921	647	-5.3

continued...

* s = 2.46 mm, w =25.4 mm and L = 281 mm

Table C.2 (concluded)

2000	232	1.010	1.107	632	-8.6
2000	226	1.193	1.121	596	-16.3
2000	144	0.129	0.310	1034	78.2
2000	144	0.154	0.354	1009	72.3
2000	139	0.178	0.402	1006	72.1
2000	139	0.203	0.438	983	67.2
2000	139	0.205	0.472	1007	72.5
2000	133	0.422	0.687	866	41.9

Table C.3: Rectangular Channel CHF Data*. From De Bortoli *et al.* (1958).

P (psia)	ΔTi (F^o)	$Gx10^{-6}$ ($lb.ft^{-2}.hr^{-1}$)	$CHFx10^{-6}$ ($Btu.ft^{-2}.hr^{-1}$)	h_c ($Btu.lb^{-1}$)	X_c (%)
2000	533	0.081	0.236	1130	99.0
2000	530	0.131	0.352	1063	84.6
2000	525	0.667	0.949	664	-1.7
2000	502	0.578	0.786	661	-2.3
2000	435	0.182	0.388	1036	78.7
2000	433	0.366	0.650	894	48.0
2000	432	0.557	0.861	803	28.4
2000	434	0.755	1.025	730	12.7
2000	433	0.971	1.164	663	-1.9
2000	409	0.571	0.695	665	-1.4
2000	341	0.130	0.300	1115	95.8
2000	334	0.185	0.351	1046	80.8
2000	335	0.333	0.573	1039	79.5
2000	333	0.370	0.582	915	52.5
2000	331	0.585	0.781	810	29.8
2000	335	0.626	0.842	871	43.2
2000	331	0.770	0.915	760	19.1
2000	330	0.858	0.786	652	-4.2
2000	354	0.926	0.938	668	-0.8
2000	329	0.947	1.072	739	14.6
2000	335	1.05	1.142	759	18.6
2000	330	1.128	1.105	724	11.4
2000	337	1.47	1.42	666	-1.2
2000	299	0.919	0.765	651	-4.5
2000	283	1.35	1.120	666	-1.2
2000	232	0.159	0.290	1100	92.5
2000	235	0.341	0.429	880	45.0
2000	233	0.424	0.504	855	39.6
2000	230	0.665	0.591	740	14.8
2000	233	0.794	0.689	729	12.5
2000	229	1.128	0.826	679	1.7
2000	234	1.32	0.920	663	-1.9
2000	156	0.037	0.066	1043	80.2
2000	153	0.185	0.286	1109	94.4
2000	141	0.390	0.474	997	70.2
2000	145	0.591	0.606	909	51.2
2000	135	0.595	0.595	932	56.6
2000	140	0.785	0.689	852	38.9
2000	137	0.891	0.713	841	36.7
2000	139	0.985	0.790	822	32.4
2000	137	1.372	0.894	762	19.4

continued...

* s = 1.27 mm, w =25.4 mm and L = 306 mm

Table C.3 (concluded)

2000	138	1.551	0.985	754	17.7
2000	136	1.740	1.032	738	14.3
2000	136	1.865	1.052	726	11.7
2000	136	1.91	0.855	700	5.6
2000	140	2.09	1.155	716	9.5
2000	82	0.229	0.211	929	55.5

Table C.4: Dumb-Bell Shape Channel CHF Data for Minimum Gap Size of 0.762 mm*. From Green *et al.* [1969].

P (Psia)	h_i ($Btu.lb^{-1}$)	$G\times10^{-6}$ ($lb.hr^{-1}.ft^{-2}$)	$CHF\times10^{-6}$ ($Btu.hr^{-1}.ft^{-2}$)	h_c ($Btu.lb^{-1}$)
2000	612	0.247	0.0897	1081
2000	485	0.252	0.1142	1069
2000	377	0.253	0.1336	1058
2000	173	0.254	0.1682	1029
2000	613	0.499	0.1345	962
2000	482	0.501	0.1831	953
2000	377	0.504	0.2263	954
2000	174	0.505	0.3009	944
2000	613	1.047	0.2147	878
2000	485	1.046	0.3033	860
2000	377	1.045	0.3862	852
2000	174	1.044	0.5243	823
2000	614	2.078	0.3134	810
2000	485	2.094	0.4483	762
2000	377	2.100	0.5919	740
2000	173	2.091	0.8191	680
2000	614	4.067	0.4324	752
2000	487	4.183	0.6773	697
2000	377	4.176	0.9294	662
2000	171	4.190	1.4214	610
1600	483	0.251	0.1266	1134
1600	377	0.252	0.1438	1112
1600	172	0.254	0.1836	1106
1600	483	0.500	0.2064	1016
1600	376	0.502	0.2462	1007
1600	174	0.504	0.3209	994
1600	488	1.041	0.3170	880
1600	377	1.045	0.3938	862
1600	173	1.043	0.5388	840
1600	488	2.079	0.4565	771
1600	377	2.088	0.6175	758
1600	175	2.088	0.8644	709
1600	486	4.156	0.6608	692
1600	377	4.174	0.9225	661
1600	173	4.169	1.3592	594
1200	485	0.250	0.1321	1166
1200	376	0.252	0.1528	1158
1200	172	0.254	0.1913	1144
1200	484	0.500	0.2450	1116
1200	374	0.504	0.2884	1112
1200	172	0.505	0.3662	1108

continued...

* for channel shape see Figure 6.1.

Table C.4 (concluded)

1200	488	1.038	0.3653	942
1200	376	1.042	0.4450	926
1200	172	1.041	0.5881	900
1200	488	2.079	0.4759	783
1200	376	2.086	0.6171	757
1200	176	2.093	0.9004	731
1200	488	4.136	0.6348	686
1200	376	4.171	0.8779	647
1200	171	4.178	1.3523	589

Table C.5: Dumb-Bell Shape Channel CHF Data for Minimum Gap Size of 0.381 mm*. From Green *et al.* [1969].

P (Psia)	h_i ($Btu.lb^{-1}$)	$Gx10^{-6}$ ($lb.hr^{-1}.ft^{-2}$)	$CHFx10^{-6}$ ($Btu.hr^{-1}.ft^{-2}$)	h_c ($Btu.lb^{-1}$)
2000	614	0.247	0.0869	1061
2000	488	0.248	0.1126	1066
2000	379	0.248	0.1310	1050
2000	176	0.247	0.1690	1045
2000	612	0.496	0.1341	956
2000	487	0.493	0.1828	958
2000	378	0.495	0.2203	943
2000	176	0.494	0.2918	927
2000	616	0.995	0.2020	874
2000	487	0.988	0.2820	849
2000	376	0.994	0.3512	825
2000	615	1.986	0.3024	809
2000	486	1.975	0.4452	773
2000	379	1.983	0.5560	736
2000	614	3.964	0.4306	752
2000	484	3.949	0.6311	707
2000	376	3.954	0.9327	677
2000	171	3.949	1.416	627
1600	378	0.992	0.3657	846
1600	179	0.991	0.5099	833
1600	178	1.972	0.8186	706
1600	486	3.932	0.6514	697
1600	377	3.946	0.9094	671
1600	173	3.951	1.4071	625
1200	489	0.2455	0.1312	1171
1200	378	0.2468	0.1520	1161
1200	177	0.2468	0.1926	1168
1200	487	0.4930	0.2453	1121
1200	378	0.4938	0.2847	1111
1200	178	0.4931	0.3600	1105
1200	487	0.9876	0.3464	933
1200	379	0.9905	0.4126	908
1200	175	0.988	0.5486	880
1200	487	1.9682	0.4440	774
1200	378	1.9653	0.5766	751
1200	377	1.9683	0.5832	753
1200	486	3.937	0.6193	686
1200	377	3.953	0.8556	653
1200	172	3.951	1.3382	603

* for channel shape see Figure 6.1.

APPENDIX D

CHF DATA FOR BILATERALLY HEATED ANNULI

Table D.1: Bilaterally Heated Annuli CHF Data*. From Becker and Letzter [1975].

#	P (BAR)	ΔT_{sub} (K)	G $(kg.m^{-2}.s^{-1})$	q_i	q_o $(W.cm_{-2})$	X_c	R
1	30.0	10.5	241.	43.7	0.0	0.443	0.0
2	29.9	9.6	499.	78.2	0.0	0.382	0.0
3	29.7	9.0	728.	99.1	0.0	0.330	0.0
4	29.7	8.5	1008.	116.7	0.0	0.279	0.0
5	29.8	9.4	1473.	142.7	0.0	0.227	0.0
6	29.8	9.4	1988.	165.5	0.0	0.192	0.0
7	29.9	10.6	2501.	189.2	0.0	0.169	0.0
8	30.4	8.8	2991.	205.2	0.0	0.156	0.0
9	30.2	7.7	3418.	217.1	0.0	0.145	0.0
10	30.1	10.5	496.	50.3	48.8	0.690	0.969
11	29.9	10.1	722.	59.5	57.6	0.555	0.968
12	29.9	8.8	1006.	68.7	06.5	0.459	0.967
13	29.8	11.1	1488.	81.7	78.3	0.356	0.958
14	30.0	10.3	1995.	93.7	89.8	0.303	0.958
15	30.2	10.9	2496.	106.9	101.8	0.271	0.951
16	30.0	9.5	2930.	115.9	109.8	0.251	0.948
17	29.9	11.3	244.	39.5	12.4	0.628	0.310
18	30.0	10.0	498.	44.4	66.5	0.821	1.497
19	30.0	10.0	732.	52.6	78.3	0.654	1.489
20	30.0	10.5	1011.	58.7	86.9	0.520	1.482
21	29.8	9.2	1482.	66.8	98.7	0.400	1.47
22	30.0	11.5	1985.	77.5	114.0	0.336	1.471
23	29.9	9.8	2821.	89.0	130.4	0.270	1.465
24	30.2	9.4	503.	39.2	69.6	0.817	1.774
25	30.1	10.2	732.	48.0	85.0	0.680	1.768
26	29.9	9.8	1005.	54.1	95.3	0.551	1.762
27	30.2	10.4	1473.	60.7	106.6	0.414	1.756
28	29.6	8.0	2005.	69.4	121.0	0.347	1.745
29	30.2	9.9	2776.	80.1	138.8	0.280	1.732
30	30.0	10.0	245.	19.6	38.5	0.909	1.968
31	30.1	9.7	500.	36.8	71.9	0.829	1.952
32	29.9	9.1	731.	43.0	89.4	0.693	2.078
33	29.9	9.8	1007.	51.7	100.5	0.568	1.944
34	30.1	10.2	1478.	59.1	113.9	0.433	1.927
35	30.0	10.8	2016.	68.7	131.9	0.362	1.919

continued...

* For annulus dimensions see table 7.1.

Table D.1 (continued)

36	30.0	9.3	2857.	76.1	145.0	0.279	1.906
37	30.0	10.8	243.	18.4	40.1	0.929	2.179
38	30.0	10.5	501.	33.2	71.9	0.806	2.165
39	30.1	9.7	733.	39.6	85.3	0.652	2.155
40	29.7	10.2	1005.	46.8	99.5	0.550	2.126
41	30.1	9.7	1472.	55.4	117.7	0.442	2.124
42	30.1	9.5	2010.	61.1	128.8	0.350	2.109
43	30.2	8.7	2705.	70.5	147.7	0.297	2.096
44	29.9	9.6	244.	17.0	39.7	0.904	2.336
45	30.1	10.2	499.	30.7	71.6	0.795	2.331
46	29.9	9.3	729.	37.1	85.9	0.651	2.315
47	29.9	9.1	1010.	43.5	100.3	0.546	2.304
48	30.0	9.3	1465.	50.0	115.1	0.427	2.301
49	30.0	10.3	1960.	55.9	127.3	0.347	2.279
50	30.0	7.1	2650.	62.2	141.8	0.289	2.278
51	30.2	9.4	2839.	67.5	152.6	0.285	2.260
52	30.1	9.7	244.	10.5	42.6	0.892	4.052
53	29.9	9.3	499.	18.5	74.1	0.757	3.995
54	29.9	8.6	728.	22.4	89.5	0.624	3.988
55	29.9	9.6	1005.	25.8	103.1	0.514	3.994
56	29.9	9.8	1438.	30.0	119.6	0.412	3.980
57	29.6	8.8	1908.	33.1	129.9	0.336	3.919
58	30.1	8.2	2800.	40.1	157.0	0.274	3.920
59	29.7	10.5	243.	0.0	44.8	0.821	∞
60	29.9	10.3	503.	0.0	79.0	0.697	∞
61	29.8	8.4	726.	0.0	99.6	0.611	∞
62	30.8	10.5	1004.	0.0	123.7	0.543	∞
63	30.1	9.7	1473.	0.0	147.9	0.438	∞
64	29.7	9.0	2001.	0.0	166.1	0.359	∞
65	30.4	10.0	2506.	0.0	183.4	0.312	∞
66	30.1	10.0	2874.	0.0	190.4	0.280	∞
67	50.0	12.6	242.	45.2	0.0	0.494	0.0
68	48.7	8.7	498.	73.0	0.0	0.389	0.0
69	49.2	9.6	728.	91.9	0.0	0.329	0.0
70	50.4	10.4	1007.	118.9	0.0	0.305	0.0
71	50.0	9.1	1478.	144.0	0.0	0.249	0.0
72	50.0	9.6	2004.	165.6	0.0	0.206	0.0
73	49.8	9.1	2519.	184.6	0.0	0.181	0.0
74	50.4	9.1	3032.	200.4	0.0	0.161	0.0
75	50.3	10.2	4038.	226.5	0.0	0.129	0.0
76	49.0	10.3	247.	27.4	27.2	0.837	0.993
77	49.8	10.1	496.	46.2	45.5	0.696	0.985
78	49.7	9.2	728.	57.0	55.5	0.579	0.972
79	49.9	9.0	1005.	67.2	65.8	0.493	0.979
80	50.2	10.4	1470.	80.0	78.0	0.391	0.975
81	50.2	11.6	2010.	93.3	90.5	0.325	0.970
82	50.0	10.1	2509.	102.9	99.9	0.287	0.971
83	50.1	10.2	3001.	111.5	107.4	0.256	0.963

continued...

Table D.1 (continued)

84	50.0	10.6	3472.	121.8	117.1	0.238	0.962
85	49.4	8.1	243.	0.0	40.9	0.822	∞
86	49.1	9.5	500.	0.0	76.2	0.738	∞
87	48.6	7.9	730.	0.0	99.2	0.658	∞
88	49.8	10.1	1003.	0.0	121.4	0.580	∞
89	49.6	10.6	1473.	0.0	142.3	0.455	∞
90	49.1	10.0	2007.	0.0	158.1	0.366	∞
91	49.3	10.0	2514.	0.0	169.2	0.309	∞
92	49.4	9.6	2993.	0.0	177.6	0.270	∞
93	49.4	9.6	3002.	0.0	140.4	0.206	∞
94	49.8	10.6	3309.	0.0	183.5	0.248	∞
95	69.7	8.9	242.	43.7	0.0	0.526	0.0
96	69.2	9.4	497.	68.3	0.0	0.391	0.0
97	69.5	9.0	500.	67.3	0.0	0.384	0.0
98	69.7	10.4	731.	88.1	0.0	0.336	0.0
99	65.6	6.8	725.	82.1	0.0	0.321	0.0
100	69.7	9.2	1009.	109.1	0.0	0.302	0.0
101	69.6	10.5	1007.	108.6	0.0	0.296	0.0
102	67.7	8.7	1469.	130.7	0.0	0.243	0.0
103	70.1	9.1	2006.	144.8	0.0	0.192	0.0
104	69.2	8.7	2501.	158.5	0.0	0.165	0.0
105	68.5	8.3	3009.	170.8	0.0	0.146	0.0
106	69.7	9.2	4002.	188.1	0.0	0.113	0.0
107	69.7	11.1	244.	35.7	0.0	0.621	0.257
108	70.0	10.7	477.	58.2	9.2	0.512	0.257
109	70.1	10.5	698.	73.5	15.0	0.437	0.255
110	69.8	10.0	1001.	86.9	18.7	0.354	0.253
111	69.7	9.9	1475.	102.5	22.0	0.277	0.253
112	69.9	11.3	1997.	118.1	25.9	0.224	0.249
113	69.9	10.1	2500.	129.0	29.4	0.195	0.248
114	69.8	10.2	3008.	141.2	32.0	0.173	0.247
115	69.8	10.0	3987.	163.2	34.9	0.147	0.246
116	70.2	11.6	244.	30.7	40.2	0.704	0.513
117	69.8	10.0	482.	51.2	15.7	0.590	0.508
118	70.0	10.2	700.	63.8	26.0	0.495	0.497
119	69.9	9.4	1005.	75.3	31.7	0.405	0.502
120	70.4	9.9	1473.	88.1	37.8	0.315	0.499
121	70.1	10.1	2016.	100.9	43.9	0.256	0.495
122	70.0	10.0	2498.	112.5	50.0	0.226	0.490
123	69.7	10.4	3000.	124.5	55.1	0.203	0.489
124	70.2	9.2	3941.	141.9	60.8	0.176	0.487
125	69.9	12.0	244.	27.7	69.0	0.777	0.750
126	70.0	11.4	479.	47.9	20.8	0.677	0.745
127	68.9	7.2	699.	57.2	42.4	0.559	0.740
128	70.0	10.4	1008.	68.4	50.2	0.447	0.734
129	70.1	10.5	1470.	79.9	58.4	0.350	0.731
130	69.8	11.2	1999.	91.7	66.6	0.286	0.726
131	69.9	10.3	2522.	99.3	72.1	0.243	0.727

continued...

Table D.1 (continued)

132	70.0	10.9	3007.	110.5	79.9	0.221	0.723
133	70.0	9.7	3911.	125.5	90.2	0.192	0.719
134	70.2	14.5	243.	26.5	26.6	0.890	1.003
135	70.3	11.0	496.	43.9	43.6	0.719	0.994
136	70.4	11.6	726.	53.6	52.9	0.588	0.987
137	69.8	10.0	1006.	61.1	59.9	0.480	0.980
138	68.2	8.2	1466.	70.6	69.3	0.377	0.982
139	68.8	8.5	1990.	80.0	78.5	0.310	0.981
140	70.3	9.0	2488.	88.6	86.7	0.270	0.978
141	70.6	10.8	3002.	98.7	96.0	0.240	0.973
142	70.1	9.6	3828.	111.4	108.3	0.212	0.972
143	70.0	10.9	244.	22.8	28.3	0.990	1.241
144	69.7	9.9	479.	40.8	50.5	0.807	1.238
145	69.7	9.7	699.	49.3	60.4	0.658	1.226
146	69.6	9.6	1004.	56.9	69.9	0.523	1.228
147	69.8	9.0	1467.	65.6	79.9	0.405	1.218
148	69.6	10.1	1993.	75.3	91.6	0.334	1.216
149	69.8	8.8	2500.	83.9	101.7	0.296	1.211
150	69.9	10.6	3006.	93.0	112.4	0.264	1.209
151	69.8	10.0	3751.	105.1	126.3	0.236	1.202
152	69.8	11.2	243.	22.2	32.8	0.981	1.476
153	69.9	11.1	479.	38.1	56.2	0.852	1.477
154	69.8	8.5	697.	45.7	67.1	0.701	1.468
155	70.1	9.8	1006.	53.9	79.1	0.564	1.468
156	69.7	10.4	1472.	63.0	91.8	0.438	1.458
157	69.4	8.9	2023.	71.9	104.7	0.362	1.456
158	70.1	9.6	2499.	80.6	116.9	0.323	1.452
159	69.8	9.8	3000.	87.6	127.0	0.288	1.449
160	69.8	10.0	3731.	100.0	142.6	0.258	1.426
161	69.9	10.8	245.	20.0	34.3	0.984	1.711
162	70.2	11.6	480.	35.8	61.9	0.999	1.728
163	70.0	8.5	700.	42.9	73.6	0.737	1.716
164	69.7	8.9	1001.	49.8	85.2	0.590	1.710
165	69.7	9.4	1469.	58.1	98.9	0.459	1.701
166	69.9	10.1	2009.	69.0	113.7	0.381	1.648
167	70.0	10.2	2509.	74.3	126.2	0.332	1.699
168	69.9	8.4	2986.	80.6	136.4	0.305	1.694
169	69.9	8.4	3641.	89.7	150.3	0.273	1.674
170	70.2	11.6	244.	19.5	35.1	0.995	1.798
171	70.0	11.2	477.	36.2	65.3	0.947	1.802
172	69.9	9.1	701.	42.6	77.0	0.759	1.710
173	69.8	10.5	1005.	50.2	89.4	0.606	1.783
174	69.9	10.1	1471.	58.2	104.1	0.475	1.787
175	70.0	9.2	2006.	66.6	118.1	0.394	1.774
176	70.0	10.0	2502.	74.7	132.2	0.348	1.770
177	69.8	9.5	3008.	81.0	143.2	0.311	1.768
178	69.9	10.6	3664.	89.2	157.6	0.274	1.768
179	69.8	11.5	244.	17.6	34.6	0.961	1.968

continued...

Table D.1 (continued)

180	69.9	10.3	480.	33.3	65.8	0.931	1.977
181	69.6	9.6	697.	40.9	80.1	0.777	1.960
182	69.9	8.6	1001.	47.0	92.5	0.622	1.970
183	69.7	10.2	1463.	54.2	106.5	0.478	1.963
184	70.5	9.5	2013.	61.0	118.6	0.385	1.944
185	70.2	8.4	2495.	66.2	128.6	0.336	1.943
186	69.9	9.4	2996.	72.4	139.4	0.297	1.926
187	70.0	9.5	3660.	75.6	154.0	0.265	1.934
188	69.8	10.5	244.	17.6	34.9	0.971	1.986
189	70.1	11.5	477.	33.0	65.9	0.933	1.996
190	69.9	11.1	701.	40.9	81.8	0.782	1.998
191	69.7	9.7	1005.	47.2	93.9	0.624	1.991
192	69.9	9.4	1472.	54.8	108.0	0.485	1.971
193	69.9	9.9	2001.	62.1	122.6	0.398	1.975
194	70.5	9.7	2508.	68.4	134.5	0.345	1.966
195	70.0	9.0	2993.	72.5	142.5	0.305	1.965
193	70.2	9.9	3679.	80.4	157.6	0.268	1.960
194	69.9	10.6	244.	15.6	34.2	0.931	2.196
198	69.9	11.3	480.	29.9	65.5	0.902	2.189
199	70.1	12.2	701.	38.4	83.9	0.785	2.183
200	70.0	9.5	1001.	45.0	98.1	0.644	2.177
201	69.8	10.5	1468.	52.1	112.9	0.495	2.169
202	70.0	8.7	2016.	58.2	126.4	0.403	2.170
203	69.9	9.9	2505.	63.0	135.5	0.340	2.151
204	70.0	9.5	3001.	67.2	144.2	0.300	2.146
205	69.9	9.4	3673.	74.7	159.0	0.268	2.129
206	69.9	12.3	243.	12.6	27.2	0.731	2.152
207	70.4	11.1	479.	30.6	65.4	0.910	2.139
208	70.0	10.7	698.	38.1	81.9	0.776	2.153
209	70.0	10.7	1001.	45.0	96.7	0.632	2.146
210	69.8	9.0	1460.	51.2	110.1	0.491	2.149
211	69.9	9.4	1983.	58.7	125.5	0.406	2.137
212	69.9	9.6	2502.	63.5	134.5	0.340	2.120
213	69.9	10.1	3001.	67.2	142.5	0.294	2.121
214	69.8	9.3	3652.	73.5	155.8	0.264	2.119
215	70.0	10.4	244.	15.2	36.7	0.982	2.410
216	69.7	11.1	476.	27.6	66.5	0.906	2.406
217	70.0	9.0	695.	34.6	82.9	0.778	2.399
218	70.0	9.0	994.	41.7	100.2	0.652	2.403
219	69.9	10.6	1479.	48.8	116.9	0.499	2.394
220	70.5	11.2	2001.	53.3	126.8	0.392	2.381
221	69.7	8.9	2501.	57.1	136.1	0.338	2.382
222	69.8	8.5	2992.	61.0	145.4	0.300	2.383
223	70.3	10.5	3722.	69.0	161.5	0.259	2.339
224	69.9	12.5	244.	12.6	36.7	0.940	2.917
225	69.8	11.7	476.	23.4	67.8	0.893	2.896
226	70.0	10.9	698.	29.2	84.2	0.754	2.884
227	70.0	10.7	1045.	35.3	101.1	0.598	2.866
228	69.8	10.2	1474.	40.9	117.1	0.486	2.866

continued...

Table D.1 (continued)

229	69.9	9.9	2007.	44.8	128.1	0.385	2.855
230	69.6	9.6	2510.	48.4	138.2	0.328	2.855
231	69.8	10.5	3009.	52.4	149.4	0.290	2.850
232	69.6	9.6	3743.	57.9	164.3	0.255	2.836
233	70.8	10.2	243.	7.9	31.6	0.781	4.029
234	69.8	9.8	501.	16.9	67.1	0.806	3.974
235	70.0	10.2	735.	21.1	83.5	0.678	3.957
236	70.4	9.6	1010.	23.6	94.1	0.551	3.982
237	69.8	10.0	1476.	27.3	107.5	0.422	3.935
238	69.7	8.7	2006.	30.0	117.7	0.338	3.922
239	69.9	9.1	2982.	34.0	133.4	0.249	3.928
240	69.9	9.4	3767.	37.2	144.6	0.208	3.892
241	69.5	10.2	244.	0.0	38.0	0.818	∞
242	69.7	11.4	498.	0.0	90.7	0.959	∞
243	69.8	9.3	498.	0.0	71.2	0.751	∞
244	69.8	9.0	732.	0.0	91.7	0.653	∞
245	69.5	9.7	725.	0.0	91.2	0.655	∞
246	69.0	9.7	1018.	0.0	109.2	0.553	∞
247	69.6	9.8	1006.	0.0	108.6	0.558	∞
248	69.2	10.2	1517.	0.0	125.2	0.416	∞
249	68.8	9.5	1472.	0.0	124.4	0.429	∞
250	69.4	10.8	2002.	0.0	136.1	0.335	∞
251	69.5	9.7	1997.	0.0	135.5	0.338	∞
252	69.4	9.4	2510.	0.0	143.0	0.279	∞
253	69.3	9.3	2510.	0.0	144.5	0.283	∞
254	69.4	9.1	3003.	0.0	150.5	0.243	∞
255	69.7	10.4	3000.	0.0	153.8	0.245	∞
256	69.4	8.9	3469.	0.0	161.3	0.224	∞
257	69.2	8.2	3636.	0.0	163.8	0.218	∞
258	99.6	10.4	241.	40.9	0.0	0.552	0.0
259	100.8	10.1	502.	60.0	0.0	0.379	0.0
260	100.1	9.3	743.	72.1	0.0	0.301	0.0
261	100.0	11.2	1011.	88.4	0.0	0.259	0.0
262	100.1	9.8	1477.	103.3	0.0	0.205	0.0
263	99.4	9.5	2048.	119.3	0.0	0.163	0.0
264	100.4	10.3	2510.	132.0	0.0	0.140	0.0
265	99.5	8.9	2991.	144.1	0.0	0.130	0.0
266	100.0	9.2	3987.	174.6	0.0	0.113	0.0
267	99.6	10.2	493.	37.9	38.3	0.711	1.008
268	99.9	10.9	739.	44.3	44.5	0.540	1.004
269	99.5	9.6	1006.	49.3	49.6	0.438	1.006
270	99.5	9.6	1467.	56.1	55.8	0.330	0.994
271	99.7	9.7	2043.	61.9	61.6	0.252	0.995
272	99.7	10.5	2499.	70.8	70.1	0.229	0.990
273	99.6	9.4	2991.	79.7	78.8	0.217	0.989
274	99.7	10.2	3968.	101.9	99.7	0.202	0.979
275	100.0	11.7	243.	24.5	25.0	0.947	1.020
276	99.9	10.6	244.	21.1	28.1	0.979	1.335

continued...

Table D.1 (continued)

277	99.9	10.6	497.	37.1	48.9	0.832	1.318
278	100.2	10.4	730.	41.3	54.4	0.620	1.317
279	99.8	9.6	1006.	48.4	63.6	0.523	1.313
280	100.0	9.7	1469.	53.9	70.5	0.387	1.308
281	100.1	10.0	2045.	58.7	76.6	0.291	1.305
282	100.1	10.5	2969.	72.9	94.8	0.240	1.299
283	99.8	10.1	4029.	80.6	104.1	0.187	1.291
284	100.0	10.2	243.	20.1	30.9	1.041	1.537
285	99.9	10.1	499.	33.7	51.2	0.835	1.520
286	99.8	10.5	736.	39.5	59.9	0.652	1.516
287	100.0	10.9	1010.	44.0	66.6	0.519	1.514
288	100.4	11.2	1474.	52.5	79.6	0.415	1.517
289	99.8	10.1	2062.	56.9	86.1	0.314	1.513
290	99.9	11.6	2894.	71.7	108.2	0.270	1.509
291	99.9	10.6	3830.	80.6	120.9	0.225	1.500
292	99.9	12.1	245.	16.6	29.7	0.948	1.793
293	99.6	10.2	501.	29.1	52.3	0.811	1.796
294	99.8	9.6	730.	33.8	60.3	0.638	1.786
295	99.7	10.0	1006.	37.6	67.2	0.505	1.788
296	99.9	9.4	1459.	43.1	76.7	0.392	1.779
297	99.9	10.6	2062.	48.4	85.7	0.296	1.773
298	100.1	10.3	2931.	58.1	102.7	0.244	1.768
299	100.0	9.7	3888.	68.0	119.6	0.211	1.760
300	99.7	11.7	244.	13.5	29.5	0.898	2.189
301	99.9	10.1	506.	23.7	51.6	0.759	2.177
302	99.9	9.9	734.	28.1	60.9	0.611	2.171
303	99.8	9.8	1008.	30.9	67.2	0.482	2.177
304	100.0	10.0	1471.	34.5	74.5	0.356	2.163
305	100.0	10.2	2044.	39.1	84.7	0.281	2.163
308	99.7	9.7	2992.	48.0	103.4	0.229	2.152
307	100.1	8.6	3988.	56.7	121.5	0.203	2.141
308	100.1	11.2	244.	0.0	35.9	0.874	∞
309	99.9	11.1	499.	0.0	57.1	0.667	∞
310	99.6	10.2	738.	0.0	69.9	0.548	∞
311	99.3	10.4	999.	0.0	80.1	0.455	∞
312	99.6	10.6	1464.	0.0	92.8	0.349	∞
313	99.7	9.5	2054.	0.0	103.3	0.272	∞
314	99.8	9.3	2487.	0.0	113.8	0.245	∞
315	99.9	10.1	3001.	0.0	125.2	0.216	∞
316	100.0	11.2	4016.	0.0	153.4	0.190	∞
317	139.9	10.7	245.	38.4	0.0	0.610	0.0
318	139.7	9.9	502.	46.8	0.0	0.338	0.0
319	140.0	11.3	740.	63.4	0.0	0.297	0.0
320	139.7	9.4	1017.	73.0	0.0	0.248	0.0
321	139.8	9.0	1481.	88.3	0.0	0.198	0.0
322	139.7	10.6	2158.	103.3	0.0	0.137	0.0
323	139.8	10.4	2991.	135.4	0.0	0.127	0.0
324	139.9	9.8	3841.	161.9	0.0	0.118	0.0

continued...

Table D.1 (concluded)

325	139.8	9.7	243.	19.3	20.1	0.918	1.039
326	139.6	9.9	500.	28.7	29.4	0.636	1.027
327	139.8	9.5	733.	35.5	36.1	0.526	1.017
328	139.8	10.2	1011.	38.7	40.4	0.406	1.048
329	139.8	10.7	1486.	48.3	49.2	0.325	1.018
330	139.9	10.0	2978.	70.8	70.6	0.219	0.997
331	140.5	10.4	3670.	71.4	71.3	0.165	0.999
332	140.0	11.8	245.	0.0	28.9	0.833	∞
333	139.9	11.7	503.	0.0	38.4	0.511	∞
334	140.0	13.4	736.	0.0	46.1	0.395	∞
335	140.1	11.8	1019.	0.0	54.3	0.333	∞
336	139.9	10.3	1474.	0.0	66.9	0.281	∞
337	138.5	11.9	2178.	0.0	83.3	0.215	∞
338	139.9	12.7	2992.	0.0	97.2	0.167	∞
339	139.8	11.9	3705.	0.0	115.4	0.161	∞